Titre: Title:	Control Strategies for Standing Column Wells in a Cold Climate
Auteur: Author:	Camille Beurcq
Date:	2019
Type:	Mémoire ou thèse / Dissertation or Thesis
Référence: Citation:	Beurcq, C. (2019). Control Strategies for Standing Column Wells in a Cold Climate [Mémoire de maîtrise, Polytechnique Montréal]. PolyPublie. https://publications.polymtl.ca/3916/

POLYTECHNIQUE MONTRÉAL

affiliée à l'Université de Montréal

Control Strategies for Standing Column Wells in a Cold Climate

CAMILLE BEURCQ

Département de génie mécanique

Mémoire présenté en vue de l'obtention du diplôme de *Maîtrise ès sciences appliquées*

Génie mécanique

Mai 2019

POLYTECHNIQUE MONTRÉAL

affiliée à l'Université de Montréal

Ce mémoire intitulé :

Control Strategies for Standing Column Wells in a Cold Climate

présenté par **Camille BEURCQ**

en vue de l'obtention du diplôme de *Maîtrise ès sciences appliquées*

a été dûment accepté par le jury d'examen constitué de :

Michel BERNIER, président
Michaël KUMMERT, membre et directeur de recherche
Philippe PASQUIER, membre et codirecteur de recherche
Massimo CIMMINO, membre

DEDICATION

‘Almost every way we make electricity today, except for the emerging renewables and nuclear, puts out CO2. And so, what we’re going to have to do at a global scale, is create a new system. And so, we need energy miracles.’

TED conference, 2010, Bill Gates

‘Chaque génération, sans doute, se croit vouée à refaire le monde. La mienne sait pourtant qu’elle ne le refera pas. Mais sa tâche est peut-être plus grande. Elle consiste à empêcher que le monde se défasse’

Discours de réception du prix nobel de littérature, 1957, Albert Camus

ACKNOWLEDGEMENTS

Pour commencer, je voudrais remercier mon directeur de recherche, le professeur Michaël Kummert pour son soutien constant et son regard vif et précis sur mon travail. Il a su m'accompagner et faire évoluer ma réflexion grâce à ses précieux conseils toujours très pertinents en partageant ses connaissances malgré une charge de travail conséquente. Je suis très reconnaissante d'avoir pu bénéficier de son encadrement de qualité, de son expertise, et de ses nombreux encouragements pendant ces deux ans de collaboration.

Mes remerciements s'adressent aussi particulièrement à mon codirecteur, le professeur Philippe Pasquier, dont les conseils, le temps accordé et l'expertise technique ont permis à ce projet de voir le jour. Je le remercie pour son soutien, sa bonne humeur, mais aussi sa patience lors de nos rencontres qui m'ont toujours (re)motivée.

Je remercie aussi Alain Nguyen qui a mis à ma disposition le modèle du puits à colonne permanente élaboré pendant son doctorat et qui est à la base de la recherche présentée dans ce mémoire.

Un grand merci à tous mes collègues du bee-lab pour nos diverses discussions, scientifiques ou non, particulièrement le bureau 317 : Sam, Alex, Louis, Gregor, Walid, Kun et Florent.

Enfin j'aimerais remercier mille fois mon équipe de rugby qui m'a permis de retrouver et de garder un bel équilibre, au prix de quelques bleus, et qui m'a ouvert les portes d'une nouvelle passion et d'un bonheur intense et partagé, comme une nouvelle famille.

Merci à mes autres amis de poly, et aux *Canadians colors*, ceux qui sont encore là et ceux qui sont rentrés, chacun m'a apporté quelque chose d'essentiel : des rires, de belles discussions ou de merveilleux souvenirs.

Enfin, même s'ils sont loin, un grand merci à ma famille, particulièrement mes parents et ma sœur pour leur soutien indéfectible et l'amour qu'ils me portent au quotidien.

Enfin, j'aimerais adresser ma plus sincère gratitude à l'Institut de l'Énergie Trottier (IET) pour le soutien financier octroyé à ce projet. Ce travail de recherche n'aurait pas été possible sans la participation financière de l'IET.

RÉSUMÉ

Les puits à colonne permanente sont des échangeurs géothermiques relativement profonds qui ont pour particularité d'utiliser directement l'eau souterraine comme fluide caloporteur. L'eau est généralement pompée à la base du puits grâce à une pompe submersible jusqu'à un échangeur à plaques. Ce dernier fait le lien entre la boucle d'eau souterraine et la boucle d'eau du bâtiment sur laquelle sont connectées des pompes à chaleurs décentralisées qui assurent le chauffage et la climatisation du bâtiment. L'eau est ensuite réinjectée en haut du puits sous le niveau dynamique à l'aide d'un tuyau de réinjection. Avant d'être réinjectée dans le puits, jusqu'à 30% de l'eau souterraine peut être déviée vers un puits d'injection (ou une autre destination) ce qui a pour effet d'attirer de l'eau, à une température proche de celle du sol non perturbé, à travers les fractures du sol dans le puits à colonne permanente et ainsi d'augmenter sa performance thermique. Ce processus est aussi appelé 'saignée'. Ce type d'échangeur implique des forages relativement longs, mais leur efficacité thermique permet de réaliser des économies par rapport à des puits en boucles fermée. La boucle d'eau du bâtiment comporte aussi des auxiliaires de chauffage et de refroidissement qui prennent le relai quand l'échangeur souterrain ne peut répondre à la demande du bâtiment, particulièrement lors des pointes de demande.

La consommation énergétique de ces systèmes provient des pompes à chaleur, de l'énergie de pompage, et de l'énergie consommée par les systèmes auxiliaires. Les coûts d'opération peuvent aussi être influencés par la pointe de puissance appelée par le système. D'un autre côté, la saignée implique des impacts environnementaux et peut être reliée à des contraintes d'opération techniques et légales, et il est donc intéressant de limiter le volume d'eau saignée du puits.

Le but de cette recherche est d'explorer et de recommander des stratégies de contrôle des bâtiments équipés de puits à colonne permanente pour le pompage, la saignée, les consignes de température du bâtiment et des systèmes auxiliaires, dans le but d'améliorer l'efficacité énergétique du système et les coûts d'opération, tout en limitant le volume d'eau souterraine saignée.

Ce travail de recherche comporte le développement d'un modèle de bâtiment de bureau détaillé en plusieurs zones chauffées et climatisées par des pompes à chaleur décentralisées. Le modèle a été réalisé avec le logiciel TRNSYS pour la partie bâtiment tandis que l'échangeur géothermique est modélisé dans Matlab. Une étude des pertes de charge dans la boucle d'eau souterraine a été

réalisée pour une meilleure précision de l'évaluation des stratégies de pompage de façon à prendre en compte l'impact de la saignée sur l'énergie de pompage.

La revue de littérature a permis d'identifier un scénario de référence qui regroupe les pratiques et recommandations pour le contrôle de système qui servira pour comparer l'impact des stratégies testées. Les simulations réalisées se séparent en trois grandes catégories : les stratégies de pompage, de saignée et de contrôle du bâtiment.

Les stratégies de pompages implémentées ont montré l'intérêt de l'utilisation des pompes submersibles à vitesse variable afin de contrôler le débit de pompage en fonction de la charge sur la boucle d'eau du bâtiment. La meilleure stratégie identifiée permet des économies de 8 % du coût d'opération par rapport au scénario de référence avec un volume d'eau saignée réduit ou identique. Les stratégies de saignée ont montré qu'à débit de saignée constant, il n'était pas nécessaire d'aller au-dessus de 15% de débit saigné. La combinaison de stratégies simples de saignée avec la meilleure stratégie de pompage permet d'obtenir différents points d'opération selon les contraintes retenues pour le volume d'eau saignée : dans une large plage d'opération, les résultats montrent une diminution quasi linéaire des coûts d'opération en fonction du volume saigné, mais la combinaison des stratégies proposées permet ici encore une amélioration significative du coût d'opération par rapport au scénario de référence, à volume d'eau de saignée égal. Des stratégies de contrôle du débit de saignée évoluant par rapport à la charge ont montré un intérêt lorsqu'elles sont basées sur l'évolution de la charge future afin de préparer les puits à répondre à une demande importante comme lors de la reprise le matin. Cependant, les économies engendrées par ces stratégies 'prédictives' sont faibles et semblent difficilement justifier le niveau de complexité introduit. Enfin, on a aussi voulu étudier le bâtiment dans son ensemble au travers des stratégies de contrôle du bâtiment en lui-même. Les simulations ont démontré que les coûts et l'énergie consommée sont très sensibles au choix de la consigne de l'auxiliaire et peuvent être facilement améliorés grâce à l'utilisation d'un profil de consigne évitant les reprises matinales rapides pour les températures du bâtiment. Ces deux paramètres ont un impact significatif sur la performance globale, et doivent donc être optimisés en même temps que les paramètres de pompage et de saignée.

ABSTRACT

Standing column wells (SCWs) are a type of ground heat exchanger which relies on relatively deep wells and uses groundwater directly as the heat transfer fluid. The groundwater is generally pumped at the bottom of the well with a submersible pump to a plate heat exchanger. This heat exchanger is the connection between the ground loop and the building loop which supplies the source side of distributed heat pumps providing heating and cooling to the building. The groundwater is then reinjected at the top of the well below the dynamic level of the aquifer with a rejection pipe. Before being reinjected, up to 30% of the groundwater may be diverted into an injection well (or another destination). This has the effect to attract groundwater at a temperature close to the undisturbed ground temperature from the ground fractures in the aquifer into the standing column well, which will increase its thermal performance. This process is also called 'bleed'. Although this type of ground heat exchanger relies on relatively deep wells, their high heat exchange capacity can lead to cost savings compared to closed-loop systems. SCW systems also include auxiliary devices for heating and cooling, which are used when ground heat exchanger is not sufficient to meet the building load, especially during peak periods.

The energy use of SCW systems comes from the heat pumps, the submersible pump, and auxiliary heating and cooling devices. Operative costs are also influenced by the peak power demand of the system. On the other hand, bleed can be associated to environmental impacts and subject to technical and legal constraints, so there is an interest to limit the volume of groundwater bled.

The goal of this research is to design and assess control strategies of the building for : pumping, bleed, and building and auxiliary setpoint temperatures with the aim of improving the overall energy efficiency and operative costs while minimizing the volume of groundwater bled.

The work performed includes the development of a detailed model of an office building that includes fifteen thermal zone heated and cooled by decentralized heat pumps. The building and HVAC system are modelled in TRNSYS while the ground heat exchanger is modelled in Matlab. A detailed assessment of the head losses in the ground loop with and without bleed was performed in order to accurately represent the impact of bleed on the pumping energy needs, as this is a key aspect of the overall control optimization.

Through the literature review, a *'good practice'* scenario was identified. This scenario combines typical practice and recommendations regarding SCW systems operation. Simulations are then performed to assess the impact of different control assumptions on the system performance, compared to this reference scenario. The simulations are separated in three main categories : pumping, bleed and building (including auxiliary) control strategies.

The pumping control strategies implemented showed the interest of variable speed submersible pump so that the pumping flow rate evolves as a function of the load on the building loop. The best strategy delivers up to 8 % savings in operating costs compared to the *good practice* scenario, with an equivalent or reduced volume of groundwater bled. The bleed control strategies showed that when implementing a constant bleed flow rate, going over a 15% bleed ratio is not beneficial. The combination of simple bleed ratio control strategies with the best pumping strategy allows to obtain different operating points depending on the selected constraints regarding the volume of groundwater bled: over a large operating range, operating costs decrease quasi-linearly with an increase of the volume bled. Here again, the combination of proposed strategies delivers significant operating cost savings with an equivalent volume of groundwater bled. The implementation of linear control for bleed flow rate shows an interest when it is based on the future load predicted on the building loop. These control strategies help the well prepare for large load demand especially before the morning start. However, the cost savings with those 'predictive' strategies are modest, especially when compared to the added complexity of implementation, and they may not be justified in the studied case. Finally, this work aimed at studying the building as a global system specifically regarding the zone setpoint temperatures and the auxiliary heating setpoint. The simulations showed that the costs savings and energy consumption are very sensitive to the choice of the auxiliary temperature setpoint. The performance is also significantly better if a "smoother" setpoint profile is used for the building zones, with long ramps to recover from the night setback/startup. These two parameters have a large impact on the overall system performance and must be optimized together with the control parameters for pumping and bleed ratio.

TABLE OF CONTENTS

LIST OF TABLES

LIST OF FIGURES

LIST OF SYMBOLS AND ABBREVIATIONS

List of Abreviations

ASHRAE	American Society of Heating, Refrigerating and Air-Conditioning Engineers
COP	Coefficient of performance
EWT	Entering water temperature (to the heat pumps)
GHE	Ground Heat Exchanger
GPM	Gallons per minutes
GSHP	Ground Source Heat Pump
HDPE	High Density Polyethylene
HP	Heat Pump
HVAC	Heating, Ventilation and Air Conditionning
HX	Heat Exchanger
LWT	Leaving water temperature (from the heat pumps)
NCBE	National Energy Code for Buildings
PVC	Polyvinyl chloride
SCW	Standing Column Well
SHGC	Solar Heat Gain Coefficient
SWH	Service Water Heating
TESS	Thermal Energy System Specialists
TRCM	Thermal resistance and capacitance model
TRNSYS	Transient System Simulation Tool
USA	United State of America
USDOE	United State Department of Energy

List of variables

A	Area (m^2)
ACH	Infiltration rate (h^{-1})
b	Aquifer thickness (m), or mean plate gap - for the heat exchanger (m)
C	Thermal capacity in the SCW model (J/K)
D	Height difference (m)
D_e	Equivalent diameter (m)
D_i	Inside diameter (m)
F	Friction factor (-)
G	Mass velocity for the heat exchanger head loss model ($kg.h^{-1}$)
g	Gravitational acceleration ($m.s^{-2}$)
I	Impression (m) – refers to the level elevation in the injection well
K	Hydraulic conductivity (m/s)
L	Length (m)
l	Head loss (m)
LR	Leakage Rate ($L.s^{-1}.m^{-2}$)
$\dot{m}$	Flow rate (kg/hr)
n	Number of nodes in the SCW model (-)
P	Power (kW)
Δp	Head loss (kPa)
Q	Heat transfer (kW)
V	Volume (m^3)
V	Speed of the fluid in head loss calculation ($m.s^{-1}$)

r	Borehole radius (m)
R	Thermal Resistance in the SCW model (K/W)
Re	Reynolds number (-)
RR	Relative roughness (-)
S	Drawdown (m) – refers to the decrease of level in the SCW
S_s	Specific storage (m^{-1})
T	Temperature (˚C)
t	Time (s)
W	Effective plate width – for the heat exchanger (m)
W_c	Compressor Power (kW)
z	Height (m)

Greek Letter

α	Coefficient referring to the kind of land around the building in infiltration modelling (-)
δ	Layer thickness in infiltration modelling (m)
ε	Roughness (mm)
η	Efficiency (-)
μ	Dynamic viscosity (Pa.s)
ρ	Density ($kg.m^{-3}$)
υ	Kinematic viscosity ($m^2.s^{-1}$)

List of indexes

air	Refers to the airflow in ventilation or heating system
bldg	Refers to the building
bleedinjectionpipe	Refers to the bleed injection pipe
cool	Refers to cooling mode
drawdown	Refers to the drawdown or diminution of the water level in the SCW
env	Refers to the envelope of the building
fan	Refers to the fan used in the HVAC system
freshair	Refers to the outdoor fresh air needed in the building
heat	Refers to heating mode
HX	Refers to the plate heat exchanger
in	Inlet (temperature, flow rate, etc.)
inj	Refers to the injection well
j	Refers to the node index in SCW model
k	Refers to the neighbouring node index in SCW model
loop	Refers to the building loop
motor	Refers to the motor of the submersible pump
out	Outlet (temperature, flow rate, etc.)
pipe	Refers to the pipes in the ground loop head loss calculation
pump	Refers to the submersible pump
risingpipe	Refers to the pipes that pump the groundwater out of the SCW
reinjectionpipe	Refers to the pipes that returns the groundwater back to the SCW
sing	Refers to the singular head losses

tot	Refers to the total head losses
weather	Refers to the weather file data in infiltration modelling
zone	Refers to the building zones

LIST OF APPENDICES

CHAPTER 1 INTRODUCTION

Global warming, energy transition and environmental crisis are expressions invading more and more our everyday life through news and social media. A sustainable development of our society will necessarily pass through an increased awareness of the world population, with political and governmental decisions, but also by research works that support the technical and innovative needs of our society, in a way that is respectful of our planet.

One of the main challenges of our society is to achieve a smooth energy transition by reducing fossil fuels consumption and greenhouse gas emissions. In Canada, the residential and commercial sectors consume respectively 34% and 24% of the electricity produced nationwide (RNCan., 2018). In the residential sector, energy is primarily used for space heating (61%), followed by water heating (19%) and cooling (3%), among others (RNCan., 2016a). This means that heating and cooling represent 83% of the energy used in the residential sector. By comparison, heating and cooling represent 69% of the energy needs in the commercial sector (RNCan., 2016b). The European commission reported in 2016 that 50% of the annual energy used in Europe was used for heating and cooling (Commission Européenne, 2016).

When implementing a long-term energy efficiency project, the use of geothermal energy may be a solution to reduce the energy consumption of buildings. For space heating and cooling, low temperature geoexchange is an efficient and environmentally friendly solution. Indeed, ground-source heat pumps (GSHPs) can efficiently provide heating and cooling since they benefit, beyond a certain depth, from a relatively constant ground temperature all year long. Their interest stands in their efficiency that is approximately three times higher than conventional electrical boilers. For example, when an electrical boiler provides one unit of heat, it uses one unit of electricity. By comparison, a GSHP system can provide around three units of heat for one unit of electricity. This high energy efficiency explains why the energy provided by geothermal heat pumps worldwide has increased by 63% and by 41% for space heating alone between 2010 and 2015 (Lund et al., 2016).

Low temperature geoexchange relies on several types of ground heat exchangers (GHEs). The most frequent GHE is the so-called closed-loop borehole as illustrated in Figure 1.1 a). This type of GHE relies on a ground loop installed in a borehole usually filled with a bentonite-based grout. A heat carrier fluid then exchanges energy with the surrounding soil and transmits it to heat pumps used for space heating or cooling. Closed-loop systems are the most widely used GHEs in practice and

benefit from a relatively strong expertise. Although the thermal efficiency of closed-loop GHEs is interesting, their construction cost, especially for well drilling, is an impediment to their democratization and wide use in the society. Indeed, the higher construction cost of closed-loop GHEs by comparison to more conventional heating and cooling systems leads to long investment payback periods that discourage their use in practice.

By comparison, open-loop systems use groundwater extracted from a nearby aquifer through a series of pumping and injection wells. The groundwater movement in the aquifer between the injection and abstraction wells allows a significant heat exchange with the soils or rocks located between the wells. To operate, open-loop systems require a large lot and specific hydrogeological conditions, such as a productive aquifer. Unfortunately, such conditions are not frequent in dense urban areas, which limits the areas where open-loop systems can be installed.

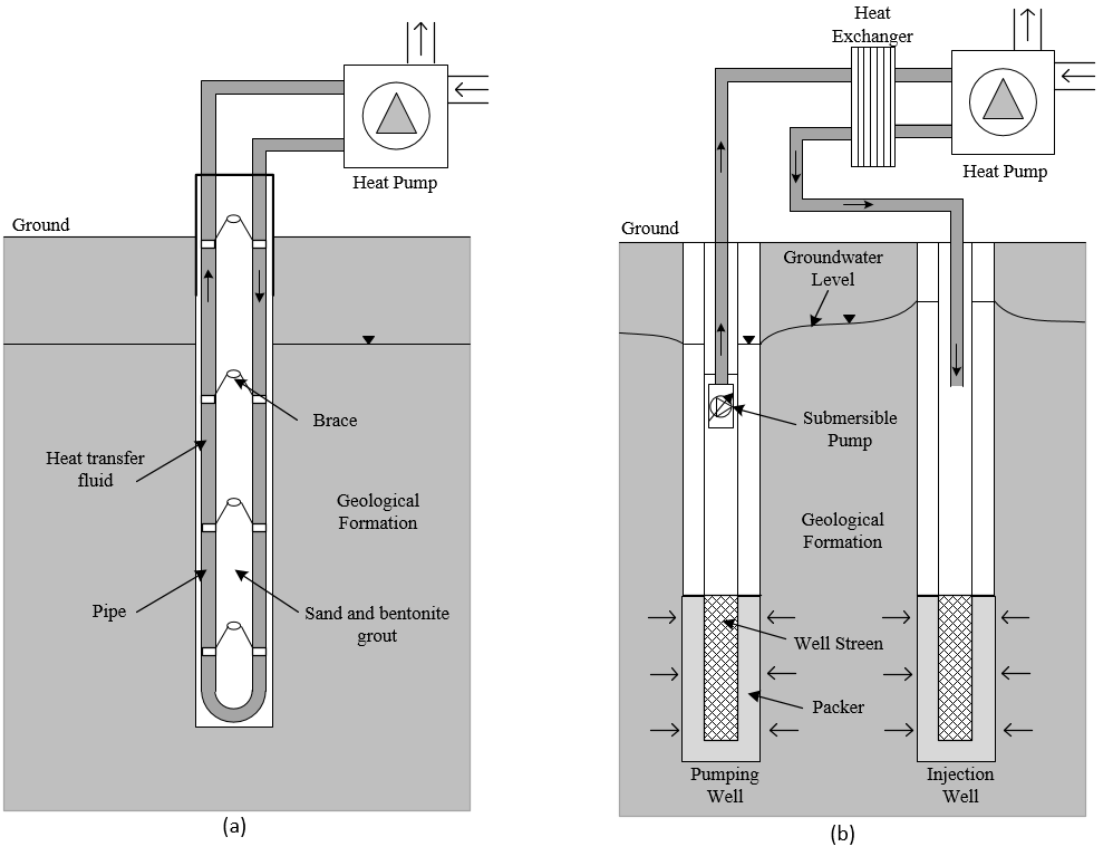

Figure 1.1: Layout of a closed-loop (a) and open-loop (b) ground heat exchanger

There is an alternative between closed- and open-loop systems called standing column wells (SCWs). In a SCW, groundwater is pumped from the base of a deep well and directed to a heat exchanger. Most of the water is then returned at the top of the SCW, while a smaller fraction is diverted, or "bled" to a nearby injection well. By comparison to conventional closed-loop systems, SCWs can lead to significant capital cost savings. According to Deng O'Neill et al. (2006), for a similar installed thermal power, SCWs can reach construction costs reductions between 49% and 78%. A 9-year monitoring study in the United States showed that a SCW system was able to generate energy savings of more than 685,000 kWh per year for a 200-ton installation with six 455m deep SCW in a relatively cold climate (Orio et al., 2006). The potential of SCWs lies in their capacity of being installed in dense urban areas or in historic districts where a lack of land area is an obstacle to the installation of a wide closed-loop system (Pasquier et al., 2016). This has been revealed lately with the retrofit of the St Patrick's cathedral in New York city for which a ground-coupled heat pump system using SCWs has been installed. Another advantage of SCWs is their ability to operate efficiently in rocky geological formations having a low permeability, where an open-loop system would not be a viable option. Despite a significant potential, SCWs are not widely used outside the north-east of the United States. This is mainly due to a lack of demonstration projects and technical expertise outside the geographical areas where SCWs initially appeared.

When integrating a SCW to a building heating and cooling system, a building loop links the decentralized heat pumps, auxiliary systems, circulating pumps and heat exchangers together. In such a configuration, the heat exchanger links the building and the groundwater loop together. The auxiliary systems ensure that the GSHPs operate at the correct temperature and is a key feature for systems using groundwater and operating in cold climates since they prevent freezing of the groundwater in the heat exchanger. In addition, reducing the groundwater volume discharged to the injection is desirable as it prevents clogging of the injection well. Although a few different control strategies are used in practice, there is no clear guidelines for the control of a SCW connected to an injection well and operating in cold climates.

1.1 Objectives

The aim of this research work is to identify control strategies adapted to SCW operating in a cold climate and to provide guidelines to reduce overall energy consumption, electrical peak power demand and total groundwater volume discharged ("bled") to the injection well. More specifically, this work seeks the following four specific objectives:

1. Objective 1 is to develop a detailed model of a typical office building in a cold climate, including a Heating, Ventilating and Air-Conditioning (HVAC) system based on distributed heat pumps supplied by a building loop, and to couple that model to an existing detailed model of the SCW.
2. Objective 2 is to identify the parameters involved in pumping energy consumption and to implement a code that computes head loss in the ground loop for different temperatures, flow rates, and pumping configurations.
3. Objective 3 is to develop and assess pumping control strategies, investigating the system temperatures and annual performance. The performance should be assessed in terms of energy, peak demand, and operating costs, and the annual volume of groundwater bled should be included in the overall assessment.
4. Objective 4 is to develop and assess control strategies for the bleed flow rate in order to use this feature more efficiently. Again, performance should be assessed by energy, peak demand, operating costs, and volume of groundwater bled.
5. Objective 5 is to assess the impact of building-related controls (zone heating and cooling setpoint profiles, and auxiliary heating setpoint) on the overall SCW system performance and to make recommendations for the efficient operation of the entire system.

1.2 Master Thesis Outline

This research work is organized as follows. After the present introduction, a literature review focusing on the research work accomplished so far on SCWs will be presented in Chapter 2. Then, Chapter 3 will present the methodology used to build an integrated simulation model in the TRNSYS and Matlab environments. Chapter 4 will present an analysis on the head loss in the

ground loop for three pumping configurations and its impact on pumping power for different temperatures, flow rates and bleed scenarios. The following three chapters will present and discuss the results obtained on the control strategies for the pumping flow rates (Chapter 5), the bleed flow rates (Chapter 6), and for the building setpoint temperatures (Chapter 7). This last chapter also includes an assessment of the overall system operation under all investigated control strategies. Finally, the last chapter will conclude this research work and propose some recommendations to simplify the design of SCW systems.

CHAPTER 2 LITERATURE REVIEW

This chapter presents some research works accomplished on SCWs that are currently available in the literature. To allow the reader to understand the operation of a SCW system, the first section will describe the features and parameters affecting the efficiency and operation of a SCW. The chapter will continue with a section on the different models developed over the years for simulating the thermal and hydraulic behaviour of SCWs. Then, some data on existing installations will be presented to illustrate the potential of SCWs for covering building cooling and heating demand. In the fourth section, the chapter will focus on describing how the bleed of a SCW impacts its thermal efficiency. Finally, the chapter ends with a summary of the key learning points from this literature review.

2.1 Standing Column Wells

A SCW consists of a long borehole mostly drilled in the bedrock and filled with groundwater as shown in Figure 2.1. Typical installations use a PVC pipe almost as long as the well within which a submersible pump is installed. In a conventional SCW, groundwater is pumped at the bottom of the well through a PVC pipe and returned below the dynamic level in the annular space of the borehole via a rejection pipe. As some soils might be unstable near the surface, a steel casing is installed to prevent the unconsolidated material to fall into the SCW.

Before reinjecting the groundwater into the SCW, part of the flow rate can be diverted into a separate injection well. This process is called “bleed” and improves the system performance by attracting water from the undisturbed neighbouring ground through aquifer fractures. The bleed induces heat transfer by advection within the borehole, which improves significantly the thermal efficiency of the SCW. The bleed fraction is dictated by local practices or by the ground hydraulic conductivity and is usually in the order of 5% to 25% of the total pumping flow rate (Pasquier et al., 2016). This means that 95% to 75% of the well flow rate is reinjected directly in the SCW, while the remaining flow rate is diverted to a nearby sewer, river or injection well. The injection well shown in Figure 2.1 is not always present, but is mandatory in some jurisdictions which require to reinject the bleed water to its original aquifer. An example of such a jurisdiction is the Province

of Québec, and a recent experimental installation close to Montréal is for example equipped with an injection well representing half the length of the SCW (Beaudry et al., 2018).

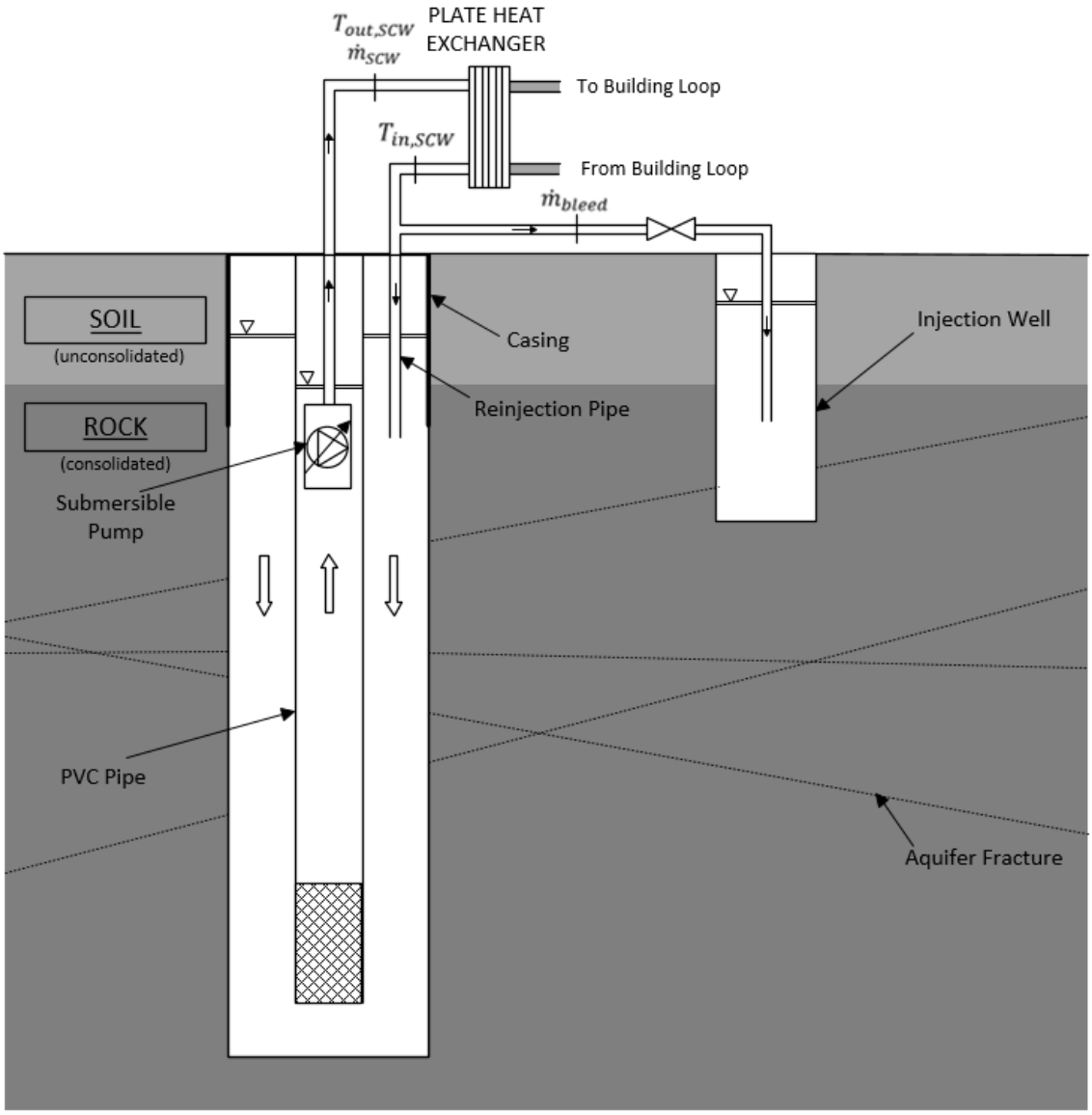

Figure 2.1: Illustration of a standing column well installation

SCWs are halfway between closed-loop and open-loop systems. When operating without bleed, SCWs are similar to closed loop boreholes, but with the advantage of a direct heat exchange with the rock surrounding the borehole and a relatively small borehole resistance. On the other hand, when a SCW bleeds a fraction of the total pumping flow rate, it is more similar to an open-loop

system since part of the pumped water comes from the surrounding aquifer, which allows heat transfer in advection mode in the surrounding ground.

In some locations where groundwater can cause fouling and scaling of the heat exchangers, a plate heat exchanger is added between the groundwater loop and the building loop to prevent groundwater from flowing through the heat pumps (Beaudry et al., 2018). Besides, the operation of the SCW will modify the ground temperature, which may lead to scaling or to bacteria growth in the SCW or system components (Pasquier et al., 2016). In some situations, the SCW can also supply domestic water to the building (Spitler et al., 2002) and this may be authorized only if the minimum water quality requirements are met for a year-round operation. To insure water quality, some installations integrate a water treatment unit such as the experimental installation described in Beaudry et al. (2018).

Several parameters can modify the response of a SCW. Spitler et al. (2002) led a parametric study on SCWs that reports the main parameters that influences SCW system performance. It appears that within all the parameters tested, the most sensitive were the bleed rate, borehole length, ground thermal conductivity and hydraulic conductivity. Some other parameters such as borehole diameter, casing depth and wall roughness were identified to have a less significant effect on the convective heat transfer and the SCW overall performance.

2.2 Simulation Models of Standing Column Wells

A model is a mathematical representation of the real situation usually used to plan, study and design systems. SCWs are a modelling challenge because of the coupled thermal and hydraulic response of the well. For SCWs modelling, the literature shows different levels of sophistication from analytical to numerical approaches. The following section describes some of these models.

2.2.1 Analytical Models

The first analytical model of SCWs was proposed by Oliver et al. (1981). The model was limited to steady-state radial heat flow and only considered conduction heat transfer. The model solved the conservation of energy equation for a control volume including the water in the SCW and surrounding ground. The model was limited to steady-state and underestimated the heat transferred

from or to the ground, and was not able to integrate the benefits brought by the activation of the bleed and the corresponding advective heat transfer.

Orio (1994) developed another model to simulate the transient temperature response in a SCW based on the Kelvin line theory. The research included a comparison with the results provided by the model of Oliver et al. (1981) and showed a difference of less than one degree Celsius between the two models.

Analytical models are easy to implement and use, but these models do not account for the effect of bleed and groundwater flow, which limits their use since bleed is an important feature for the efficiency of SCWs. In fact, the advective heat transfer induced by the bleed leads to a coupled problem, which makes difficult the use of analytical solutions for transient simulations. In addition, analytical models do not consider the residence time of the groundwater in the SCW and its thermal capacity, two features helping the operation of SCWs in cold climates.

2.2.2 Numerical Models

Numerical approaches can be used to model SCWs and get around the analytical model drawbacks. Indeed, numerical models combine and solve equations describing heat transfer and groundwater flow within the well and surrounding aquifer. Yuill et al. (1995) developed a quasi-two-dimensional (radial-axial) model converting the governing equations into finite difference equations. The model introduced an equivalent thermal conductivity term to consider the higher heat transfer induced by vertical groundwater flow in the well but neglected the advective heat transfer in the aquifer caused by the bleed. Their model assumes a steady-state solution for the hydraulic head in the well. The model was able to compute radial heat transfer at specific depths but is not a full two-dimensional model.

More recent SCW numerical models solve the advection-diffusion equation for heat transfer and the continuity equation for groundwater flow. The solution of the resulting system of partial differential equations is usually solved by the finite element method (Abu-Nada et al., 2008; Croteau, 2011; Nguyen et al., 2012) or finite volume method (Ng et al, 2011; Rees et al., 2004). It is worth noting that finite element models coupling thermal, hydraulic and chemical processes have been used to locate and mitigate scaling problems in SCWs by Eppner et al. (2017a, 2017b).

Numerical models can integrate complex boundary conditions and geometries and can provide efficient and accurate results. However, this is usually achieved at the cost of a significant computation time that limit their use in practice.

2.2.3 Thermal Resistance and Capacity Models

Thermal Resistance and Capacity Models (TRCM) are a good compromise between analytical and numerical models in terms of accuracy and computational time. In this category, Deng (2004) first proposed a 2D axisymmetric model of SCWs integrating a bleed flow rate. Due to the intensive computational time of this model, a simplified 1D axisymmetric model was also developed and integrated to the TRNSYS environment.

More recently, Nguyen et al. (2013, 2015a) developed a 2D axisymmetric TRCM integrating the groundwater movement in the SCW and surrounding ground and fracture flow (Nguyen et al., 2015b). A Haar wavelet solver was also proposed by Nguyen et al. (2015c) to reduce the computation time. The TRCM proposed by Nguyen was evaluated by comparing a finite element model and the TRCM. The comparison showed mean absolute error for the entering water temperature (EWT) and leaving water temperature (LWT) of 0.05 ˚C, which is deemed more than acceptable for HVAC applications. Since the TRCM developed by Nguyen et al. will be used in this work, a more complete description of the simulation model will be presented in Chapter 3.

2.3 Installations and Operational Data

Throughout this literature review, information about different facilities installed with SCWs were collected and compared to figure out what are the common practices for this kind of ground-source heat pump system. Gathering this information will help setting the industry practices and habits for the operation of SCWs and identify some design parameters, such as flow rates, borehole length, control sequences, etc.

The main source of information comes from Spitler et al. (2002) who performed a study on SCWs sponsored by ASHRAE. Their report summarizes the results of a questionnaire sent to contractors and drillers in the US North-East. The information covers 21 locations (eleven residences and ten commercial/school buildings) representing a total of 34 wells. All the installations have the common point of being heating dominated.

2.3.1 Capacity and Sizing

In this first section, we gathered information about SCWs system capacity and length from different sources and summed them up in Table 2.1. The typical capacity to length ratio for SCWs system is from 175 W/m to 250 W/m. By comparison, closed-loop systems usually show values of 75 W/m to 120 W/m. The strength of SCWs systems stands in that difference, their thermal performance is 2 to 3 times higher compared to closed-loop systems and leads to a smaller borehole length that lowers the construction costs (which is usually a drawback for geothermal installations).

We also observe that the length of the boreholes increases with the capacity of the system. Common closed-loop systems are implemented with 150 m deep boreholes. In the case of SCW system the average length is 158 m for residential buildings and 377 m for commercial ones. McGowan (2018) and Orio et al. (2006) report boreholes up to 500 m deep. SCW systems often have fewer deeper boreholes than closed-loop systems, the maximum depth being limited by drilling capacity and drilling costs.

Table 2.1: Summary of the data collected on SCWs systems. (The parentheses contain the range reported in the questionnaire.)

	Installed Capacity (kW)	**Well Depth (m)**	**Capacity/Depth (W/m)**	**Static Water Level (m)**
Residential*	27.1 (17.6-52.8)	158 (73–274)	196 (136–359)	14.6 (0.9-36.6)
Commercial*	200.6 (35.2-352)	377(183-457)	236 (176–385)	6.1 (4.9-12.2)
Cathedral NYC**	880	502.9	175	\
Public School ***	704	455	258	\

* Source : (Spitler et al., 2002); ** Source : (McGowan, 2018); *** Source : (Orio et al., 2006)

2.3.2 Pumping flow rate

The work of Spitler et al. (2002) indicates that conventional submersible pumps can provide circulation flow rate corresponding to 3 GPM per ton of heating or cooling capacity

(0.054 L s^{-1} kW^{-1}). This flow rate value is also recommended and used in Orio et al. (2006) and is deemed as a conservative design criterion (Orio et al., 2014). Some installations have provided additional operating data, such as the Maine Audubon visitor's centre which used a pumping flow rate of 2.7 GPM/ton, while the residence Raymond uses a 2.97 GPM/ton flow rate (Spitler et al., 2002). The pumping power in all facilities is between 0.1 to 0.3 HP per ton, which corresponds to 73.6 W/ton to 220.8 W/ton (21 to 65 W/kW, i.e. W of pumping power per kW of heating or cooling capacity).

Cho et al. (2016) conducted two experiments on their deep geothermal SCW with two pumping flow rates of 70 L/min and 50 L/min, which corresponds in their case to 3.7 GPM/ton and 2.6 GPM/ton. Those pumping flow rates induce respectively a pumping power of 2.5 kW and 1.75 kW for the submersible pump (corresponding to 140 and 100 W/kW respectively). In their exploratory paper for the development and validation of a SCW model, Nguyen et al. (2013) used flow rates of 2.9 GPM/ton and 1.75 GPM/ton.

The information found on pumping flow rates indicates a recommended good practice around 3 GPM/ton for SCW operation, which will be the value used by the reference scenario in this work.

While the flow rate is usually reported for case studies and research investigations found in the literature, no systematic study of the impact of the flow rate on the SCW performance was found.

2.3.3 Case Studies Presenting Operating Data

Massachusetts school

The operation of a SCW system over a ten-year period in a public middle school in Massachusetts was reported by Orio et al. (2006). The building, of 6 700 m^2 floor area, is fully heated and cooled via the geothermal system connected to twenty water to water heat pumps, each having a nominal capacity of 10 tons (35 kW). The system started to operate in 1996. At that time the technology of submersible pumps was limited, and the submersible pump was operated continuously. To ensure no thermal interference, the wells were separated by 23 m. Thanks to this installation, the energy needed for heating was decreased by a factor of five while maintaining an outlet temperature of the wells above 4.4 °C in winter and below 26 °C in summer.

New Hampshire nursing home

Orio et al. (2014) described the operation of a nursing home in New Hampshire over a ten-year period. The building covers an area of 23,600 m^2 and its energy needs are mostly dominated by heating. The system has a capacity of 615 tons (2160 kW) through 236 heat pumps. It was decided to have small units for each zone to prevent viruses/bacterias transfer between patient rooms. The facility has 18 boreholes of a depth of 115 m and separated by distance of 15 m to 23 m. The operation of the system was able to maintain temperatures at the outlet of the SCW between 10 °C and 22 °C. Unlike most systems found in the literature, this design does not include a heat exchanger, and the groundwater flows directly on the source side of the heat pumps.

Residence Raymond

A summary of the information gathered by Spitler et al. (2002) is shown in Table 2.1. Some facilities gave additional information, for instance the residence Raymond specified that their system is designed with a 25% safety margin. They drilled one Standing Column Well of 213 m depth and their annual bleed volume is 340 m^3 when operating under a 4.8% bleed rate.

Deep Geothermal Well in Korea

Cho et al. (2016) describe an experimental SCW installation using a deep geothermal well (2383 m) with a diameter of 40 cm for the first kilometre and then a diameter of 20 cm for the lower part of the SCW. For this experimental installation, the submersible pump was designed to provide a maximum flow rate of 400 L/min with a power of almost 30 kW. The ground loop is connected to a 5-ton (17.6 kW) heat pump through a plate heat exchanger. The water-to-water heat pump provides heating to a thermal storage tank of 200 L, which is itself connected to a fan coil unit of 14.5 kW. The aim of this project was to heat a greenhouse with a ground source heat pump and compare the construction cost, operation cost and return on investment with an alternative diesel installation for three types of greenhouses. The payback time was found to be between 6 and 9 years.

In the scope of their research project, Cho et al. (2016) also conducted two experiments with different pumping flow rates and setpoint temperatures for the fan coil unit. Their results indicated a heat pump coefficient of performance (COP) of 5.5 and 5.8, which is possible because the outlet

temperature of their deep SCW is close to 40 °C. Computing the overall COP of the system, considering the energy needed for pumping groundwater, the COPs dropped to 3.1 and 3.6. The authors mentioned that if the submersible pump operation was optimized, higher COPs would be possible.

2.4 Bleed Application

As explained in section 2.1, bleed is a special characteristic of SCW and allows attracting groundwater into the well through ground fractures. This groundwater flow induced by bleed comes from the surrounding ground with a temperature closer to the undisturbed temperature of the aquifer. This feature helps increasing the borehole temperature during the peak heating period (or decrease it in peak cooling period) which leads to a higher system efficiency.

The operational parameters of SCWs vary with the geological and hydrogeological conditions. The bleed rate (or bleed ratio), expressing the ratio between the bleed flow rate and the (total) pumping flow rate, is usually between 5 and 25% (Spitler et al., 2002). All examples found in the literature use a constant pumping flow rate, but recent advances in variable-speed submersible pumps make it an interesting option, which will be considered in this work. This will require a redefinition of the bleed rate, which will be expressed as the ratio between the bleed flow rate and the maximum pumping flow rate (as opposed to the ratio between the bleed flow rate and the current flow rate).

Bleed is a key feature for SCW as shown by Spitler et al. (2002) in a parametric study. The results showed that the main parameters that influences SCW installations design and performance are: bleed rate, borehole length, rock thermal conductivity and hydraulic conductivity, in this specific order. Furthermore, the study also illustrated that the influence of bleed rate decreases the sensitivity of the borehole length. It is important to note that the bleed capacity of a borehole is directly related to the hydraulic conductivity of the aquifer in the vicinity of the SCW.

Spitler et al. (2002) also observe that the performance of SCWs improves when using bleed in the well operation, with diminishing returns over a 10% bleed rate. However, it is also mentioned that higher bleed rates may be interesting to implement during peak heating or cooling period. Bleed is always beneficial for the thermal performance of SCW systems (Pasquier et al, 2016), but also comes with drawbacks, as discussed in the next section.

2.4.1 Bleed Impacts and Issues

Using bleed during well operation shows great advantages but there are also some drawbacks that need to be understood. To begin, when a part of the pumping flow rate is diverted from the SCW, it induces a drawdown in the SCW and a water level rise in the injection well. The submersible pump has to overcome the level difference and its energy consumption has to be studied as bleed modifies the head loss in the ground loop. Rees et al. (2004) showed that increasing bleed rate with low water table level could lead to a smaller system overall efficiency due to the pumping energy needed. Rees et al. (2004) studied two cases of water table level: 5 m and 30 m. After computing energy costs, it appears that the difference observed is three times higher at a bleed rate of 20% than a bleed rate of 2.5%.

The system also has to be carefully controlled to maintain the submersible pump under the water level – the SCW cannot be operated at all if that condition is not met. If the system includes an injection well, the drawdown in the SCW also means an elevation of the injection well level. It is important to prevent overflowing the injection well, especially in a cold climate since the water flowing on the ground surface could rapidly freeze.

Furthermore, depending on the geological conditions, bleed may lead to fracture clogging on the long-term use. Those fractures are essential to dissipate in the injection well the bleed flow rate. It is interesting to limit bleed to preserve the SCW system efficiency as high as possible during its lifetime. the necessary permits may also be easier to obtain from the responsible authorities when a smaller amount of groundwater is bled. For example, in Québec, if the volume of water bled is more than 75 m^3 per day, the project needs specific environmental authorization.

To conclude, studying bleed control strategies for SCW systems seems required.

2.4.2 Control Strategies for Bleed

The previous section revealed an interest in studying control strategies for SCW in order to use bleed wisely. This section aims at gathering the bleed control strategies known and found in the literature.

Dead-Band Control

Most of the control strategies implement a constant 10% bleed rate (Spitler et al., 2002) with an ON-OFF control (i.e. the bleed rate is either 10% or there is no bleed). The first strategy identified is a dead-band control with different temperature thresholds on the heat pump entering water temperature for winter and summer. When the heat pump entering water temperature (EWT) is lower than 5.83 °C, bleed starts until the temperature increases again over 8.6 °C for the winter design. For the summer period, bleed starts when the temperature entering the heat pump is over 29.2 °C and stops when it falls below 26.4 °C. The dead-band control is also used by Deng O'Neill et al. (2006), but it is applied to the SCW outlet temperature, with different thresholds: in winter, bleed starts when the temperature coming back from the well is under 8 °C and stops when it is over 10.8 °C.

In Spitler et al. (2002), the system considered does not implement a plate heat exchanger between the ground heat exchanger and the building heat pumps. In that case, the entering water temperature to the heat pump is equal to the outlet temperature of the SCW.

Temperature Difference

Spitler et al. (2002) shows the implementation of another kind of control based on the temperature difference between the inlet and outlet temperature of the well, which also corresponds to the inlet and outlet temperature of the heat pump if the system uses groundwater directly on the source side of the heat pump. In that case, bleed starts when the temperature difference is under 5.6 °C. This threshold value was set to lead to the same amount of groundwater bled volume while operating under temperature difference control compared to the dead-band control. It appears that the temperature difference strategy led to a slightly higher minimum temperature when simulating the system for January and February.

Spitler et al. (2002) implements four simulations: no bleed, the dead-band and temperature difference control strategies, and a 10% continuous bleed. For the first case, the heat pump entering water temperature reaches a minimum value of 2 °C, which means that the SCW will experience temperature under the freezing point. When bleed is implemented, the well is always operating above the freezing point. The constant bleed rate shows the best thermal performance, without taking into account any technical or legal constraints restricting the volume of water bled.

Other Control Strategies

Most other articles refer to a continuous 10% bleed (Ng et al., 2011) or to simple controls with a threshold but no dead-band. For example, the bleed implementation is specified in Deng et al. (2005) where bleed starts when the outlet temperature of the SCW goes under 4.4 °C for a 30-minute cycle before reconsidering if bleed has to stop or remain regarding the new outlet temperature value. In that article, there is no bleed control during the summer operation. The bleed control specification is provided for the model validation with bleed. Orio et al. (2006) use an emergency bleed when the outlet temperature goes under 5.6 °C, and no bleed control is implemented during the summer period.

An eight-year operation study in the north of New Hampshire (Orio et al., 2014) on a nursing home installed with a geothermal system reports that the bleed rate was adapted from 10% to 5% because analyses showed that the bleed of 16 SCWs would produce a groundwater volume too important for the capacity of the selected absorption pond. The automated bleed rate starts when the inlet temperature to the heat pump goes outside of its operative temperature limits (10 °C to 24 °C). It is interesting to note that the control implemented has never been used since the system start up, although the bleed was used manually for periodic maintenance. The state of New Hampshire asks commercial buildings to keep track of the water volume bled, which illustrates the interest of modelling tools which assess the volume of water bled as well as the thermal performance of SCW systems.

Three-Level Bleed Controls

A 3-level bleed control strategy with an ON-OFF sequence for the heat pumps is proposed, in Nguyen et al. (2012, 2013), with different thresholds and maximum bleed rates. The strategy simulated by Nguyen et al. (2012) is illustrated in Figure 2.2. Bleed rates of 10, 20 and 30% starts with three different temperatures thresholds respectively at 7, 6, and 5 °C are reached. When the SCW cannot cover the building needs and the temperature still drop while a maximum bleed rate is operated then, at a setpoint of 4 °C, the ON-OFF sequence starts, and auxiliary heating is used. The ON-OFF sequence consists of the shut down of heat pumps every 10 minutes until the temperature in the well returns above the 4 °C limit.

In the second article (Nguyen et al., 2013), the authors simulated four cases without bleed control and without ON-OFF sequences and a case that combines bleed control and ON-OFF sequences. This combination is shown to be an interesting option to maintain the heat pump operating temperatures in their optimal range.

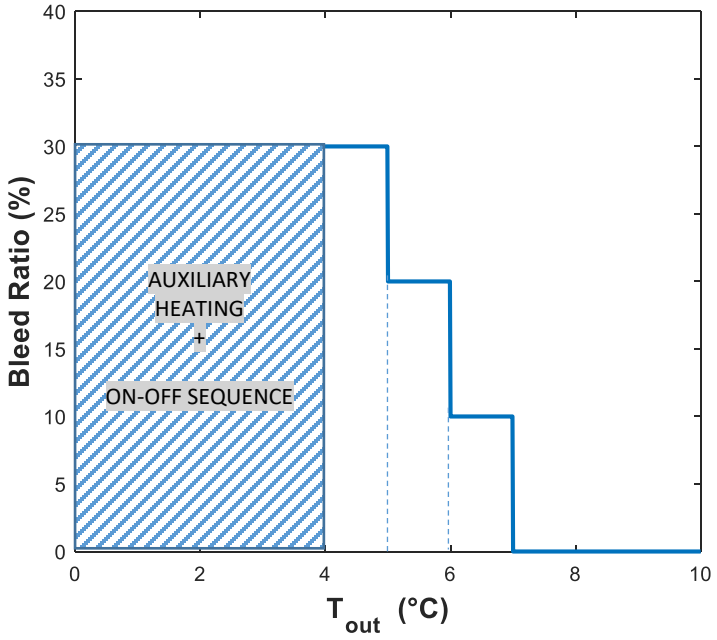

Figure 2.2: Three level bleed control and ON-OFF sequence

To conclude, most of the control strategies found in the literature implement a constant bleed rate of 10%. More advanced strategies are all temperature-dependent, and rarely include bleed rates above 10%, although several authors mention that higher bleed rates can be useful during peak heating or cooling periods (Pasquier et al., 2016 ; Spitler et al., 2002,). Pasquier et al. (2016) mention the absence of studies investigating predictive control for SCW bleed rate, and our literature survey did not find such studies.

2.5 Summary

In conclusion, SCW systems are an interesting alternative to closed-loop systems as they show higher thermal performance and lower construction costs. Moreover, their implementation in dense

urban areas is possible, where the installation of a wide field of closed-loop boreholes would be challenging or impossible.

On one hand, the lack of expertise outside of the US explains why their wide adoption is still not common in other parts of the world. The lack of design tools and models is also an obstacle to their widespread use.

A SCW system comes with different and multiple parameters that influence the system overall efficiency. The most important parameter found through this literature review is the bleed flow rate as it helps the well by inducing a groundwater flow that has a more suitable temperature.

The published literature shows a consensus to recommend a pumping flow rate of 3 GPM/ton (0.054 L s^{-1} kW^{-1}), but no detailed investigation of the optimal flow rate was found. The market availability of variable-speed submersible pumps also opens the door to more sophisticated control strategies which need to be investigated. The literature shows more studies on bleed flow rate control, but is restricted to relatively simple strategies which do not focus on cold climate operation and/or pay no attention to the amount of groundwater bled during SCW operation. This confirms the interest of addressing the objectives presented in Chapter 1.

CHAPTER 3 SYSTEM MODELLING: BUILDING, HVAC AND GROUND LOOP

This chapter describes the methodology used to construct a building model and the heating and cooling system connected to a SCW. The system studied in this chapter is illustrated in Figure 3.1 and will be used throughout this work and represents a medium office of three floors and composed of fifteen thermal zones. Each thermal zone is served by a decentralized water-to-air heat pump (which could represent several heat pumps operating in parallel). The source side of each heat pump is connected to a building loop filled with a water/glycol solution. Each heat pump is controlled by a thermostat located in the zone, with a setpoint profile that is presented in this chapter and discussed in chapter 7.

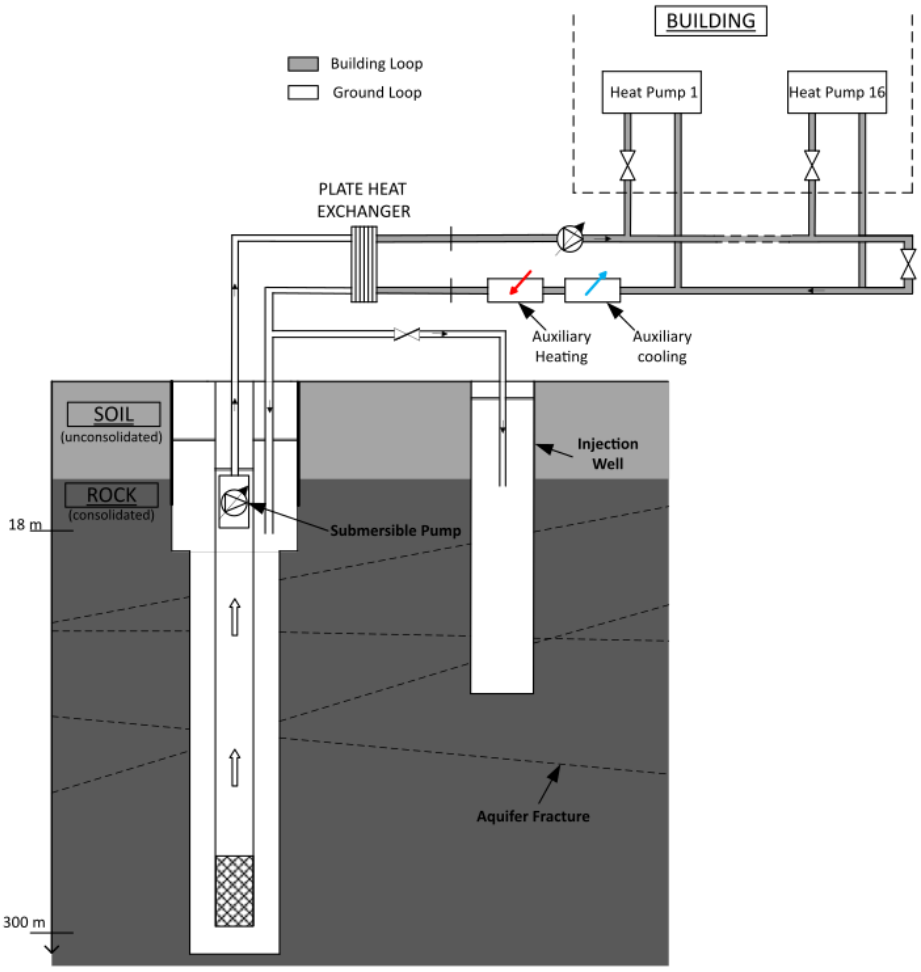

Figure 3.1: System simulated

The building loop is connected to the ground loop through a plate heat exchanger. It includes a circulating pump and auxiliary heating and cooling devices located at the inlet of the load side of the plate heat exchanger. This configuration aims at maintaining the SCWs inlet temperature within the operative limits.

The building and HVAC system up to the plate heat exchanger are modelled in TRNSYS (Klein, 2018), while the SCW is modelled in Matlab (The MathWorks, 2017a), which is linked to TRNSYS through a dedicated component known as Type 155.

3.1 The Building

3.1.1 Geometry

A medium three-storey office is modelled in TRNSYS using the 3D Sketchup plugin and the TRNBuild interface. The building is based on the "Medium Office" archetype included in the U.S. Department of Energy Prototype Buildings (USDOE-BTO, 2017), with performance data adapted according to the Canadian National Energy Code for Buildings, NECB (CNRC, 2011). The simulation uses a typical weather file for Montreal, QC (Environnement Canada, 2016).

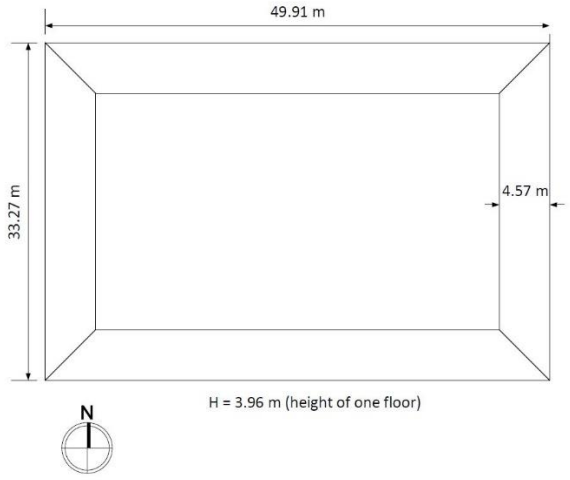

Figure 3.2: Building dimensions

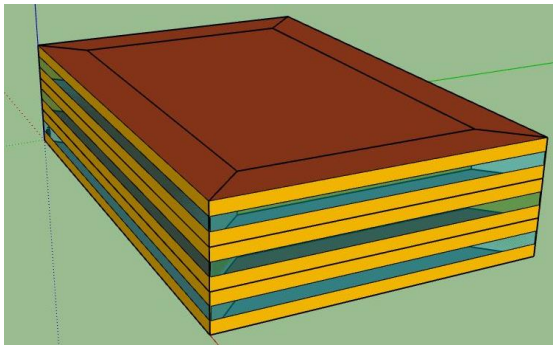

Figure 3.3 : 3D view of the building

Figure 3.2 and Figure 3.3 give an idea of the global geometry of the building office we modelled here. The building has three floors and each one is divided in 4 perimeter zones and one core. The

geometry is implemented in SketchUp via the TRNSYS plugin. The .idf file is then imported in TRNBuild to set the rest of the building attributes (wall thermal properties, schedules, gains, etc.). Table 3.1 shows several general characteristics of the building.

Table 3.1: General values describing the medium office building

Floor area	**5000 m^2**
Aspect Ratio	1.5
Window-to-Wall Ratio	33%

3.1.2 Building Envelope

The building envelope is composed of different construction types which include five types of walls made of eleven layers and one type of windows. The construction types were set according to the DOE Archetypes from EnergyPlus (USDOE-BTO, 2017), but their thermal resistances (summed up in the next tables) were adjusted to match values recommended by the NECB 2011.

Table 3.2: Summary of the different walls, their layers and overall resistance

Wall name	Layers	U-Value ($W \cdot m^{-2} \cdot K^{-1}$)
External Wall	Gypsum board Exterior Wall Insulation Gypsum board Stucco	0.210
Roof	Metal Surface Roof Insulation Built up Roofing	0.163
Ground Floor	Carped Pad Ground Floor Insulation Concrete Floor	0.203
Adjacent Wall	Gypsum Board Air layer (wall) Gypsum Board	2.060
Adjacent Ceiling	Acoustic Ceiling Air Layer (plenum) Concrete Floor Carpet Pad	1.043

Table 3.3: Characteristics of massive layers

Layer's Name	Conductivity ($W \cdot m^{-1} \cdot K^{-1}$)	Capacity ($kJ \cdot kg^{-1} \cdot K^{-1}$)	Density ($kg \cdot m^{-3}$)
Gypsum Board	0.16	1.09	800
Stucco	0.72	0.84	1856
Metal Surface	45.2	0.50	7824
Built up Roofing	0.16	1.46	1120
Concrete Floor	2.31	0.83	2322
Acoustic Ceiling	0.057	1.34	288

Table 3.4: Characteristics of massless layers

Layer's Name	Resistance ($m^2 \cdot K \cdot W^{-1}$)
Exterior Wall Insulation	4.36
Roof Insulation	5.94
Carped Pad	0.22
Ground Floor Insulation	0.85
Air plenum	0.30
Air wall	0.15

The Medium Office archetype implemented in EnergyPlus includes a thermal zone representing the plenum above each floor. We chose to model the plenum as a layer of air within the ceiling construction type. Double-glazed windows with Argon, a low-emissivity film, and a "solar control" film is modelled. The center-of-glazing properties are a U-value of 2.16 $W \cdot m^{-2} \cdot K^{-1}$ and a solar heat gain coefficient (SHGC) of 20%. Insulated frames represent 15% of the window, with a U-value of 1.7 $W \cdot m^{-2} \cdot K^{-1}$ (all listed U-values include film coefficients).

3.1.3 Internal Gains

Three types of gains are modelled (occupants, lights, and equipment) by a nominal density (expressed in $W.m^{-2}$) which is modulated by a schedule. Nominal values are provided in Table 3.5. Schedules are shown in Figure 3.4 to Figure 3.6.

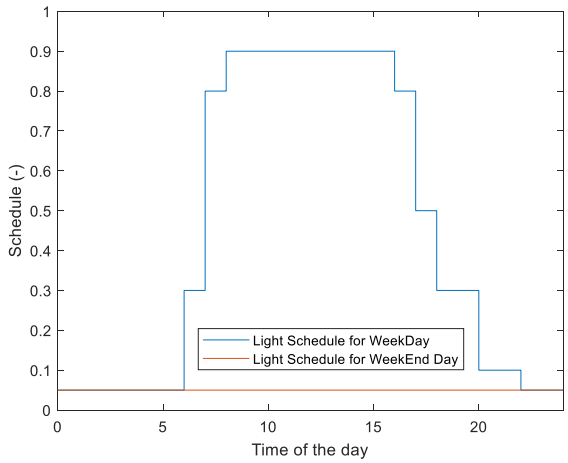

Figure 3.4: Schedule for light gains

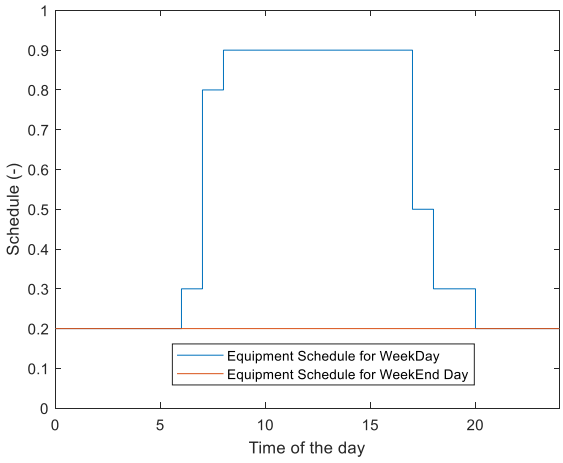

Figure 3.5: Schedule for equipment gains

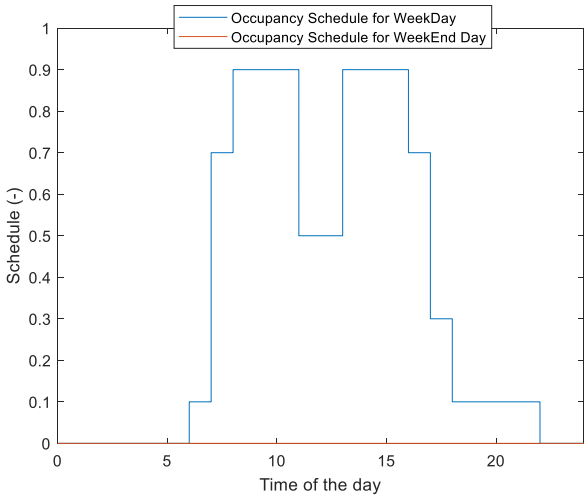

Figure 3.6: Schedule for occupancy from NECB 2011

Table 3.5: Internal gains

	Total Value	**Sensible, convective**		**Sensible, radiative**		**Latent**
	($W \cdot m^{-2}$)	**%**	**($W \cdot m^{-2}$)**	**%**	**($W \cdot m^{-2}$)**	**($W \cdot m^{-2}$)**
People	3.0	42	1.25	58	1.75	2.2
Light	9.7	30	1.5	70	6.8	-
Equipment	7.5	80	6	20	2.9	-

3.1.4 Infiltration

Infiltration refers to the air leakage that occurs through the building envelope as a result of pressure differences caused by wind and temperature differences (stack effect). A simple model recommended by Gowri (2009) is used to model wind-driven infiltration, neglecting stack effect. The model uses the Leakage Rate measured (or assumed) at 75 Pa, LR_{75}, as shown below:

$$LR = LR_{75} \times 0.112 \times 0.224 \times V \times f \tag{3.1}$$

$$f = (1 - 0.75 \times FanSchedule) \tag{3.2}$$

where V is the local wind speed, and f is a factor that reduces infiltration when the building fans are in service, assuming that the ventilation system is designed to slightly over-pressurize the building (hence reducing infiltration). $FanSchedule$ is a flag that is 1 when fans are ON, and 0 when they are OFF. A value of 9.14 L s^{-1} m^{-2} is assumed for LR_{75} (Gowri, 2009). The leakage rate expresses the flow rate per square metre of external envelope area, so infiltration is only modelled in thermal zones that are in contact with the exterior. The calculated LR is converted into an infiltration rate expressed in air changes per hour (ACH, expressed in h^{-1}) to be used in TRNSYS Type 56. The conversion is:

$$ACH = LR \times \frac{A_{env}}{V_{zone}} \times \frac{3600 \text{ s/h}}{1000 \text{ L/m}^3} = C \times LR \tag{3.3}$$

where A_{env} is the exterior envelope area (m^2), V_{zone} is the zone volume (m^3), and the last factor represents the unit conversion factor to obtain ACH in h^{-1}. C is the multiplication factor used for a given zone, and Table 3.6 shows the values obtained for the model.

Table 3.6: Values for factor C in infiltration regime types

Zone			A_{env}	V_{zone}	C
Type	**Orientation**	**Floor**	**m^2**	**m^3**	**-**
Perimeter	North & South	1 & 2	198	821	0.867
Perimeter	North & South	3	405	821	1.776
Perimeter	East & West	1 & 2	132	519	0.913
Perimeter	East & West	3	263	519	1.822
Core	-	3	983	3894	0.909

As shown in equation (3.1), LR depends on the local wind speed, which needs to be calculated from the wind speed measured at the weather station (ASHRAE, 2013a):

$$V = V_{weather} \times \left(\frac{\delta_{weather}}{z_{weather}}\right)^{\alpha_{weather}} \times \left(\frac{\delta}{z}\right)^{\alpha} \quad (3.4)$$

The selected coefficients for the simulated building represent open terrain for the weather station and city center for the building, and are shown in Table 3.7.

Table 3.7: Coefficient for wind approximation at building height

	Weather Data	**Office building**
Exponent α (-)	0.14	0.33
Layer thickness δ (m)	270	460
Height z (m)	10	11.88

3.1.5 Ventilation

The fresh air ventilation flow rate is set at 0.43 L/s·m^2 to match the value in the Commercial Prototype Buildings (USDOE-BTO, 2017), which results from the requirements of ASHRAE Standard 62.1-2010. This flow rate is modulated by a schedule which shuts ventilation OFF at night, as shown in Figure 3.7. Outdoor air is delivered to each zone by a dedicated system, as shown in Figure 3.8. Air is conditioned and is supplied to every zone at 13 ˚C.

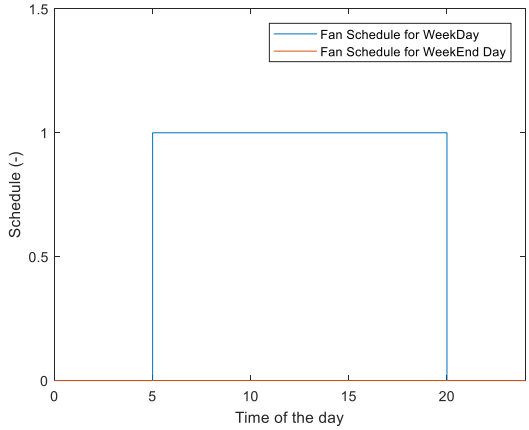

Figure 3.7: Schedule for fan operation

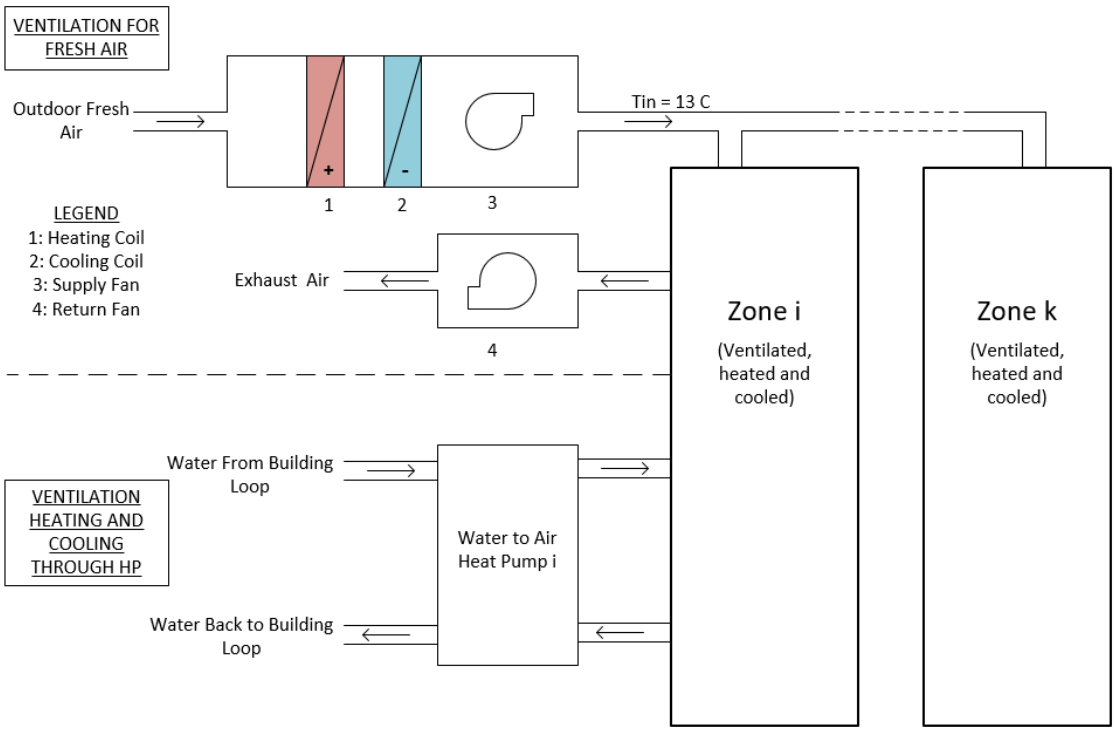

Figure 3.8: Ventilation for a zone i in the detailed simulation

3.1.6 Heating and Cooling Setpoint Temperature

The heating and cooling setpoint profiles have a large impact on energy use and peak demand, so they were part of the overall optimization process for SCW systems. Three different configurations were modelled, as illustrated in the figures below. Figure 3.9 shows a constant setpoint profile used to size the heat pump in each zone and the SCW system, as would typically be done in a heat load calculation. Figure 3.10 shows the schedule used in the NECB 2011 for office buildings. Early simulation results showed that, as other heat pump systems, SCW systems are affected by sudden changes in heating and cooling setpoints, which impose larger peak loads at the source side of heat pumps. A "milder" setpoint strategy, shown in Figure 3.11, was developed to mitigate that problem by increasing the ramping-up (or down) period in the morning. This setpoint profile will be referred to as the "ramping profile". Chapter 7 discusses the impact of setpoint profiles on the SCW system performance in terms of yearly energy use, peak demand, and operating costs.

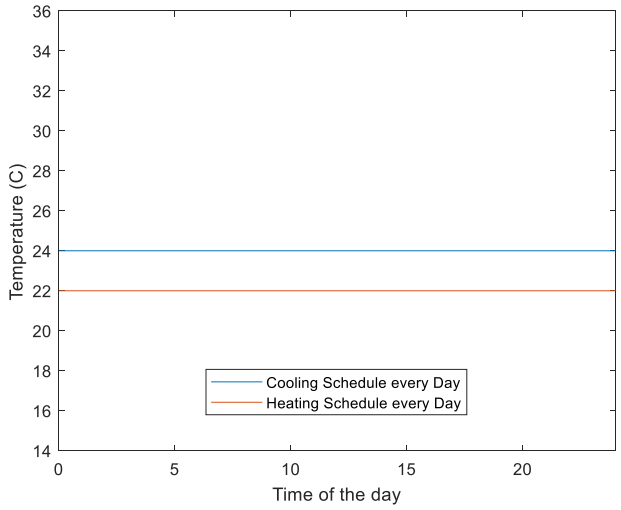

Figure 3.9: Constant setpoint profile for cooling and heating

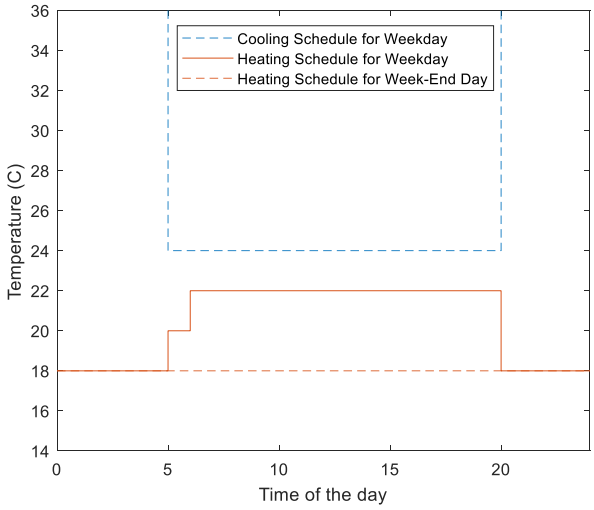

Figure 3.10: NECB setpoint profile for cooling and heating

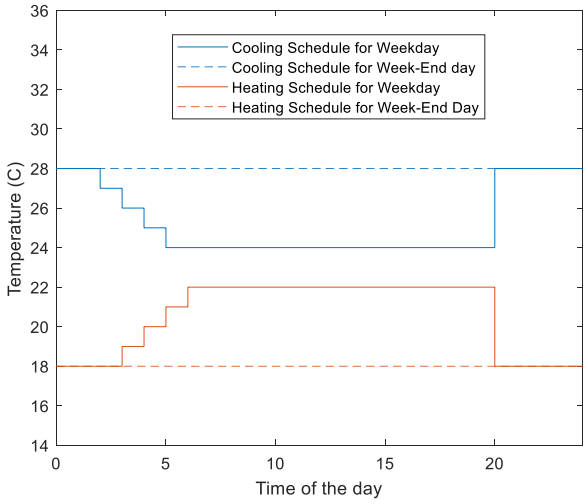

Figure 3.11: Ramping setpoint profile for cooling and heating

3.1.7 Internal Mass

A simple assumption is used to represent furniture and other thermal mass absent from the model: the actual thermal capacity of the air inside each zone is multiplied by 10.

3.1.8 Other Energy Uses

3.1.8.1 Service Water Heating

The nominal power density for Service Water Heating (SWH) is calculated based on the following assumptions from NECB 2011:

- 90 W per person
- 25 m^2 per person

This results in a nominal power for SWH of 17.93 kW, which is modulated by the schedule shown in Figure 3.12. As SWH represents a minor energy load in office buildings, it is modelled outside of the central heating and cooling system, and assumed to be met by electrical (Joule effect) heating with a COP of 1. The electrical power demand is simply added to other uses such as equipment and lighting.

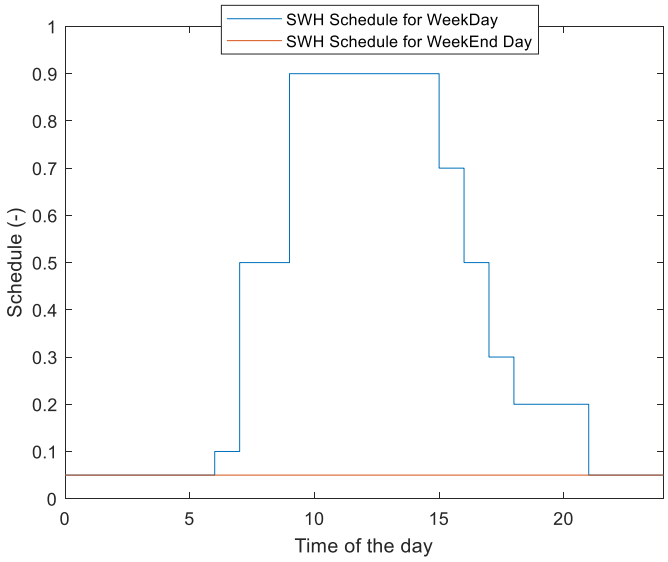

Figure 3.12: Schedule for Service Water Heating

3.1.8.2 Exterior Lights

The lighting zone for the building is assumed to be zone 2 from NECB 2011, resulting in a power of 700 W for exterior lights. A simple schedule is assumed, ON from 9 pm to 6 am and OFF outside of that period.

3.1.8.3 Elevators

The nominal power, number of elevators, and operating schedule (Figure 3.13) are taken from the "Medium Office" in the US DOE prototype commercial buildings (USDOE-BTO, 2017), which assumes two elevators (16.2 kW each).

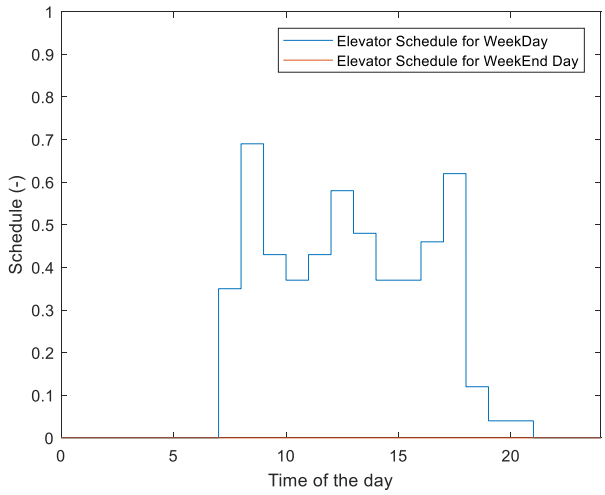

Figure 3.13: Schedule for Elevators Use

3.1.9 Ground Coupling

The first-floor cooling and heating needs are influenced by ground coupling, which is modelled by imposing the boundary temperature of the floor slab external surface. A detailed 3-D model known as Type 1244 is available in TRNSYS to model ground coupling. It meshes the ground below the building and calculates the dynamic heat transfer through a finite volume model. This model results in long calculation times, so a 2-step approach was adopted: first, detailed simulations (with Type 1244) were performed to obtain boundary temperatures imposed to the slab surfaces in each first-floor zone; secondly, these precalculated temperatures were used in further simulation variants comparing different SCW control strategies. This assumes that the slight variations in indoor temperatures from one simulation to the other are sufficiently small that ground heat transfer can be assumed to be similar for a given group of simulations.

Simulations were performed using Type 1244 for each setpoint configuration (see above) and for 2 years, discarding the first year as a warm-up period and keeping the second year as precalculated

ground temperatures. These simulations used a simplified model with ideal heating and cooling systems. Figure 3.14 shows an example of the boundary temperatures obtained for a ramping setpoint profile. The ground temperature below the core zone is relatively constant, while the boundary temperature for core zones (which is an area weighted average for all zones) shows a more pronounced yearly cycle.

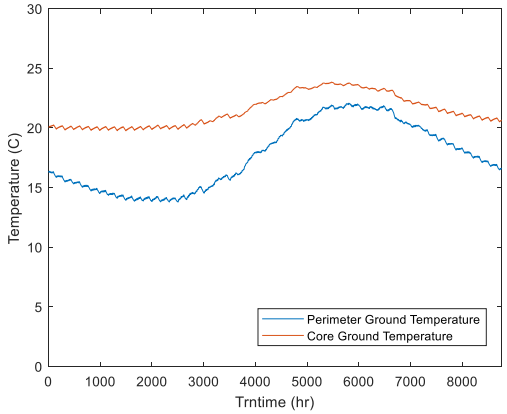

Figure 3.14: Floor slab boundary temperatures for setpoint in configuration 4

3.1.10 Annual Building Energy Loads

Figure 3.16 shows the daily mean and maximum heating/cooling power of the building over the year with the assumptions presented above (using the ramping setpoint profile).

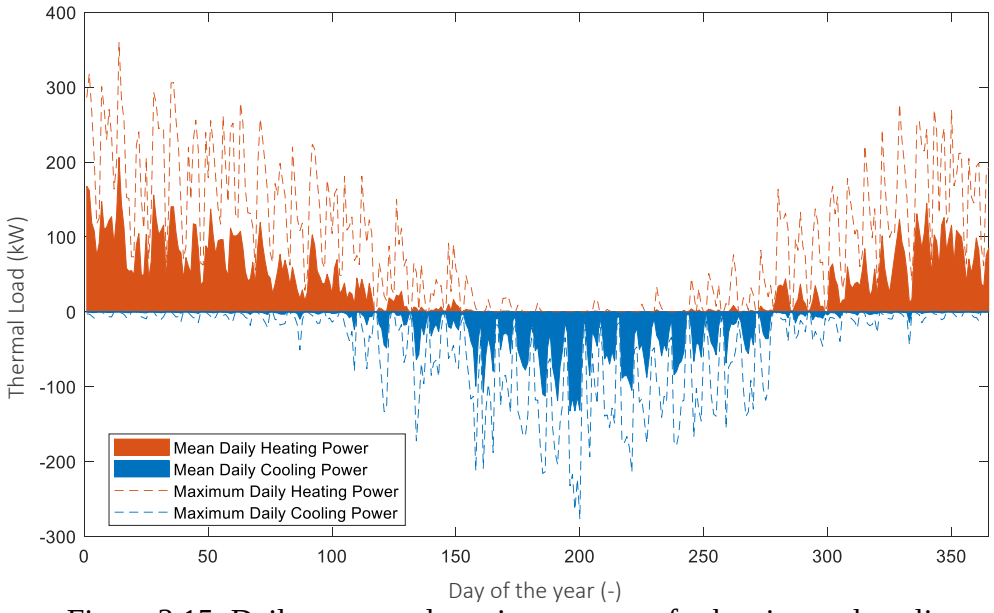

Figure 3.15: Daily mean and maximum power for heating and cooling

The yearly energy loads are presented in table 3.8. Note that values for heating and cooling represent heat, not electricity, as no COPs are introduced in the calculation at this stage.

Table 3.8: Yearly energy load for the building

	Thermal Load (kWh)	**Electrical Load (kWh)**
Heating		\
Zones	219 100	\
Fresh air	105 200	\
Cooling		\
Zones	70 100	\
Fresh air	96 400	\
SWH	44 500	\
Fan (fresh air)	\	17 500
Light	\	142 000
Equipment	\	138 500
Elevator	\	45 600

Assuming a heating COP of 1, the maximum power demand occurs in heating mode and represents 391 kW with the ramping setpoint profile.

3.2 Building Loop

The building loop contains a glycol water solution that supplies the fifteen modelled zone heat pumps as well as the heat pump used for fresh air conditioning. It also includes a variable-speed pump, the auxiliary heating and cooling devices, and the plate heat exchanger.

3.2.1 Heat Pumps

Heat pumps are modelled by the component known as Type 919 (TESS, 2012), which models a water-to-air heat pump (also known simply as a water-source or water-loop heat pump) with normalized performance maps. Four data files are needed for Type 919: cooling and heating performance (function of water inlet temperature, water and air flow rates), and heating and cooling correction factors (function of indoor wet bulb and dry bulb temperature). Appendix A provides more details on how those performance maps were derived. Typical models were selected from a commercial catalog (Trane, 2018). The selected heat pump series (Axiom Vertical) offers a range from 0.5 to 25 tons (1.8 to 88 kW) with a selection of different fans for each model. For each heat pump, a representative fan was selected by attempting to match the recommended maximum fan power in ASHRAE Standard 90.1 (ASHRAE, 2013b) as shown in equation 3.5 It should be noted that Type 919 requires heating and cooling capacity data including the fan power (which adds heat, hence increasing the heating capacity and reducing the cooling capacity), so performance data was adjusted accordingly. Appendix B shows the fan choice for each heat pump model.

$$P_{fan} = 0.0017 \, \frac{kW}{L/s} \times \dot{m}_{air,nominal} \tag{3.5}$$

The selected heat pumps are summarized in Table 3.9. Available capacities are given for inlet water temperatures of 25 ˚C in cooling and 0 ˚C in heating.

Table 3.9: Table of heat pumps capacities in cooling and heating before and after fan correction

In kW	Original Capacity		Corrected Capacity	
Heat Pump	**Heating**	**Cooling**	**Heating**	**Cooling**
GEV036	8.8	11.0	9.4	10.5
GEV042	9.9	12.6	10.5	12.1
GEV048	10.0	15.0	11.2	13.9
GEV060	13.7	18.8	14.8	17.7
GEV072	16.0	23.1	17.1	22.0
GEV090	19.2	27.0	21.5	24.7
GEV120	26.5	36.1	29.9	32.7
GEV150	35.3	46.6	38.7	43.2
GEV180	42.1	56.3	47.7	50.7
GEV240	52.1	75.6	60.6	67.1
GEV300	68.8	92.5	77.2	84.0

Heat pump selection was performed for each zone based on a dedicated simulation using constant setpoints, without internal gains for heating, and with internal gains for cooling. Security factors are added using recommendations from ASHRAE Standard 90.1 (ASHRAE, 2010): +25% in heating and +15% in cooling (Table 3.10, column 2 and 3). The machine with the closest capacity equal or above the desired value for cooling and heating is selected (heating capacity is the deciding factor for all zones except the core zones of levels 1 and 2).

As shown in Table 3.10, 4 models of heat pumps were selected. In that table and hereinafter in this work, 'Per' corresponds to a perimeter zone and 'Core' is for central zones. The number indicates the floor and the suffix letter informs on the zone orientation. For example, 'Per1S' is a perimeter zone on the first floor oriented towards South. Appendix C shows the parameters used for Type 919. The peak heating and cooling loads presented in the table include safety factors (respectively 125% and 115%), so the ratios presented in the last two columns should ideally be close to 1.

Table 3.10: Overview of the heat pump sizing

Building Thermal Zone	Peak Heating Load	Peak Cooling Load	Heat Pump Choice	Heating Capacity of heat pump	Cooling Capacity of heat pump	Heating Ratio	Cooling Ratio
	(125% in kW)	(115% in kW)		kW	kW		
Per1S	19.5	11.7	GEV090	21.5	24.7	1.10	2.11
Per1E	13.1	7.3	GEV060	14.8	17.7	1.13	2.41
Per1N	19.7	8.7	GEV090	21.5	24.7	1.09	2.84
Core1	10.8	14.5	GEV060	14.8	17.7	1.37	1.22
Per1W	13.1	9.8	GEV060	14.8	17.7	1.14	1.79
Per2S	18.4	12.0	GEV090	21.5	24.7	1.17	2.06
Per2E	12.6	7.5	GEV060	14.8	17.7	1.18	2.37
Per2N	18.9	9.6	GEV090	21.5	24.7	1.13	2.58
Core2	9.2	16.7	GEV060	14.8	17.7	1.62	1.06
Per2W	12.5	10.0	GEV060	14.8	17.7	1.19	1.77
Per3S	30.5	19.4	GEV120	29.9	32.7	0.98	1.69
Per3E	20.1	11.6	GEV090	21.5	24.7	1.07	2.13
Core3	65.7	40.7	GEV300	77.2	84.0	1.17	2.06
Per3N	30.9	17.6	GEV120	29.9	32.7	0.97	1.86
Per3W	20.1	15.2	GEV090	21.5	24.7	1.07	1.62

3.2.2 Outdoor Air

Fresh air provided to the building is conditioned by a heat pump, which is modelled with a different approach since the ON/OFF nature of Type 919 would result in poor control of the supply air conditions. Figure 3.16 shows how the load on the building loop is calculated. First, the airside heat transfer required to obtain the desired supply temperature (13 °C) is calculated by a simple coil model assuming a constant bypass fraction (15 %). The heat pump is then modelled by simple equations using the coefficient of performance (COP). The compressor power (Wc) is added to the zone heat pumps overall consumption as the ratio of the air load divided by the COP using the following formulas:

$$Q_{loop} = Q_{bldg} - W_c \qquad Q_{loop} = Q_{bldg} + W_c$$

with $COP_{heat} = \frac{Q_{bldg}}{W_c}$ with $COP_{cool} = \frac{Q_{bldg}}{W_c}$

$$Q_{loop} = Q_{bldg}\left(1 - \frac{1}{COP_{heat}}\right) \qquad Q_{loop} = Q_{bldg}\left(1 + \frac{1}{COP_{cool}}\right)$$

HEATING COOLING

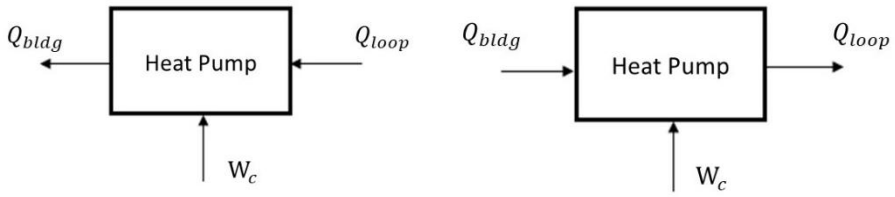

Figure 3.16: Heat pump in heating mode (left) and cooling mode (right)

The equations shown in Figure 3.16 depend on the COP, which is estimated based on the same performance data as for the zone heat pumps. The coldest temperature from the weather file is -27.2 ˚C, so the required heating rate for the maximum flow rate (9232 kg/h) is:

$$Q_{freshairHEAT} = 9232 \times 1.004 \times (-27.18 - 13) = -376100\frac{kJ}{h} \qquad (3.6)$$

$$Q_{freshairHEAT} = 104.47\ kW$$

The required heating rate is slightly higher than the largest available heat pump, but the performance data from that heat pump is used and approximated by a linear regression of the COP as a function of the entering temperature for heating and cooling performance data and nominal water and air flow rate (equations 3.7 and 3.8). R^2 values for both regressions are 0.976 and 0.970 respectively.

$$COP_{Heat} = 0.0543 \times T_{in,water} + 3.5136 \quad (3.7)$$

$$COP_{cool} = -0.1334 \times T_{in,water} + 8.9134 \quad (3.8)$$

3.2.3 Building Loop Variable-Speed Pump

The building loop pump is a variable speed pump modelled in TRNSYS with Type 110. This type allows the user to modulate the outlet mass flow rate between zero and a rated value. The outlet changes linearly according to a control signal. This signal is the ratio of the total flow rate called by the heat pumps and the maximum flow rate of the building loop. For the flow rate called by zone heat pumps, we will multiply the operative flow rate (Table 3.11) of a heat pump by its conditioning control signal (which is 0 or 1 depending whether a heat pump is OFF or ON) and add them all. The heat pumps are provided with a 2.5 GPM/ton (0.044 L s^{-1} kW^{-1}) flow rate on their source side.

Table 3.11 :Operative Flow rate of the Heat Pumps

Heat Pump	Flow rate L/s
GEV060	1.06
GEV090	1.70
GEV120	2.27
GEV300	5.68

The water flow rate required by the heat pump conditioning the outside air is assumed to be proportional to the load of that heat pump (which is modelled differently from the zone heat pumps, as described above). It is calculated assuming a fixed 3 °C temperature difference on the source side of the heat pump.

The flow rate in the building loop is simply the sum of all flow rates required by the zone heat pumps which are currently ON and the flow rate required by the heat pump used to condition outside air.

3.2.4 Auxiliary Heating and Cooling Devices

The auxiliary heating system maintains a minimum temperature of 0.5 °C in the building loop at the inlet of the plate heat exchanger with the ground loop to avoid freezing the ground water. It is assumed to be heated by electrical resistances with a COP of 1. The auxiliary cooling device has a setpoint temperature of 35 °C, to avoid warming up ground water above that level and to ensure efficient operation of the building heat pumps. The auxiliary cooling device is assumed to be a conventional chiller with a fixed COP of 3. Both auxiliary devices are assumed to have a sufficient capacity to maintain their setpoints at all times. Their electricity use is included in the cost assessment.

The impact of the auxiliary heating setpoint on the SCW performance is discussed in Chapter 7.

3.2.5 Pipes

The simulation model includes a simplified representation of the piping network inside the building. Pipes are modelled with TRNSYS Type 31, which takes into account the thermal losses and the transport delay. The piping network includes 30 m of pipes (with a 0.2 m diameter) for each distributed heat pump.

3.3 Ground Loop

3.3.1 SCW Model

The SCW model used to perform the simulations is the Thermal Resistance and Capacity Model (TRCM) developed by Nguyen et al. (2015a, 2015b). The model is written in Matlab and integrates the geometry, thermal conductivity and diffusivity of the surrounding ground, vertical pipes and groundwater through a network of interconnected thermal resistances and capacities. The well and the aquifer around are discretized into a nodal network of thermal resistances and capacities as illustrated in Figure 3.17. Figure 3.18 shows the sub-domains that account for all SCW

components. Thanks to the coaxial geometry of SCW, each sub-domain is divided into annular regions in the radial direction and in vertical layer. Each regions is interconnected through the network of thermal resistances. Nguyen et al. (2015a) evaluates and describes each resistance and capacity used to solve the governing equation of heat transfer:

$$C_j \frac{dT_j}{dt} = \sum_{k=1}^{n_j} \frac{T_k - T_j}{R_k} \quad \forall \text{ j} = 1 \ldots . \text{n} \tag{3.9}$$

with n is the total number of nodes in the network, j is the node index, n_j is the number of surrounding nodes and k is the index of the neighboring node. This network has to be connected to a groundwater flow model that accounts for the transient groundwater velocity and drawdown when operating under bleed control. The model relies on the Theis analytical equation shown in section 3.3.3 and the Darcy law couples the heat transfer model to the groundwater flow model through:

$$v_D(r,t) = K \frac{ds}{dr} \tag{3.10}$$

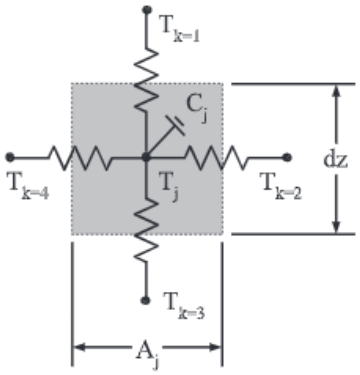

Figure 3.17: Illustration of the resistance and capacity distribution for one node from Nguyen et al. (2015a)

The model also takes into account the vertical displacement of the groundwater in the SCW and the groundwater flow in the aquifer induced by bleed. Bleed results in a reduction of the water level

in the extraction well (drawdown D) and in an increase of the water level in the injection well (impression I).

This model relies on different assumptions. First, there is no thermal short-circuit with the injection well, only one SCW is modelled, and no thermal or hydraulic interaction is accounted for. The aquifer is confined, fully saturated, homogeneous, infinite, and obeys Darcy's law. In the SCW. the flow direction is vertical and fully turbulent.

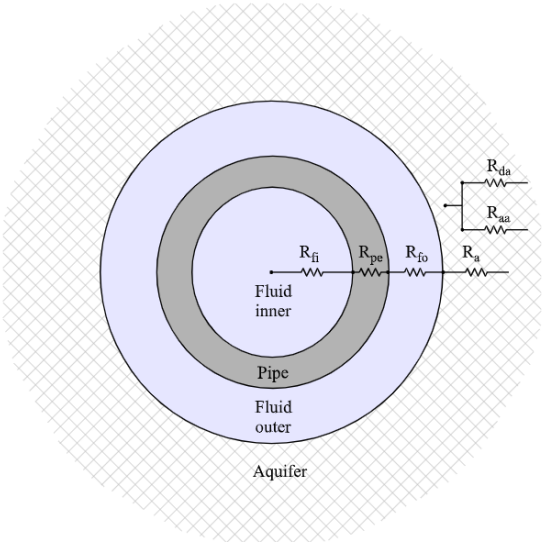

Figure 3.18: SCW coaxial geometry and the radial thermal resistances associated from Nguyen et al. (2015a)

Table 3.12: Parameters of the SCW.

Parameter	Value
Borehole Length	300 (m)
Hydraulic conductivity	5.7e-7 (m/s)
Borehole diameter	0.15 (m)
Pump pipe diameter	77.5 (mm)
Porosity	2 (%)

The Matlab model is linked to the simulation via Type 155 in TRNSYS. The main parameters of the SCW used are shown in Table 3.12 and were recently measured from the experimental system described by Beaudry et al. (2018). During the simulations, the model receives inputs from TRNSYS and sends back the outputs summarized in Table 3.13.

To limit computational time, Type 155 calls the Matlab model of the SCW at the end of each time step, after the other TRNSYS components have converged. This "ping-pong" communication mode avoids iterations between the two subsystems, at the cost of introducing a slight time difference between the two models. This time difference is deemed to be acceptable given the long reaction time of the SCW and the relatively short selected time step (7.5 min). This assumption was validated by comparing 2 selected simulations using both modes. In iterative mode, the two programs were performing up to 25 iterations between themselves (each of them involving internal iterations within one program), leading to computation times over 30 h for a yearly simulation. The "ping-pong" mode reduced simulation time to 3 hours while the simulated heat pump consumption was within 1 % of the original results. Appendix 4 provides some details on this comparison.

Table 3.13: Inputs and outputs of type 155.

N°	Input		Output	
	Name	**Unit**	**Name**	**Unit**
1	Inlet Temperature to the well - $T_{in,SCW}$	°C	Outlet Temperature of the well - $T_{out,SCW}$	°C
2	Inlet flow rate to the well - $\dot{m}_{in,SCW}$	kg/h	Outlet flow rate of the well - $\dot{m}_{out,SCW}$	kg/h
3	Bleed flow rate - $\dot{m}_{bleed}$	kg/h	Bleed flow rate - $\dot{m}_{bleed}$	kg/h
4	-	-	Drawdown – S	m
5	-	-	Pressure Drop	kPa
6	-	-	Impression in the injection well - I	m

3.3.2 SCW Sizing

There is no recognized design tool for SCW systems, so an ad-hoc procedure was used to size the simulated system. Typical borehole depths are between 150 and 450 m, and a fixed 300-m depth was used. As for heat pump sizing, a dedicated simulation without gains is used to obtain the maximum building load, which occurs at 7 AM on February 13 for the selected weather data file. The maximum building heating load is 397 kW (296 kW in the zones and 101 kW for outside air), and the corresponding building loop heating load is 309 kW assuming a COP of 4.5.

As shown in Chapter 2, the design heat extraction load for SCWs is between 176 and 385 W/m with an average value of 236 W/m for commercial buildings. Assuming the mean value, the required mean SCW length is:

$$L = \frac{397\,000\,W}{236\,W/m} = 1682\,m \tag{3.11}$$

The selected configuration includes 6 SCWs of 300 m, or 1800 m, which results in an extraction rate of 220 W/m (or 52 ft/ton).

3.3.3 Drawdown in SCW and Impression in Injection well

Drawdown in the well is calculated with the Theis relation shown in equation 3.12 for confined aquifer (Bear, 1979) and the hydraulic parameters described in section 3.3.1.

$$\mathrm{S} = \frac{Q}{4\pi kb} \times \int_u^\infty \frac{e^{-u}}{u}\,du \tag{3.12}$$

with $u = \frac{r^2 S_s}{4kt}$

In the previous equations, Q is the bleed flow rate in $m^3 \cdot s^{-1}$, k is the hydraulic conductivity in m s^{-1}, b is the aquifer thickness in m, r is the borehole diameter in m, S_s is the specific storage (dimensionless) and S the drawdown in m.

The impression is a simple proportional relationship between drawdown, well length and efficiency showed in equation 3.13 and Table 3.14.

$$I = S \times \frac{\varepsilon_{SCW}}{\varepsilon_{inj}} \times \frac{L_{SCW}}{L_{inj}} \text{ (in m)} \tag{3.13}$$

A condition on the impression well level has to be added that virtually prevents the well from overflowing in the simulation. The literature review showed that water table in commercial systems is around 6 m. We chose to limit the well level elevation below 5 m. If this condition is not met, the simulation re-run the time step with a smaller bleed flow rate.

Table 3.14: Characteristics included in drawdown and impression modelization

	Efficiency	Length
SCW	0.85	300 m
Injection Well	0.6	150 m

3.3.4 Pumping

The main goal of this research project is to optimize control strategies for the pump flow rate and bleed flow rate. Chapter 4 details how head losses in the ground loop are calculated and their implications on the pumping power, and chapters 5 and 6 discuss the control strategies themselves.

3.3.5 Heat Exchanger

The last part of the system is the plate heat exchanger. It links the ground loop to the building loop so that groundwater is not used directly into the building HVAC system. It is modelled assuming a constant effectiveness of 80 %, but head losses on the ground water loop side are assessed in more detail as explained in Chapter 4.

3.4 Operating Cost Assessment

Maintenance costs are not considered in this study, so operating costs are equivalent to electricity costs.

3.4.1 Hydro-Québec – Rate M

Since this research is focusing on a cold climate, we chose to use Hydro-Québec electricity rates for medium power customers for the calculation of costs related to energy consumption and power needs.

The general rate for medium power customers (Rate M) applies to customers that have a maximum power demand superior to 50 kW at least once during a 12 months period (Hydro-Québec, 2018). The next rate (L) is for customers with a minimum billing demand of 5000 kW or more, so the modelled building clearly fits within the “M rate” category. The M rate is divided between energy and power costs on a monthly basis. The energy cost is 4.99 ¢/kWh for the first 210 000 kWh and

then 3.70 ¢/kWh for the remaining consumption. The monthly price for power is 14.46 $/kW. This rate is applied every month to the 15-min peak power demand of the current month. There is a minimum monthly charge for power, equal to 65% of the maximum power demand charge for the preceding winter period (this is sometimes known as a demand ratchet). This means that reducing the maximum power demand in winter will have an impact on the peak demand for the whole year.

3.4.2 Peak Power Demand Calculation

In the previous section, we saw that part of the costs is related to peak power demand. Our simulation uses a 7.5 minutes timestep. Hydro-Québec documentation on electricity rate states that '*power demands are determined for integration periods of 15 minutes'* (Hydro-Québec, 2018), so 15-min results are calculated by averaging 2 successive time steps before calculating the peak demand.

Power demand costs are assessed for the building as a whole, including HVAC electricity use and all other uses (lighting, equipment, elevators, service water heating), and also for these other categories only (i.e. without the HVAC electricity use) to assess the impact of HVAC control strategies.

3.4.3 Peak Power Demand and On/Off Control Effect

Initial simulation results showed that a non-predictable "noise" was added to calculated costs due to the ON/OFF nature of heat pump controls and the discrete nature of the simulation process. Small variations of the control strategies can lead to large changes in the number of heat pumps in operation at a specific time step, leading to strong impacts on the peak demand. This is compounded by the simplified schedules used for equipment and lighting, which cause large time-step-to-time-step variations in the electrical demand. In a real building equipped with a Building Energy Management System, measures would very likely be put in place to restrict the peak demand, and the natural randomness of user behavior and ON/OFF thermostats would most probably introduce some diversity in the electrical loads.

To eliminate this "apparent randomness" in peak loads, the peak demand cost is calculated by averaging the 5 largest 15-min values over a simulation, rather than taking the absolute largest 15-min peak. Figure 3.19 shows the effect of this calculation method on the peak power demand using

one of the best control scenarios which will be presented in the following chapters. Averaging 5 timesteps largely reduces the peak demand for March, April, and November in that particular simulation. The figure also shows that averaging the 10 largest 7.5-min values does not cause a significant difference, which indicates that averaging 5 values is apparently sufficient to avoid the undesirable apparent randomness in monthly peak demand calculation.

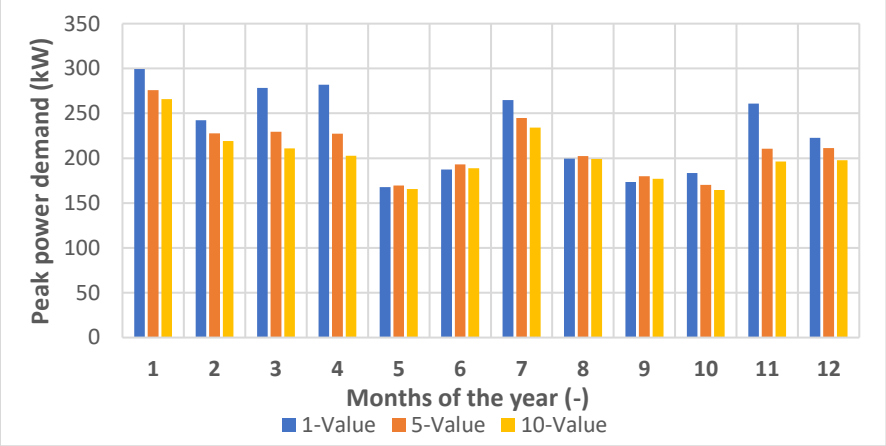

Figure 3.19: Graph of the monthly peak power demand calculated for 15-min, and by averaging 5 and 10 timestep values.

3.5 Reference Scenarios

The reference scenarios to assess the different control strategies investigated in this master thesis will be compared to 2 reference scenarios which use the same SCW design (six 300-m wells) and only differ by the control strategies:

- *Good Practice 1* is inspired by (Spitler et al., 2002)
  - The pumping flow rate is set to 3 GPM/ton (0.054 L s^{-1} kW^{-1}) with a simple ON/OFF control (the pump is switched off if there is no heating or cooling load).
  - The bleed rate is controlled by a dead-band strategy on the SCW outlet temperature: bleed is activated if the outlet temperature falls below 5.83 °C, and stops if it increases above 8.6 °C. When activated, the bleed rate is constant at 10%.
- *Good Practice 2* is inspired by (Nguyen et al., 2013)
  - The pumping flow rate is set to 3 GPM/ton (0.054 L s^{-1} kW^{-1}) with a simple ON/OFF control (the pump is switched off if there is no heating or cooling load).

- Three bleed rates can be activated based on the SCW outlet temperature, as described in Chapter 2: 10% below 7 °C, 20% below 6 °C, and 30% below 5 °C (bleed is deactivated if the SCW outlet temperature is above 7 °C).

Another basis for comparison is a conventional building equipped with the same HVAC system (same decentralized heat pumps and ventilation system), and for which the building loop is heated by an electrical boiler (with a COP of 1) and cooled by a typical chiller (with an assumed seasonal COP of 3). This scenario will be referred to as "No SCW".

Comparisons presented in the following chapters will present the performance in two graphs that aim at representing the necessary trade-off between thermal performance and volume of groundwater bled on an annual basis. Figure 3.20 shows the annual operating cost (calculated as the electricity bill with Hydro-Québec "M" rate) as a function of the total daily average volume of groundwater bled on an annual basis. An optimal system would reduce the operating cost while keeping the volume of water bled as low as possible, i.e. moving towards the lower left corner of the graph.

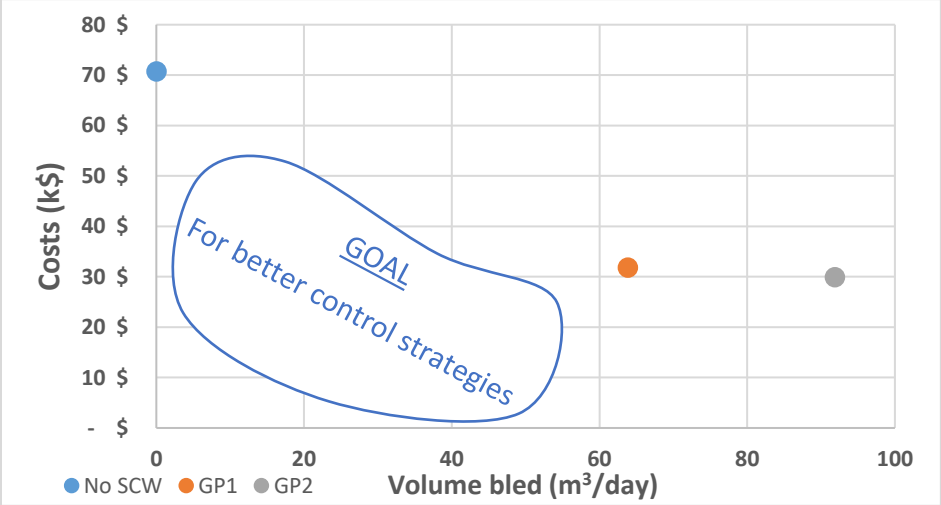

Figure 3.20: Annual operating cost vs. annual volume of groundwater bled

Figure 3.21 shows the same variable on the x-axis (daily average volume of groundwater bled) but represents the annual COP on the y-axis. The annual COP is defined as the sum of all heating and cooling energy (heat delivered to or extracted from the building, including the outside air conditioning) divided by the sum of the electricity used by all heat pumps and by the circulating

pump. The fan power used by zone heat pumps is included, as well as the fan power dedicated to outdoor air system. In this graph, the optimal system would increase the annual COP while keeping the volume of water bled as low as possible, moving towards the upper left corner of the figure.

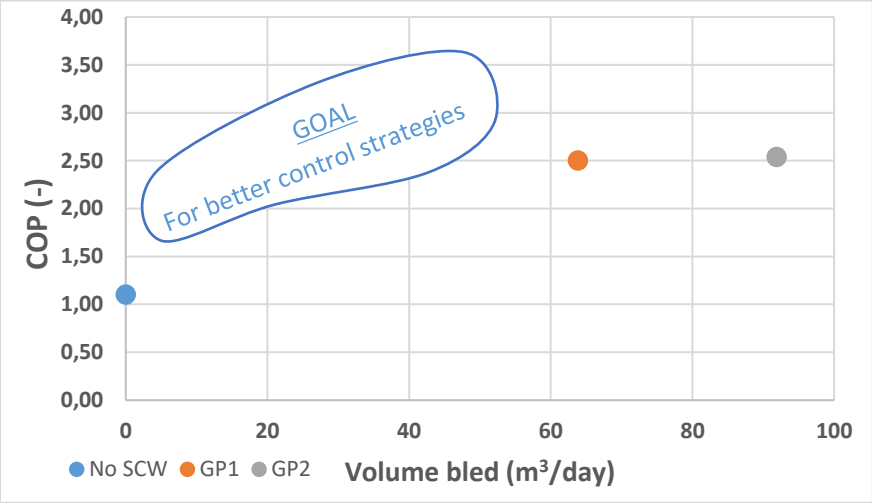

Figure 3.21: Annual COP vs. annual volume of groundwater bled

CHAPTER 4 HEAD LOSS AND IMPAC ON PUMPING POWER

In this chapter, an assessment of the head loss in the underground loop is accomplished for a later use in the detailed modelling. Indeed, since the detailed simulations will be used to elaborate control strategies for the pumping and bleed flow rates, such assessment is required. Among the various parameters included in this analysis, the groundwater temperature (from 0 to 35 °C), pumping flow rate (from 1.5 to 3.5 GPM per ton), drawdown and impression induced by pumping and bleed are considered. This chapter will consider the following part in the ground loop network: pipes, elbows, valves, tees and heat exchangers. The calculation of the head loss is designed to consider whether there is or not bleed in operation. Figure 4.1 is a diagram of the experimental SCW installation that is the foundation of the assumptions and work illustrated in this section.

4.1 System Configuration

In the literature review, we described the SCW system considered in this research. In this section, we will focus on the head loss in the system with, or without bleed. If there is no bleed of the SCW, as seen in Figure 4.1, the pump has to overcome the head loss in the system (heat exchanger, pipe, valves, elbows) and the height difference between the two levels in the SCW. It is important to note that there is no real pipe between the end of the rejection pipe and the beginning of the rising pipe. The borehole acts like a pipe but considering the diameter of the borehole the head loss in this part are neglected.

Pumping in the SCW immediately decreases the level in the rising pipe and increases the level in the annular section which is considered symmetrical. The reduction of the level in the rising pipe, called *h*, is equal to the head loss through the rising pipe which is calculated in section 4.2.2.

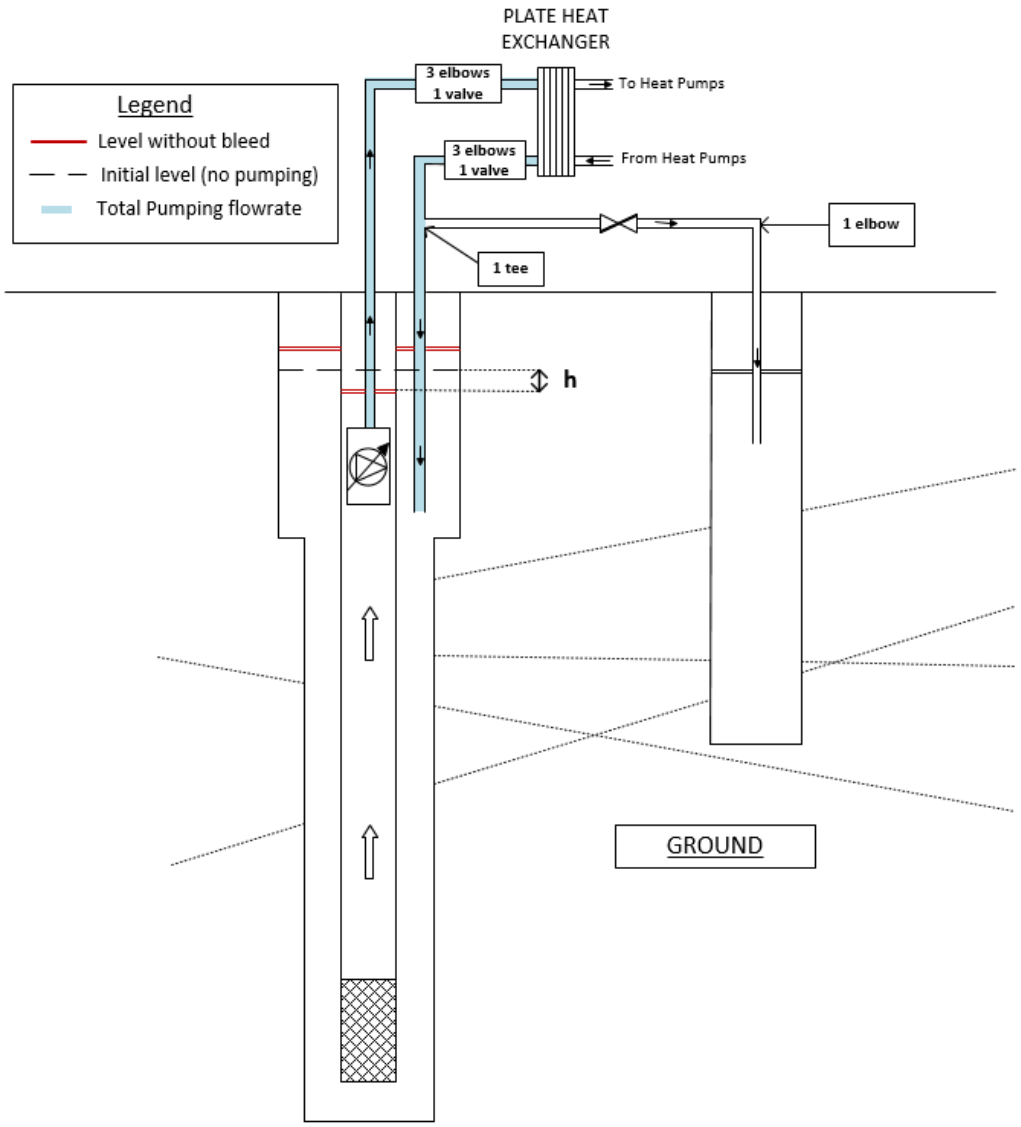

Figure 4.1: Installation configuration working without bleed for a groundwater withdrawal at the bottom of the SCW

If the bleed is activated, water will flow through the bleed injection pipe and a new part of the system needs to be considered for the head loss calculation: bleed pipe, valve, tee, elbow. Bleed will also have an impact on the flow rate going through each pipe as shown in Figure 4.2. In this Figure, the color of each pipe indicates the flow rate considered for the head loss calculation and illustrates the fact that the flow rate in the rejection pipe will be lower when the SCW operates with bleed.

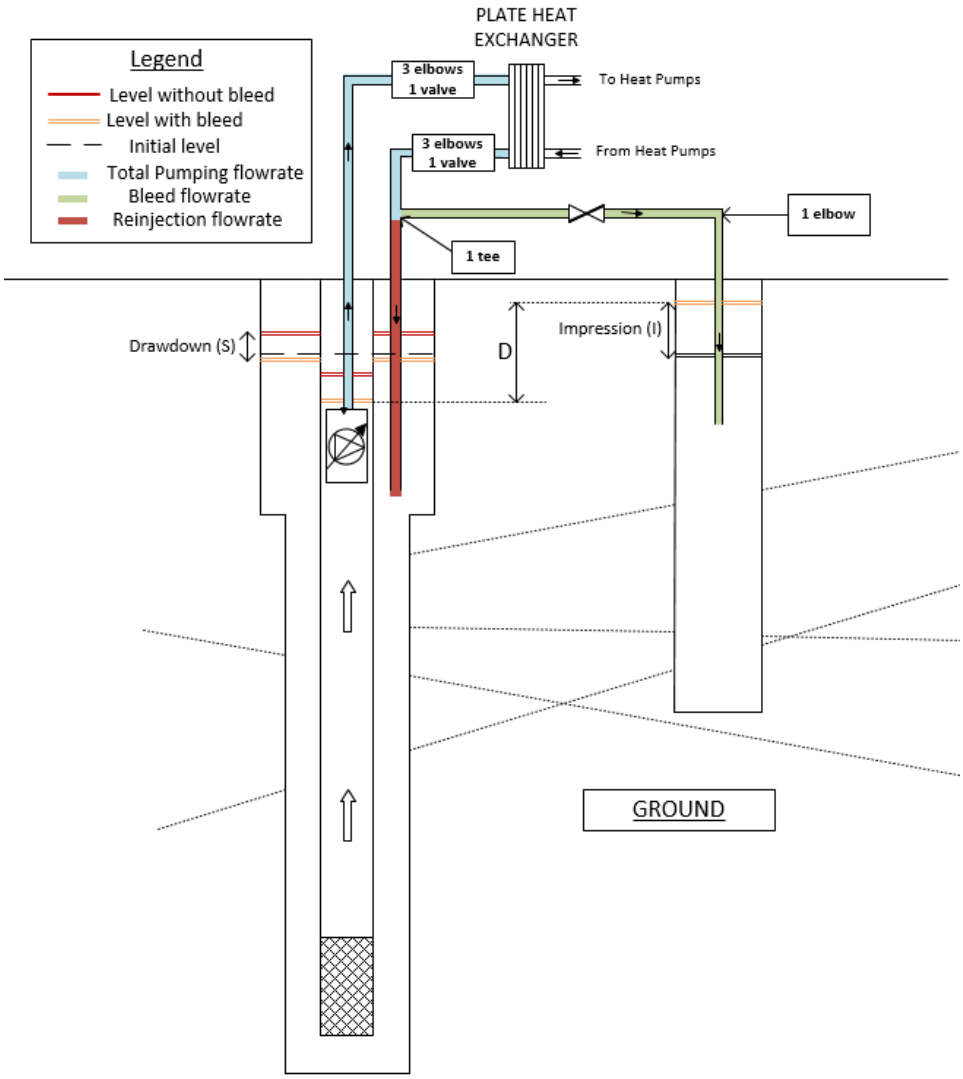

Figure 4.2 :Installation configuration working with bleed for a ground water withdrawal at the bottom of the SCW

When the bleed flow rate is directed towards the injection well, an open-loop is created. This induces a reduction of the groundwater level in the SCW, called drawdown, and a rise of the groundwater level in the injection well called impression. This induces a height difference *D* that must be overcome by the pump. A section about drawdown and impression calculation was presented in chapter 3 with a strategy to compute drawdown and impression values for specific pumping and bleed flow rates.

4.2 Head loss Calculation and Assumptions

Most of the data used in this section are taken from an experimental installation described in Beaudry et al. (2018) but other assumptions were made regarding the head loss estimation and it will be explained in the following paragraphs. Table 4.1 is summing up the main characteristics of each part of the system needed for calculation (pipe length, number of elbows, etc.).

Table 4.1 : Summary of the parts considered in head loss calculation

Type	Quantity	Characteristics
Rising Pipe 1	1	$L = 282\ m$ and $D_{i,risingPipe1} = 101.5\ mm$
Rising Pipe 2	1	$L = 28\ m$ and $D_{i,risingPipe2} = 51.9\ mm$
Reinjection Pipe 1 – Before bleed	1	$L = 10\ m$ and $D_{i,reinjectionPipe1} = 51.9\ mm$
Reinjection Pipe 2 – After bleed	1	$L = 18\ m$ and $D_{i,reinjectionPipe2} = 51.9\ mm$
Bleed injection pipe	1	L=15+15 = 30 m and $D_{i,bleedinjectionPipe} = 51.9\ mm$
Elbows	7	3 before the heat exchanger, 3 after the heat exchanger and 1 on the bleed injection pipe each for a $D_i = 51.9\ mm$
Valves	3	1 before the heat exchanger, 1 after the heat exchanger and 1 on the bleed injection pipe each for a $D_i = 51.9\ mm$
Tee	1	Divider of the flow rate between injection in SCW and bleed
Heat Exchanger	1	Plate heat exchanger see 1.1.4.
Height difference induced by bleed	/	From 0 to 7 meters, explanation in section 1.1.5. D = Impression – Drawdown

4.2.1 Fluid properties

In order to assess the head loss, the fluid properties are calculated as a function of the temperature. The following equations for density and dynamic viscosity were found via EES and the curve fitting function of EES. These equations are valid for temperatures from 0 to 40 ˚C, which corresponds to the SCW operation range.

$$\mu = 0.00179129 - 0.000612913 \times T + 0.0000150225 \times T^2 - 2.40367 \times 10^{-8} \times T^3 + 1.75534 \times 10^{-10} \times T^4 \quad (4.1)$$

$$\rho = 999{,}83 + 0.0770336 \times T - 0.00950223 \times T^2 + 0.0000947295 \times T^3 - 6.11558E \times 10^{-7} \times T^4 \quad (4.2)$$

with $T = \frac{T_{in,SCW} + T_{out,SCW}}{2}$ and $\nu = \frac{\mu}{\rho}$

4.2.2 Pipe head loss

The head loss in the pipes are the result of a calculation using the Churchill equation (4.3) (Churchill, 1977) that is a function of Reynolds number and relative roughness. We chose to use this correlation because there is no restriction on its application and the equation can be used whether there is turbulent or laminar flow. Note that a pipe roughness of 0.0000212 m (Kavanaugh, 1998) was used for the HDPE pipes while a roughness of 0.0000015 m was retained for the 4'' rising pipe in PVC.

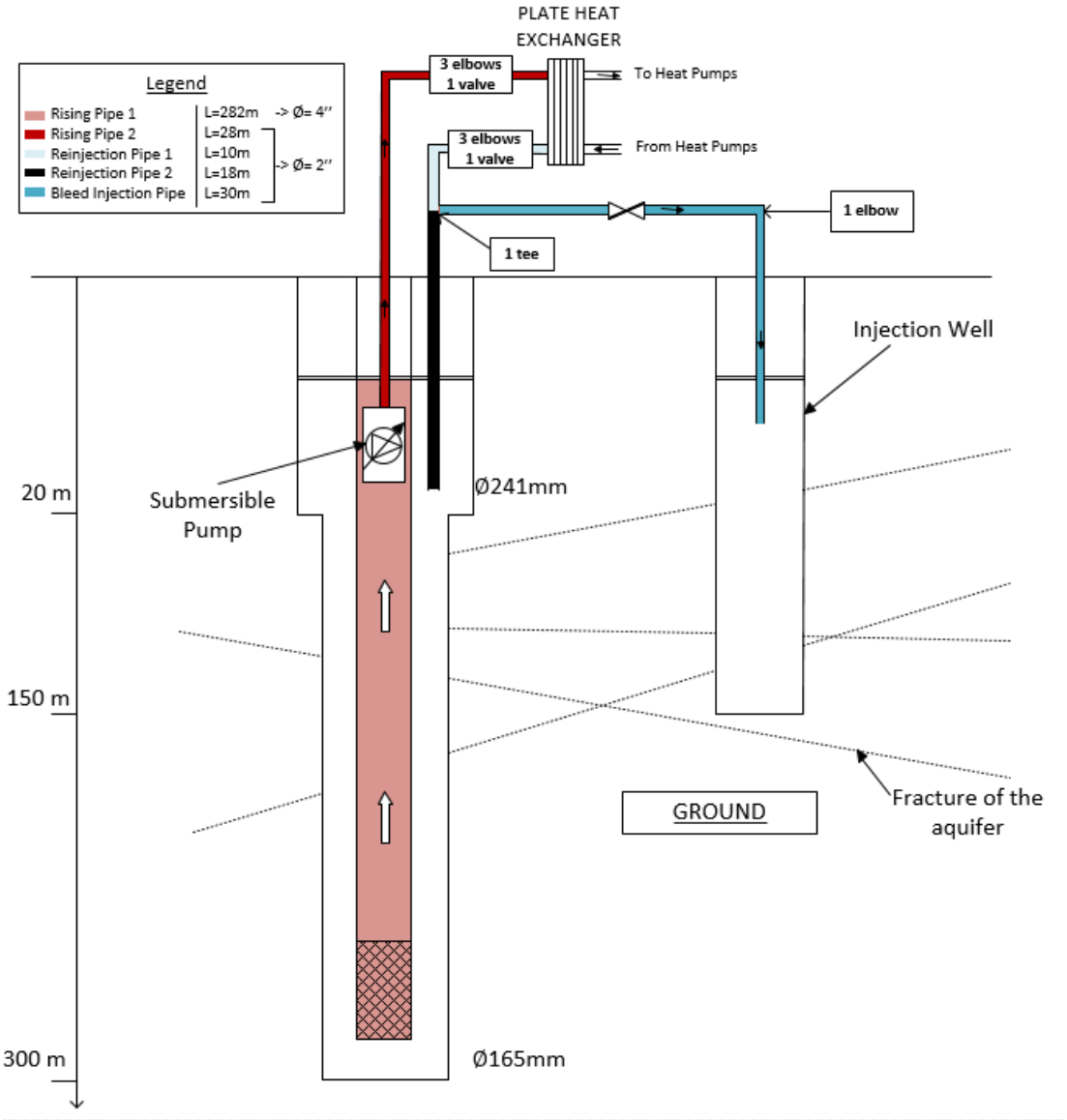

Figure 4.3: Pattern of each pipes and their dimension considered in head loss calculation

$$f = 8 \times \left(\left(\frac{8}{Re}\right)^{12} + \left(\left(2.457 \times ln\left(\frac{1}{\left(\frac{7}{Re}\right)^{0.9} + 0.27 \times RR} \right) \right)^{16} + \left(\frac{37530}{Re}\right)^{16} \right)^{-1.5} \right)^{1/12} \quad (4.3)$$

With $Re = \frac{V \times D}{\nu}$ and $RR = \frac{\varepsilon}{D}$

$$\text{Then } l_{pipe} = \frac{f \times L \times V^2}{2 \times D \times g} \text{ (m)} \tag{4.4}$$

4.2.3 Singular Head Loss in Elbows and Valves

The head loss caused by elbows and valves in the system are estimated as following:

$$l_{sing} = K \times \frac{V^2}{2 \times g} \tag{4.5}$$

The pipe fitting coefficient *K* are chosen according to Hydraulic Institute (1990) for a 2'' diameter and are summed up in Table 4.2 according to the diameter considered.

Table 4.2: Coefficient *K* for head loss calculation

Coefficient K	**2''**
Regular screwed 90˚ elbow	1.0
Gate valve screwed (open) – 2 units	0.15
Globe Valve screwed – 1 unit	6.8
Tee – Flowline	0.9
Tee – Branchline	1.4

4.2.4 Heat Exchanger Head Loss

The head loss estimated for the plate heat exchanger are a combination of the manufacturer data from the one installed in the experimental installation and the heat exchanger design handbook (Thulukkanam, 2013). This documentation gives an approximate equation for the pressure drop on one side of the plate heat exchanger such as:

$$\Delta p = \frac{4 \times f \times L \times G^2}{2 \times g_c \times \rho \times D_e} \times \left(\frac{\mu_w}{\mu_b}\right)^{0.14} \quad (4.6)$$

In our case the fluid on the side of the ground loop is ground water and $g_c = 1$ in SI Units so the equation 4.6 is simplified into:

$$\Delta p = \frac{4 \times f \times L \times G^2}{2 \times \rho \times D_e} \quad (4.7)$$

The following terms were also defined:

- $f = \frac{2.5}{Re^{0.3}}$, the friction factor has this form for typical plate heat exchangers
- $A_0 = W \times b$ in m^2
- $G = \frac{M}{A_0}$, the mass velocity in $kg \cdot m^{-2} \cdot s^{-1}$, is the ratio of M in $kg \cdot s^{-1}$ and A_0
- $D_e = \frac{4 \times W \times b}{2 \times (W+b)}$ the equivalent diameter.

Table 4.3 sums up the size of the heat exchanger used. Note that the curve found with equation 4.7 was corrected with a factor to match the operation data provided by the manufacturer and presented in equation 4.8.

$$\Delta p_{corrected} = C \times \Delta p \quad \text{with C=18.24} \quad (4.8)$$

Table 4.3: Size of the plate heat exchanger used

Symbol	Name	Value (m)
W	Effective plate width (gasket to gasket)	0.394
b	Mean plate gap	0.0116
L	Flow Length	0.726

Table 4.4: Operation data of the heat exchanger

Symbol	Value	Unit
Flow rate	11356	$kg \cdot hr^{-1}$
Temperature	38	˚C
Pressure drop	62.5	kPa
Density	977	$kg.m^{-3}$
Mean viscosity	0.69	cP

4.2.5 Drawdown and Impression

The drawdown in the SCW and the impression in the injection well are time-varying outputs of the SCW model. For the purpose of evaluating various D values, four different bleed flow rates were used to compute drawdowns and impressions. Table 4.5 provides a summary for each case. Note that a reference pumping flow rate of 3 GPM per ton, which corresponds to a total flow rate of 214 L/min and a bleed rate of 10% were used.

Table 4.5: Values for s, I and D considered for head loss observation when operating at 214 L/min

Situation	Bleed rate (%)	Drawdown (s in metre)	Impression (I in metre)	Level Difference (D in metre)
1	0	0	0	0
2	10	1.14	3.25	4.39
3	15	5.00	1.75	6.75
4	25	2.85	0	2.85

4.3 Pump Hypothesis

The submersible pump is responsible for the flow rate on the source side of the plate heat exchanger. The pump is designed with a variable frequency drive that is meant to provide the best efficiency at every time step. The efficiency of the motor and the pump are then set to constant values for our simulation.

Table 4.6: Parameters for the submersible pump.

Parameter	Value (unit)
Pump efficiency	0.6 (-)
Motor efficiency	0.76 (-)

The simulation of the submersible pump is a key component in the simulation because the electrical consumption of the submersible pump has a significant impact on the overall consumption of the system. The pump consumption is a function of the flow rate and pressure drop in the ground loop. In the detailed simulation, we will use type 742 to calculate the pump consumption according to pressure drop and inlet flow rate with the efficiency assumptions made above. Type 742 simply resolves the following equation:

$$P_{pump} = \frac{\Delta p \times \dot{m}}{\rho \times \eta_{tot}} \tag{4.9}$$

with Δp in kPa, $\dot{m}$ in kg/hr and $\eta_{tot} = \eta_{pump} \times \eta_{motor}$.

and $\Delta p = \Delta p_{pipes} + \Delta p_{sing} + \Delta p_{HX} + \Delta p_{Drawdown}$

4.4 Pumping Power Assessment

Figures 4.4, 4.5 and 4.6 presents the pumping power corresponding to the various systems' components. First, in all graphs we observe that the pipes, the water level difference (*D*) and heat exchanger are generating most of the head loss when there is no bleed. Singular head loss due to elbows and valves are not making a major difference but still needs to be considered in the calculations.

Figure 4.4 shows that the variation of the flow rate leads to the widest variation of head loss and will be significative while studying pumping strategies. The temperature has a comparatively small impact (Figure 4.6) but it is still interesting to consider it in the study as in cold climates we will be working at low temperatures during winter. The impact of the bleed flow rate on the pumping power is illustrated in Figure 4.5. The addition of the bleed pipe, elbow and valves with the reduction of the flow rate in the rejection pipe seems to have inverse effects that do not show much variation on the head loss. The main impact results from the water level difference that the pump must overcome when more groundwater is bled from the SCW. The variation observed is significant.

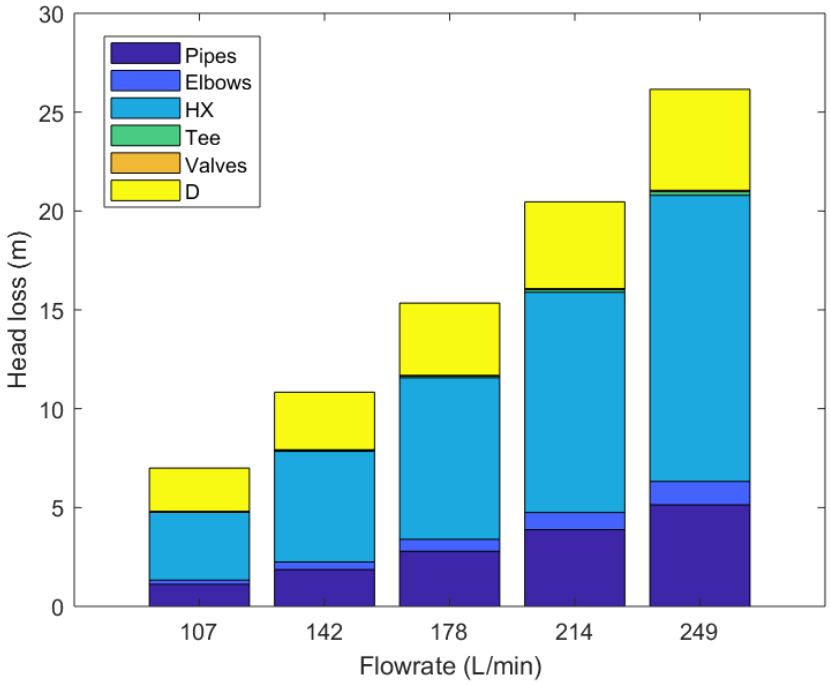

Figure 4.4: Head loss as a function of the flow rate with a 10% bleed rate and a temperature of 5 °C

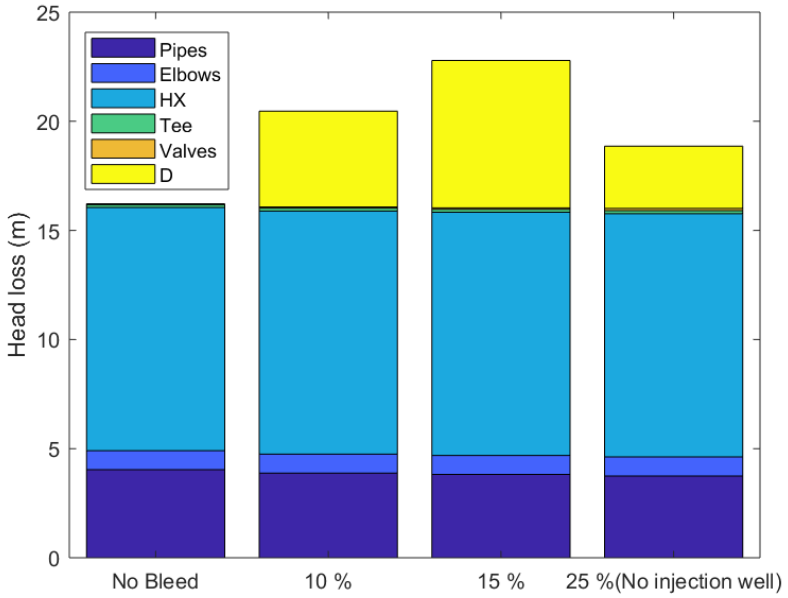

Figure 4.5: Head loss for various bleed scenarios for a total flow rate of 214 L/s and 5 °C

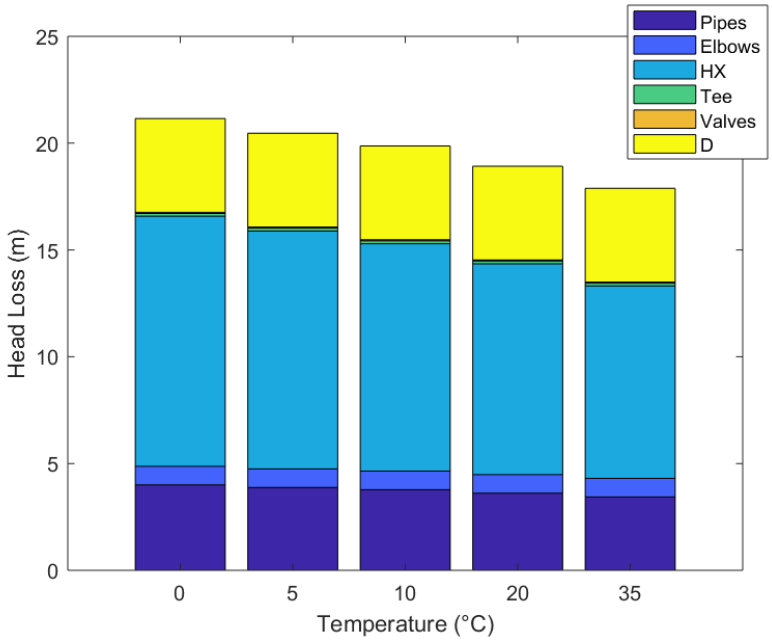

Figure 4.6: Head loss as a function of temperature for 214 L/s and a bleed rate 10 %

CHAPTER 5 PUMPING FLOW RATE CONTROL STRATEGY

Through the literature review, we were able to identify two major control variables for standing column wells: pumping (or circulating) flow rate and bleed flow rate. This chapter studies the impact of the pumping flow rate on SCW operations. First, section 5.1 compares different settings for constant flow rate strategies while section 5.2 presents simple variable-speed strategies. Finally, section 5.3 presents a sensitivity analysis on the thresholds used for the variable-speed strategies.

5.1 Constant Pumping Strategies

5.1.1 Simulations and Scenarios

In this section, we compare scenarios with a constant pumping flow rate from 1.5 to 3.5 GPM/ton (0.027 to 0.063 L s^{-1} kW^{-1}). The flow rate in the SCW is constant, unless no load is applied on the building loop, in which case the pump is shut off and there is no flow rate in the SCW. The same bleed flow rate control strategy is assumed in all cases, inspired by the recommendations found in the literature (Spitler et al., 2002). A bleed ratio of 10% (based on a constant flow rate of 3 GPM/ton) is assumed with an ON/OFF control using the dead-bands and thresholds on the outlet temperature (see Chapter 2).

5.1.2 Behavior During Peak Heating Day

In this section the simulation results obtained with 1.5 and 3.5 GPM/ton are compared for a representative peak heating day. The comparison is based on the inlet and outlet temperature of the SCW, energy exchange on the source side of the plate heat exchanger, energy consumption of the auxiliary heating system and COPs of the distributed heat pumps.

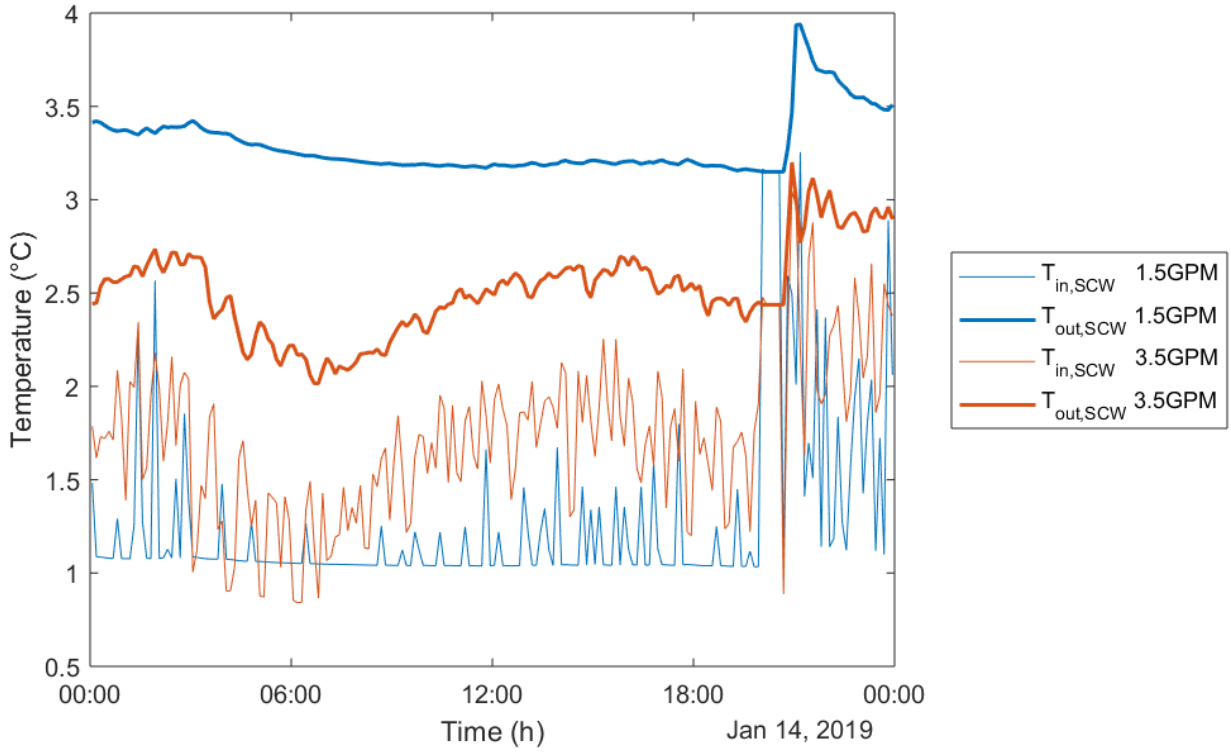

Figure 5.1: Inlet and outlet temperature of a SCW for 1.5 and 3.5 GPM/ton

The peak heat demand occurs on January 14 for the selected weather data file (see Chapter 3). Figure 5.1 shows the inlet and outlet temperature of the SCW for 1.5 GPM/ton in blue and 3.5 GPM/ton in orange. The lower flow rate causes a higher temperature difference in the heat exchanger, leading to a larger temperature difference visible between the two blue lines. This also results in a longer residence in the SCW, which leads to a significantly higher EWT (outlet temperature) to the heat pumps. The lower saturation of the SCW inlet temperature around 1 °C is caused by the auxiliary heating, which maintains the minimum temperature on the building side of the heat exchanger above 0.5 °C.

The heating power provided by the SCW is obtained with the product of the flow rate and the temperature difference on the source side of the heat exchanger and is shown in Figure 5.2. Both flow rates lead to similar heat transfer across the heat exchanger, with a more pronounced difference during the morning peak period (4 peaks seen between 2 and 6 AM), where the higher flow rate leads to a higher heat exchange. The outlet temperature and heat transfer are steadier at a small pumping flow rate, which has an impact on the energy used by the auxiliary heater, as seen

in Figure 5.3. During the morning peak period, the lower flow rate leads to a slightly higher auxiliary energy use, while this trend is reversed during the rest of the day.

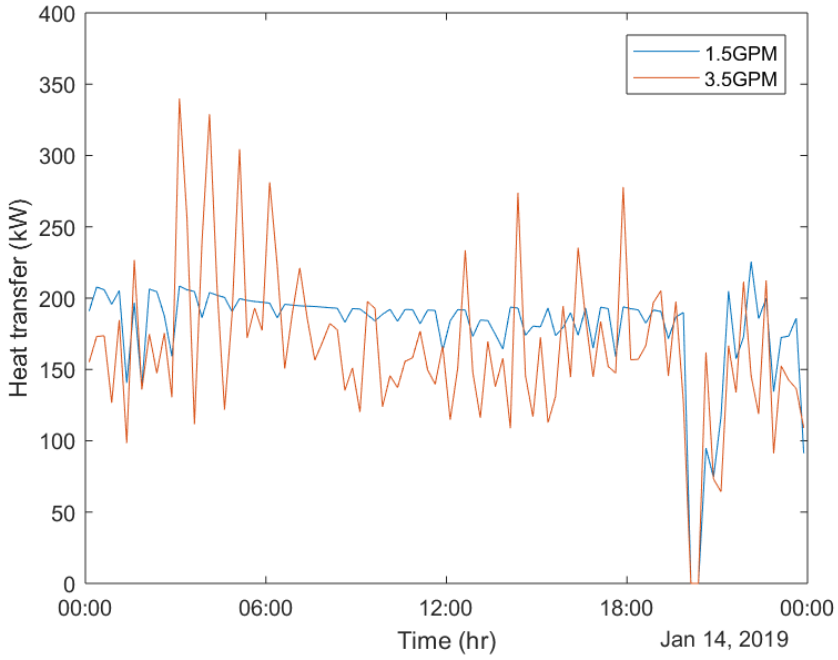

Figure 5.2: Energy exchanged on the source side of the heat exchanger for 1.5 and 3.5 GPM/ton

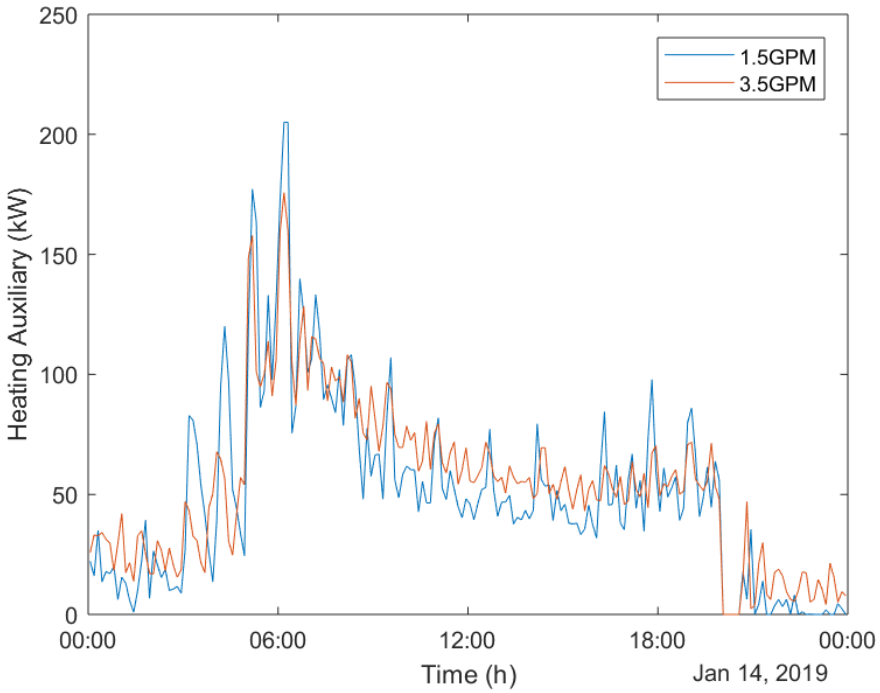

Figure 5.3: Heating energy of the auxiliary system for 1.5 and 3.5 GPM/ton

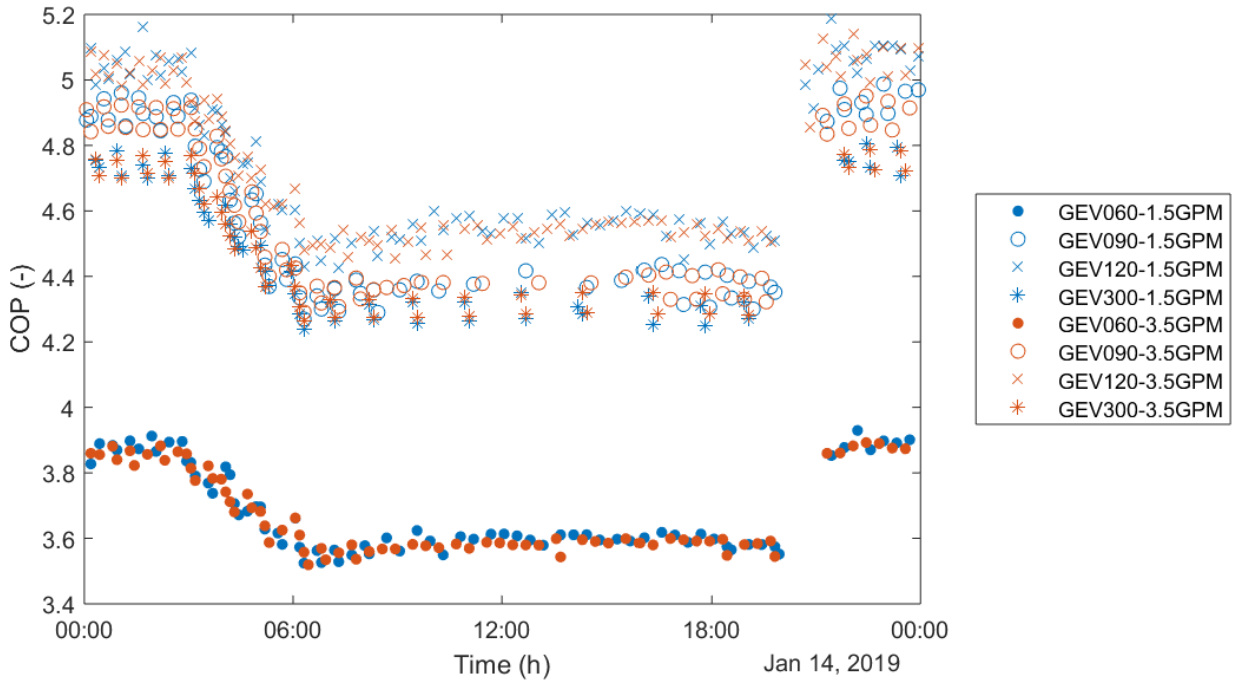

Figure 5.4: COP of the heat pumps for the four models implemented at two flow rates

The Figure 5.4 shows the coefficient of performance (COP) for the heat pumps models of 4 selected thermal zones (see chapter 3). The marker corresponds to the heat pump model, and the color corresponds to the pumping flow rate strategy. The impact of the higher outlet temperature with a lower flow rate is very small, and the heat pump COPs are similar in both cases. The differences between the COPs of individual heat pumps can be attributed to their different design. This is especially visible for the smaller heat pumps model (GEV060), which has a lower COP than the other selected heat pumps.

5.1.3 Annual Simulation Results

Figure 5.5 shows the annual energy use for the pumping flow rate strategies. Unsurprisingly, the pumping energy use is strongly influenced by the flow rate, with a non-linear relationship. For example, the pumping energy for 3.5 GPM/ton is 7 times as high as for 1.5 GPM/ton. The heat pump energy use for heating is essentially the same in all cases and the impact of the different strategies on their COP is very limited. The auxiliary energy use for heating increases with the flow

rate, leading to a total heating energy use increase. The energy use for cooling is not affected by the different scenarios.

The impact of different pumping strategies on the maximum power demand shown in Figure 5.6 shows an opposite trend: increasing the flow rate above 1.5 GPM/ton leads to a reduction of the peak electrical demand, which always occurs in heating in the modelled building. This is achieved by a reduction in auxiliary heating, as larger flow rates are beneficial in peak conditions. Flow rates higher than 2.5 GPM/ton do not improve the performance further, and the share of pumping power in the total peak demand increases with the flow rate, so that the best value seems to be located around 2.5 GPM/ton. It is interesting to note that an increased flow rate leads to more auxiliary energy use over the year, but a lower auxiliary peak demand.

Using Hydro-Québec rate M, we can see in Figure 5.7 that the computed annual cost is relatively constant, with energy and power being affected in different directions. Rate M includes a significant power cost, which represents about 60% of the total cost in our case. A detail of costs is presented in Table 5.1, showing that the minimum cost is obtained for a constant pumping flow rate of 2 GPM/ton with savings of 2.4% compared to the good practice value of 3 GPM/ton. This is equivalent to a modest reduction of 1600 $ of the annual bill, but the flow rate reduction can be implemented without cost (or lead to additional cost savings if a smaller pump can be selected).

Figure 5.8 shows the total volume of water bled annually. All strategies use the same nominal bleed flow rate (10% of 3 GPM/ton), but bleed is activated based on thresholds and dead-bands based on the SCW outlet temperature. The outlet temperature is affected by total pumping flow rate, and lower flow rates (i.e. longer residence times) lead to higher temperatures in heating, in turn leading to a reduction of bleed periods. This reinforces the attractiveness of operating the SCW with a reduced total flow rate, as bleed increases the environmental impact of SCW operations.

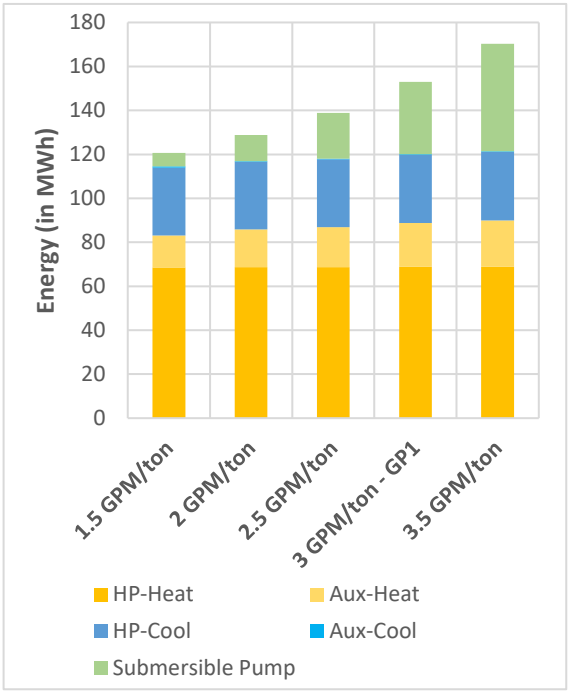

Figure 5.5: Annual energy used for heating and cooling

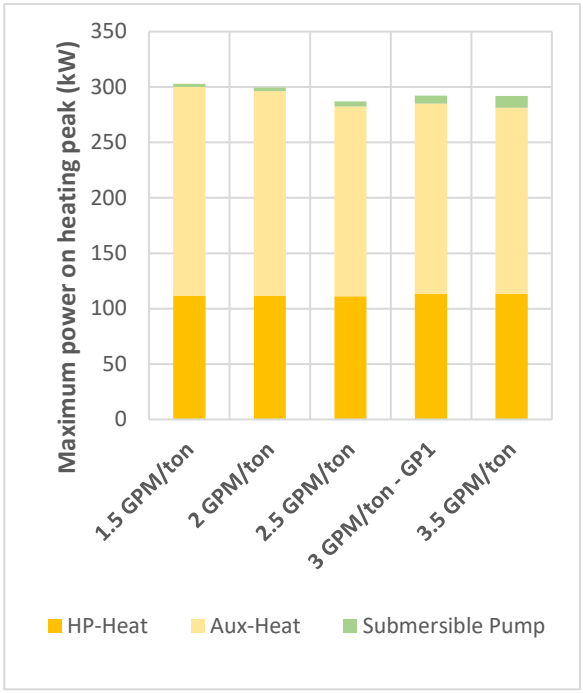

Figure 5.6: Annual maximum peak power

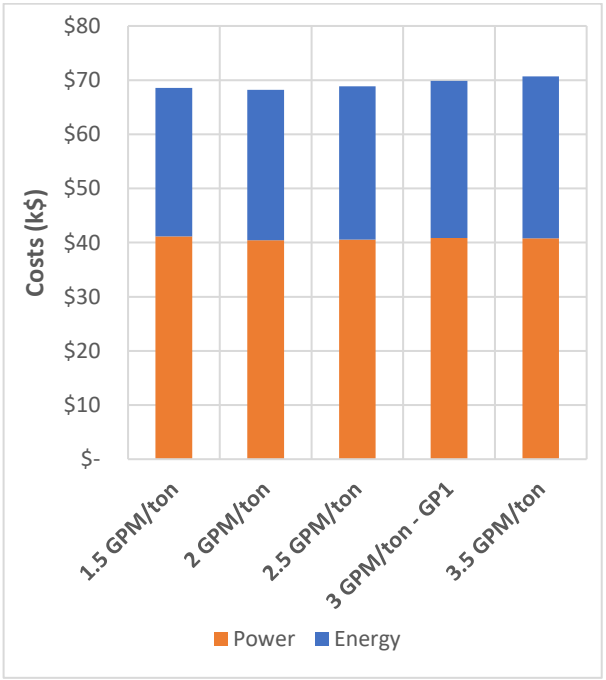

Figure 5.7: Annual operation costs for the medium office building

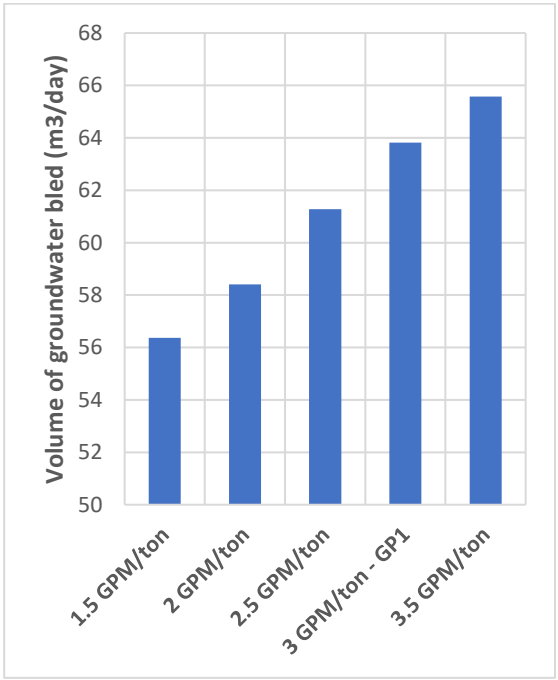

Figure 5.8: Groundwater volume bled

Table 5.1 : Summary of energy, power and total costs for constant control

	Annual Costs					
	Energy		Power		Total	
1.5 GPM/ton	27 410 $	-5,6%	41 120 $	0,7%	68 530 $	-1,9%
2 GPM/ton	27 830 $	-4,2%	40 410 $	-1,1%	68 240 $	-2,4%
2.5 GPM/ton	28 330 $	-2,4%	40 550 $	-0,7%	68 880 $	-1,5%
3 GPM/ton	29 040 $	0,0%	40 850 $	0,0%	69 890 $	0,0%
3.5 GPM/ton	29 910 $	3,0%	40 780 $	-0,2%	70 690 $	1,2%

5.2 Variable Speed Pumping Strategies – Load Proportional

5.2.1 Simulation and Scenarios

In this section, a simple variable flow rate strategy is investigated by varying the flow rate proportionally to the heating or cooling load on the building loop. Figure 5.9 represents such a strategy, showing the normalized pumping flow rate (i.e. the ratio between the flow rate and the maximum flow rate for that configuration) as a function of the normalized building loop heating or cooling load (i.e. the ratio between the heating or cooling load on the building loop and its maximum value). As previously, the maximum flow rate tested in each simulation goes from 1.5 to 3.5 GPM/ton unless there is no load on the building loop (in which case the pump is OFF). This results in five different simulations that will be compared between each other and with the *good practice 1* for annual results.

We assume that a variable speed pump is used and that its efficiency is constant (see chapter 3) as long as the pump operates above 25% of its maximum flow rate. In other words, there is a minimum acceptable flow rate to maintain the assumption of a constant pump efficiency. In the following figure, the linear control is applied between 20% and 70% of the maximum load. The sensitivity of these thresholds is studied in section 5.3.

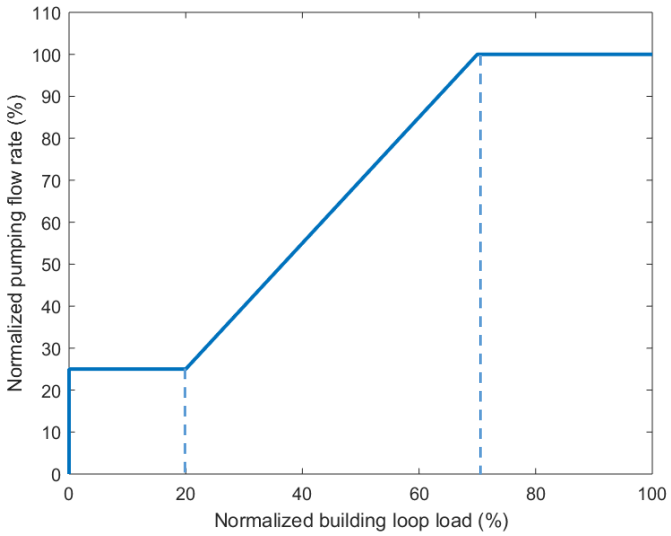

Figure 5.9: Linear flow rate control strategy

As the control strategy will modify the load on the building loop (i.e.: the heat pump performance is function of the entering temperature which is modified by the control strategy), we are not able to predict the maximum building loop load before the simulation. Considering this, a building loop load file has been designed based on *good practice 1* and is used in all the linear control strategies. (see Appendix 5).

5.2.2 Constant versus Linear Pumping Strategy during Peak Heating Day

The same curves are provided for this example as previously for the comparison between high and low pumping flow rate Figure 5.10. shows the variation on pumping flow rate when the linear control is applied compared to the constant control. On this figure, we can see that the flow rate is reduced during the night and higher during daytime when the building has to provide thermal comfort to users. Also, the pumping flow rate increases sharply during the morning peak when the heating system brings the temperature in the zones back to their “day” value.

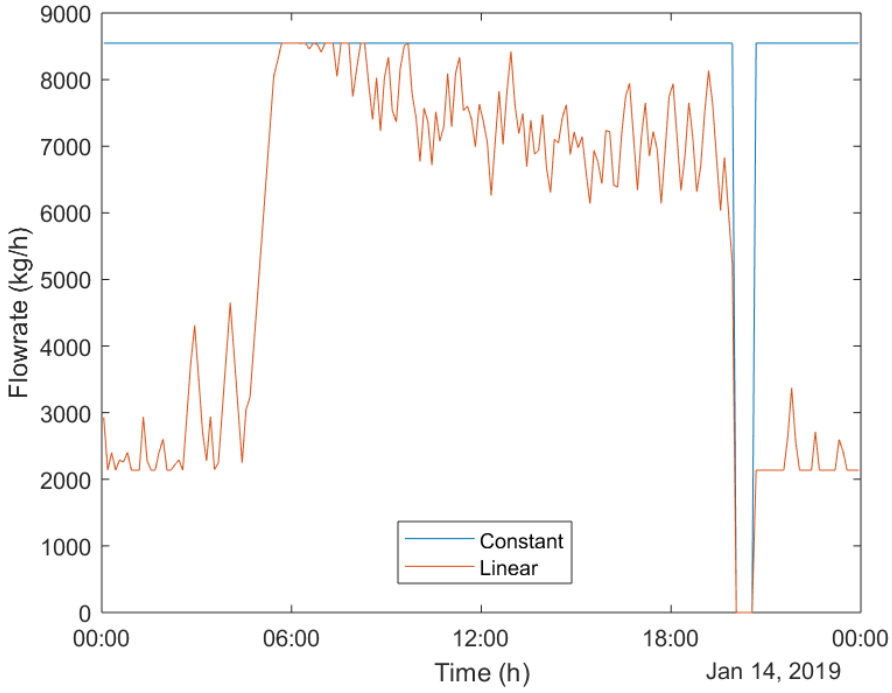

Figure 5.10: Pumping flow rate on the source side of the heat exchanger for constant and linear controls

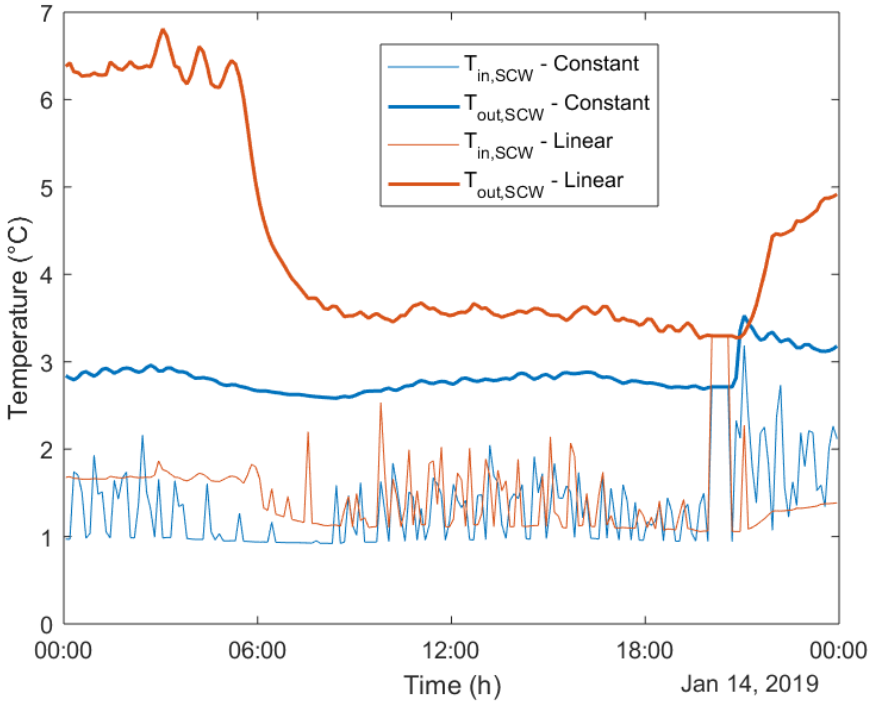

Figure 5.11: Inlet and outlet temperatures of the SCW for constant and linear controls

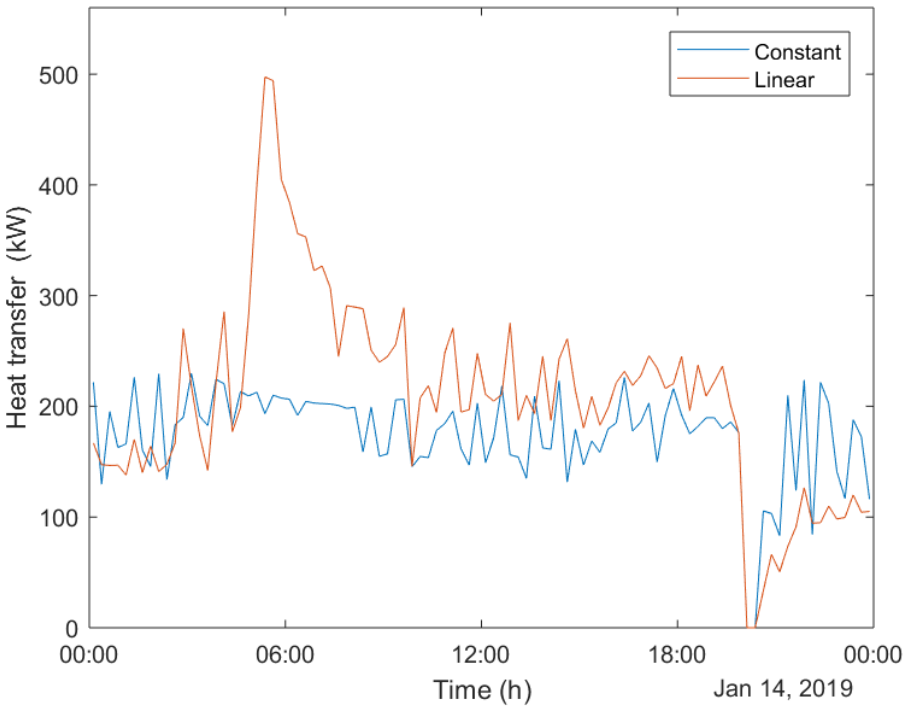

Figure 5.12: Heating energy transferred for constant and linear control

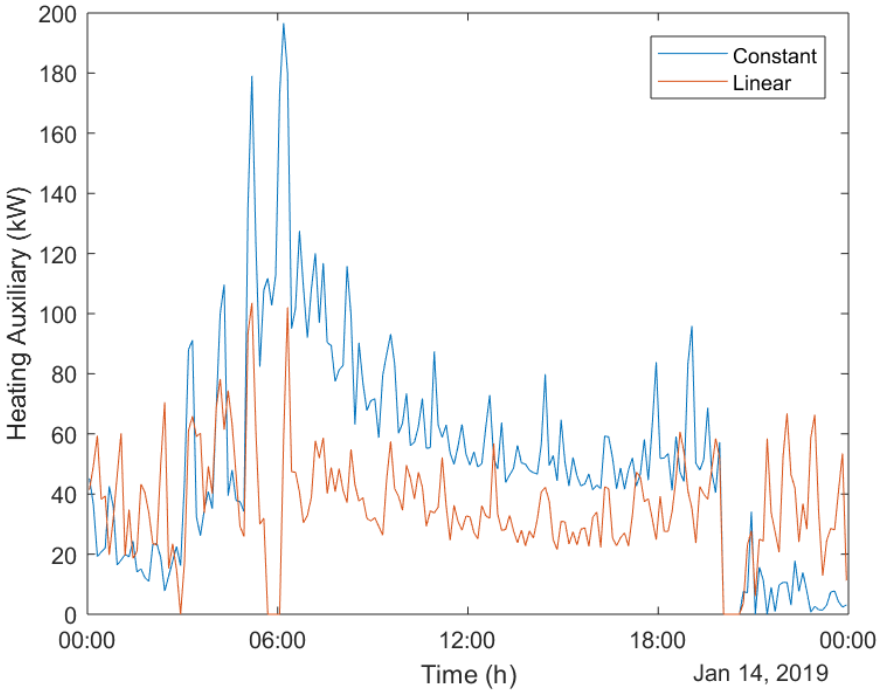

Figure 5.13: Heating auxiliary energy for constant and linear controls

The linear control has an important effect on the residence time of the groundwater into the well, and the SCW outlet temperature is significantly higher with the variable flow rate strategy, especially during the night, as shown in Figure 5.11. The results observed on temperature have a direct impact on the energy exchanged, as shown in Figure 5.12. At the peak, the energy exchanged at the plate heat exchanger is twice as large for the linear control as for the constant strategy. This has a direct impact on the heating auxiliary energy use, which is divided by two at the peak (see Figure 5.13). This will have a major impact on the annual simulation results. Reducing the peak power demand of auxiliary system leads to reduced operating costs, and potentially reduced capital costs if a smaller system can be installed.

5.2.3 Annual Simulation Results

In this section, the variable pumping strategies are compared to *good practice 1*, which is denoted as "GP1" in Figures 5.14 to 5.17. In those figures, linear variable pumping strategies denoted by "Linear 1.5", "Linear 2", etc. correspond respectively to a linear variation with a maximum flow rate of 1.5 GPM/ton, linear variation with a maximum flow rate of 2 GPM/ton, etc.

Figure 5.14 shows the annual energy use for heating and cooling. Variable flow rate control achieves a large reduction in pumping energy use. Between the good practice scenario and the linear scenario using the same maximum value of 3 GPM/ton, we observe that the pumping energy has been divided by almost six. The impact on heating energy use (heat pumps and auxiliary) is minimal, and cooling performance is generally improved, but very low flow rates have a detrimental impact on cooling energy use (the linear 1.5 GPM/ton has the worse cooling energy use).

The best peak power demand is achieved by the linear 2.0 GPM/ton scenario, which seems to offer the best combination of residence time and heat exchange for minimizing auxiliary and heat pump peak power demand.

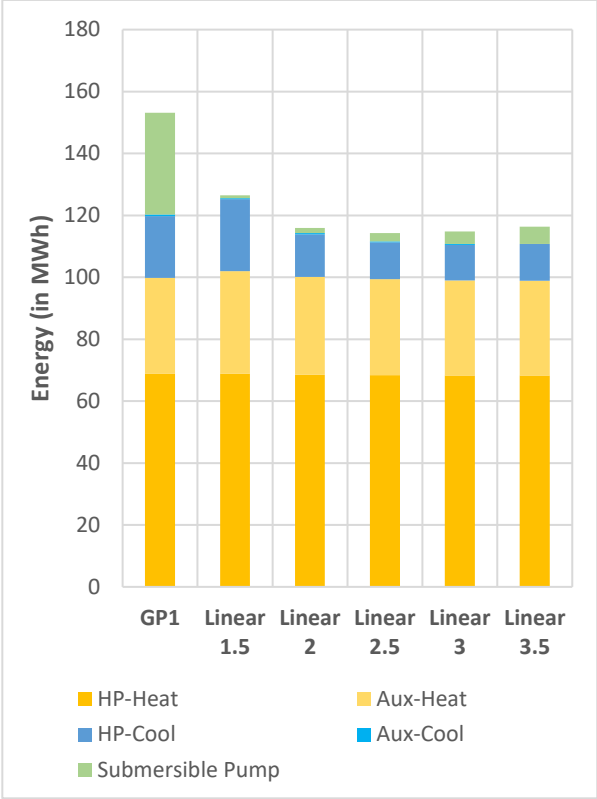

Figure 5.14: Annual energy consumed

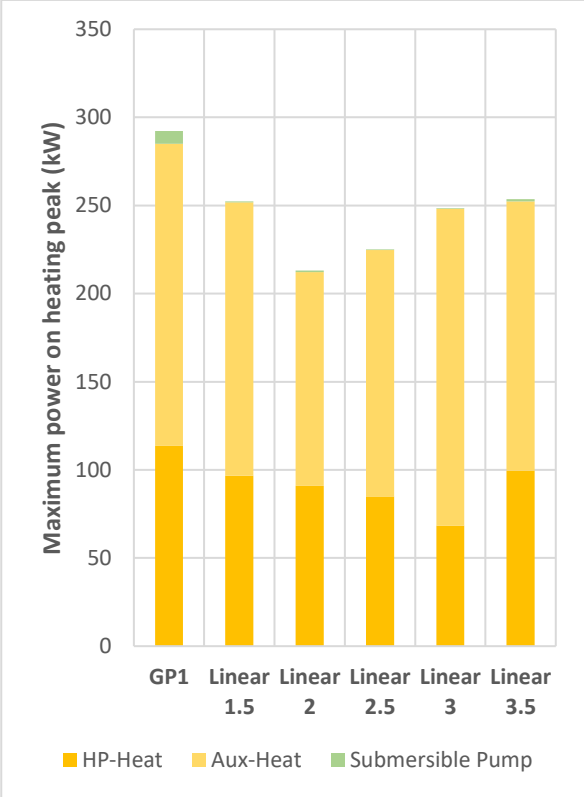

Figure 5.15: Annual peak power demand

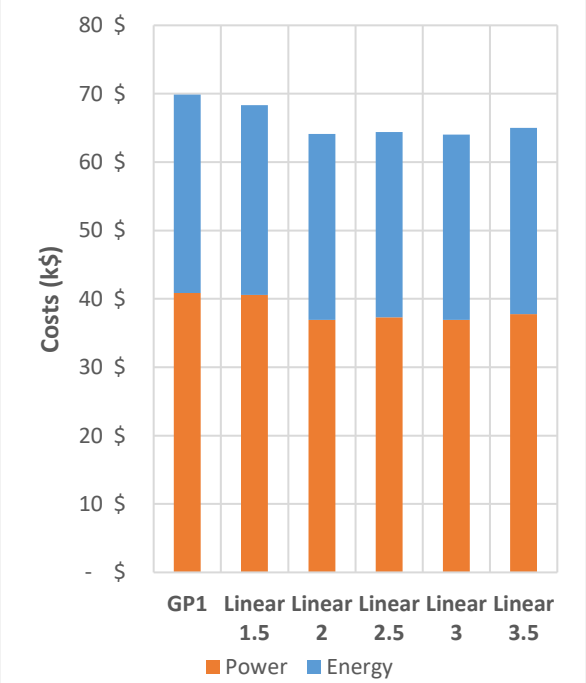

Figure 5.16: Annual costs for the medium office building

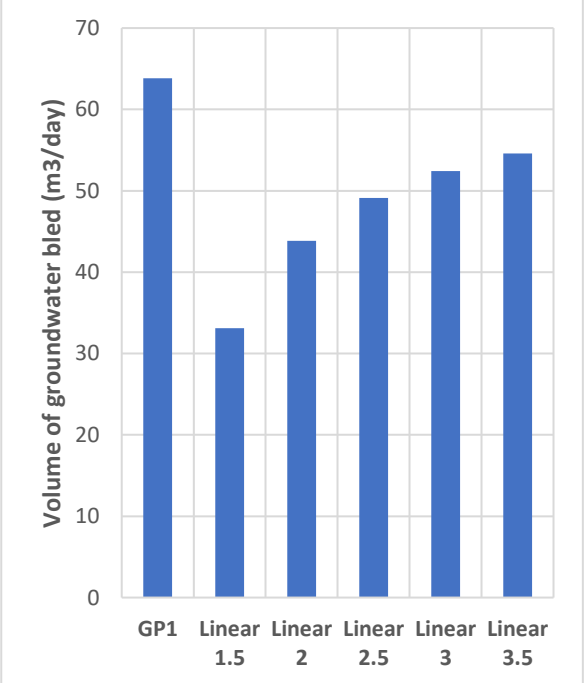

Figure 5.17: Groundwater volume bled

Pumping power makes a very small contribution to the peak power demand, which is partly explained by the fact that the overall building peak demand occurs at a time when the heating load is high.

The linear control strategies studied in this section achieve significant operational cost savings (Figure 5.16), mainly through reduced peak power costs. The largest savings are observed for the 2 GPM/ton linear strategy, with savings of 8.3% on the total annual energy bill of the building (Table 5.2). As observed in the previous section, the total volume of bled water favors strategies with a reduced flow rate (Figure 5.17). Even if the operating costs are close to each other, this would indicate that the preferred scenario is the linear control with a maximum value of 2 GPM/ton.

Table 5.2: Energy, power and total costs for linear control

	Annual Costs					
	Energy		Power		Total	
REF	29 040 $	0,0%	40 850 $	0,0%	69 890 $	0,0%
1.5 GPM/ton	27 750 $	-4,4%	40 570 $	-0,7%	68 320 $	-2,2%
2 GPM/ton	27 190 $	-6,4%	36 910 $	-9,7%	64 100$	-8,3%
2.5 GPM/ton	27 100 $	-6,7%	37 290 $	-8,7%	64 390 $	-7,9%
3 GPM/ton	27 110 $	-6,6%	36 910 $	-9,6%	64 020 $	-8,4%
3.5 GPM/ton	27 210 $	-6,3%	37 790 $	-7,5%	65 000 $	-7,0%

5.3 Linear Control Thresholds Sensitivities

5.3.1 Simulations and Scenarios

The previous sections discussed the results of linear control strategies using the thresholds presented in Figure 5.9. In this paragraph, we investigate the impact of modifying the thresholds used in the control strategies. The considered configurations are summed up in Figure 5.18, while Table 5.3 shows which parameters were modified. All the simulations were run with a maximum flow rate of 2 GPM/ton, which showed the best performance, and the scenario using the thresholds shown in Figure 5.9 (20% and 70%) is referred to as “Reference” in this section.

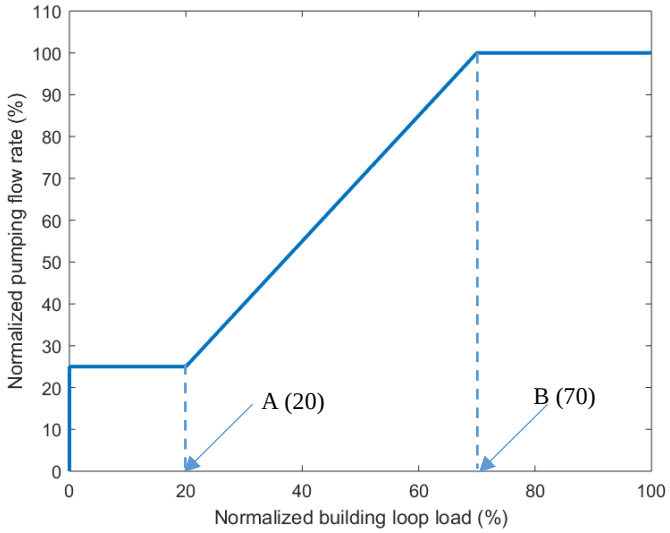

Figure 5.18 : Compared linear control variables

Table 5.3 : Tested thresholds

	A	B
Reference	20	70
Scenario 1 (S1)	10	70
Scenario 2 (S2)	30	70
Scenario 3 (S3)	20	60
Scenario 4 (S4)	20	80

5.3.2 Annual Simulation Results

Annual operating costs with Hydro-Québec rate M (energy and power) are presented in Table 5.4. The thresholds used in section 5.2 offer the best performance, and other scenarios show relatively small differences, with power costs within 4% and energy costs within 1% of the reference (total costs are within 2.5% of the reference).

Table 5.4: Energy, power and total costs for different thresholds

	Annual Costs					
	Energy		**Power**		**Total**	
Reference	27190 $	0,0%	36910 $	0,0%	64100 $	0,0%
Scenario 1	27090 $	-0,4%	37520 $	1,7%	64610 $	0,8%
Scenario 2	27360 $	0,6%	38310 $	3,8%	65670 $	2,5%
Scenario 3	27180 $	0,0%	37280 $	1,0%	64460 $	0,6%
Scenario 4	27235 $	0,2%	37580$	1,8%	64820 $	1,1%

5.4 Conclusion

This chapter aimed at comparing improved control strategies for the circulating (total) flow rate in the SCW, compared to a constant flow rate of 3 GPM/ton (0.054 L s^{-1} kW^{-1}) recommended in the literature. Reducing the constant flow rate increases the residence time in the SCW and reduces the pumping power. The best compromise seems to be significantly lower than the recommended value, at 2 GPM/ton, leading to modest operating cost savings and to a reduced volume of water bled annually.

Figure 5.19 presents an overview of all annual results, showing the volume of water bled and the operating costs on an annual basis. Each dot corresponds to one configuration discussed in the sections above. In the top right corner, we find, in orange, the constant control simulations. The blue dot corresponds to the good practice scenario. All the simulations implemented with linear pumping control (grey dots) operate with reduced operating costs and ground water bled, with an optimum found for the linear 2 GPM/ton strategy, shown as LIN 2 in the figure. Interestingly, even the variants with non-optimal thresholds (Scenarios 1 to 4 discussed in section 5.3) give a better performance than any constant flow rate strategy. The best control strategy (linear flow rate control with a maximum of 2 GPM/ton and the thresholds shown in Figure 5.9) is identified by a triangle (in grey) in the Figure 5.19.

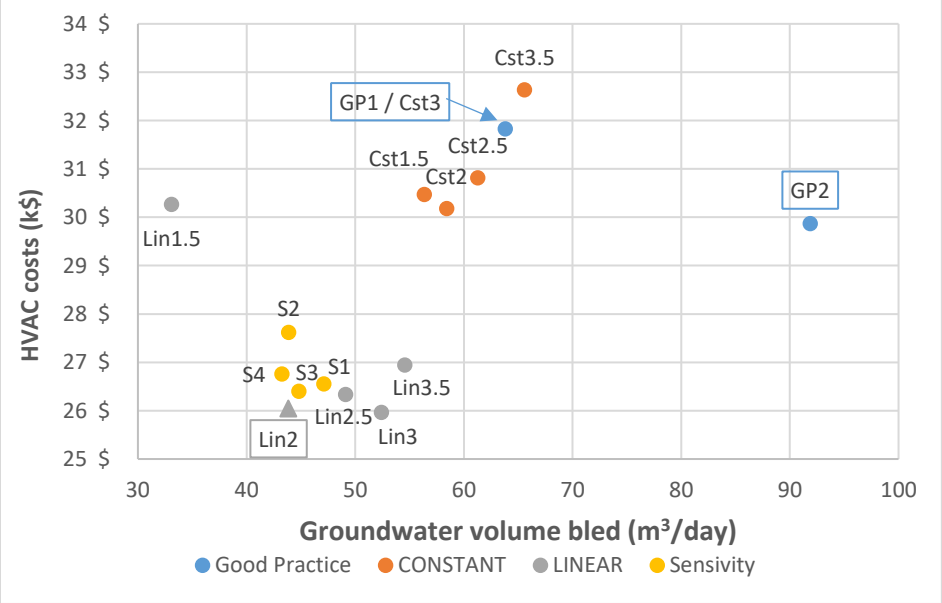

Figure 5.19: Annual operating cost vs. annual volume of groundwater bled

Figure 5.20 shows the annual COP as a function of the average volume of groundwater bled on an annual basis with the same color code as figure 5.19. All scenarios except for the constant 3.5 GPM/ton operates at a better annual COP compared to the good practice scenarios while the volume of groundwater is reduced. From that perspective, an optimum is found for the 2.5 GPM/ton linear strategy. However, the COP is an indicator that focuses on the energy consumption versus the energy provided to the system. Figure 5.19, with the cost calculation, shows a different optimum because the electricity rate includes a condition for peak power demand.

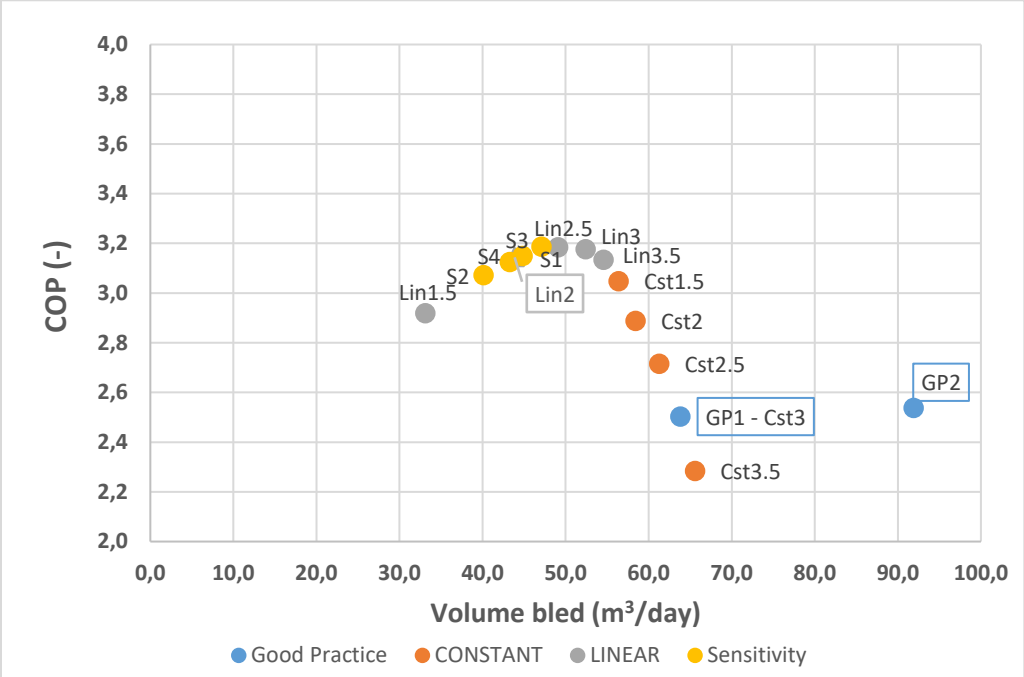

Figure 5.20: Annual COP vs. annual volume of groundwater bled

CHAPTER 6 BLEED FLOW RATE CONTROL STRATEGY

The total pumping flow rate discussed in the previous chapter is one of the two control variables chosen to optimize the operation of a SCW. The bleed flow rate, i.e. the fraction of the total flow rate which is diverted to an injection well instead of being reinjected into the SCW, is the second control variable. This chapter investigates different control strategies for the bleed flow rate and their impact on energy use, peak power demand, operating costs, and volume of water bled. This master's thesis focuses on cold climate operation, so the different control strategies are optimized and assessed in heating mode only. In cooling mode, a reference bleed flow rate control strategy from the literature is used (Spitler et al., 2002) which relies on thresholds and dead-bands (see chapter 2). Section 6.1 presents an overview of the different bleed ratio control strategies that will be compared. Section 6.2 shows the impact of these strategies on the system operation on the peak heating day, and section 6.3 presents annual results.

6.1 Control Strategies

In the following discussion, the bleed ratio is always expressed as a percentage of the maximum total pumping flow rate. For example, if a strategy uses the best pumping flow rate strategy identified in the previous chapter, the total flow rate will be linearly modulated between 0.5 and 2 GPM/ton (0.009 and 0.036 L s^{-1} kW^{-1}). In that case, a bleed ratio of 10 % would represent 10 % of 2 GPM/ton, not 10 % of the actual total flow rate at that time.

All control strategies studied in this chapter are presented in Table 6.1. The reference scenarios named *Good practice 1 and 2*, are described in section 3.5. The first set of simulations covers a constant bleed ratio of 0%, 5%, 10%, 15%, and 25 % of the maximum pumping flow rate with a dead-band control inspired from the literature (Spitler et al., 2002). The second set is based on a linear control of the bleed ratio with a 25% maximum and a 0% or 5% minimum. These control strategies are illustrated in Figure 6.1. The third and fourth sets of control strategies modulate the bleed ratio as a function of the maximum load over a prediction horizon (3, 6, 9, 12 or 24 hours ahead) – the difference between the 3rd and 4th sets is the minimum bleed ratio (see Table 6.1). All sets (1 to 4) use the pumping flow rate control strategy that was shown to deliver the best

performance in the previous chapter: 2GPM/ton maximum flow rate with a linear modulation according to the load.

Table 6.1: Summary of the control strategies implemented for bleed ratio

Scenario		**Maximum Bleed Flow Rate (% max pumping)**	**Minimum Bleed Flow Rate (% max pumping)**	**Predictive Control**	**Pumping Flow Rate**
Good practice 1		10% (Dead-Band control)	No	No	3GPM/ton
Good practice 2		25% (3-level bleed)	No	No	
Constant (activated with dead-band)	1.a	0	No	No	2GPM/ton with linear modulation (see chapter 5 for a description of the modulation)
	1.b	5%	No	No	
	1.c	10%	No	No	
	1.d	15%	No	No	
	1.e	25%	No	No	
Linear	2.a	25%	No	No	
	2.b	25%	5%	No	
Predictive Linear with min	3.a	25%	5%	3h	
	3.b	25%	5%	6h	
	3.c	25%	5%	9h	
	3.d	25%	5%	12h	
	3.e	25%	5%	24h	
Predictive Linear no min	4.a	25%	No	3h	
	4.b	25%	No	6h	
	4.c	25%	No	9h	
	4.d	25%	No	12h	

Note that in Table 6.1, Scenario 1.d is in fact the same as the best scenario in Chapter 5. In that chapter, the bleed ratio was expressed compared to a fixed reference of 3 GPM/ton, to clarify the discussion. In this chapter, bleed ratio is expressed compared to the maximum pumping flow rate of each control strategy. Thus, Scenario 1.d uses 15% of 2 GPM/ton, which is equivalent to 10% of 3 GPM/ton.

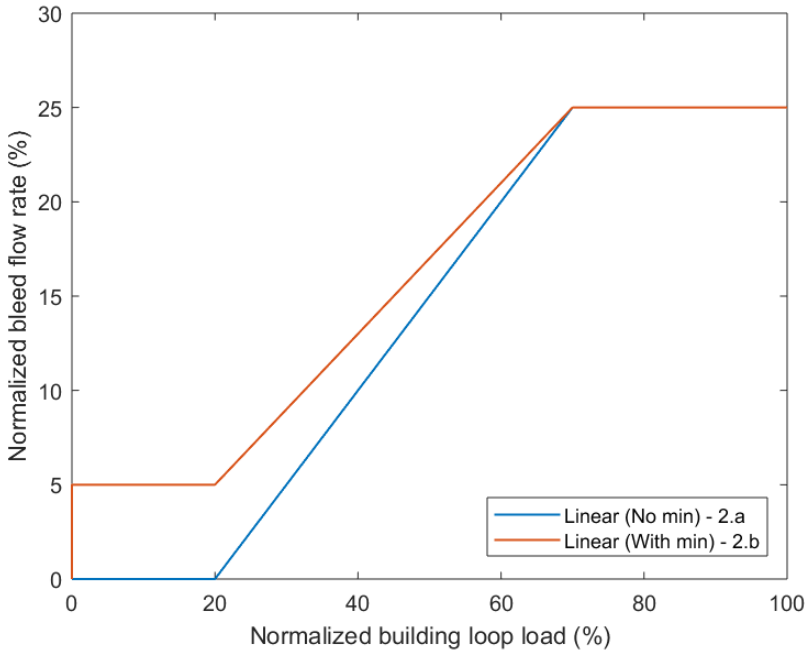

Figure 6.1: Bleed ratio linear control with minimum (orange) without minimum (blue)

6.1.1 Building Load for Predictive Strategies

As mentioned above, strategies 3 (3a to 3e) and 4 (4a to 4d) rely on a prediction of the heating load for a given horizon. The heating load which is of interest here is the building loop load, as opposed to the actual heating load of the building. The heat pump COPs are influenced by the building loop supply temperature, so an accurate prediction of the building loop load would require an iterative process in which the predicted load would depend on the SCW behavior. A simplified approach was adopted, where average annual COPs are used for all distributed heat pumps. With that simplification, the actual heating load of each zone (and that of fresh air) can be converted into a load on the building loop. We assume perfect forecasts of the weather data and occupant behavior, so that heating loads are simply taken from a previous simulation which uses the good practice SCW control strategy (circulating flow rate of 3GPM/ton and bleed flow rate of 10% of 3 GPM/ton controlled by dead-band). The calculated building loop load is processed by calculating the maximum value over different prediction horizons, which are then written to a file to be read during simulations of “predictive control” strategies.

6.2 System Behavior on the Peak Heating Day

6.2.1 Control Strategies with Constant Bleed Ratios (1.a to 1.e)

The literature review indicated that a 10 % bleed ratio is commonly used for SCWs. However, higher bleed ratios could help the system to cope with peak loads (Spitler et al., 2002), and SCWs are typically capable of operating with bleed ratios between 0 and 30 % (Pasquier et al.,2016). It seemed interesting to investigate the impact of different constant-bleed strategies on the system behavior in peak conditions.

Figure 6.2 shows the SCW inlet and outlet temperatures for three different cases: No bleed, 10% bleed ratio (*good practice* 1) and 25% bleed ratio. The heating load is high between 6 AM and 8 PM, when the building is occupied, heating setpoints are at their "day" value (22 °C) and the ventilation system conditions large amounts of fresh air. During this period, the outlet temperature is below 3 °C without bleed, while the inlet temperature is around 1 °C, indicating that auxiliary heating is activated. This is confirmed in Figure 6,3, which shows large peaks in auxiliary heating power. The behavior is slightly improved with a 10 % bleed ratio, with a slightly higher SCW outlet temperature and a slightly reduced auxiliary heating power. A much larger bleed ratio (25 %) increases the heat transfer on the heat exchanger source side significantly (Figure 6.4), showing a higher amount of heat extracted from the SCW and a higher outlet temperature. The auxiliary heating power is much reduced in this case. First, we can observe that the inlet temperature in the three cases are close to each other especially for the first two cases (no bleed and 10%). The difference between inlet temperature is the smallest during day time when the load needed from the SCW is important. In fact, every building zone need fresh air and a temperature maintained at 22 ˚C. During the night, the load needed is low and the impact of bleed ratio is more visible, with a higher difference between the cases. But the main difference is on the outlet temperature or more specifically on the temperature difference between inlet and outlet temperature of the SCW. In the case where bleed is not used, the temperature difference reaches at most around 3.5 ˚C during the night and is only 2 ˚C during the day. For the 10% bleed ratio the values are respectively 4.5 ˚C and 2.5 ˚C while they are 6 ˚C and 3 ˚C for the case with a 25% bleed. This relates to Figure 6.4, the energy exchange with a higher bleed ratio is more important and helps to lower the peak demand from auxiliary heating system (figure 6.5).

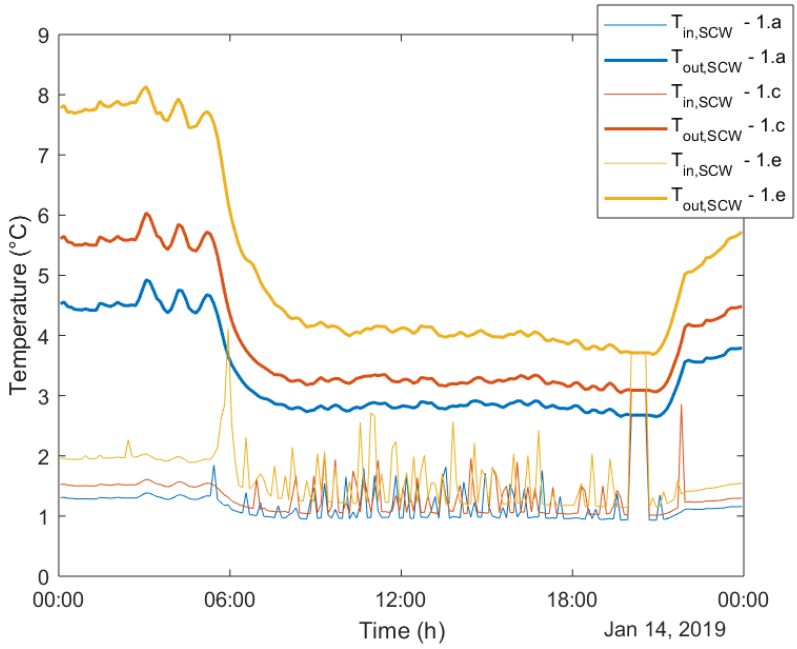

Figure 6.2: Inlet and outlet temperature of SCW for No bleed (1.a), 10% (1.c) and 25% (1.e) bleed ratio

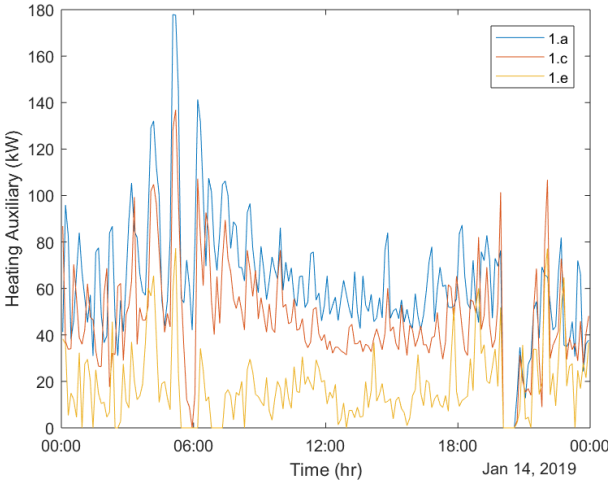

Figure 6.3: Heating auxiliary power for No bleed (1.a), 10% (1c) and 25% (1.e) bleed ratio

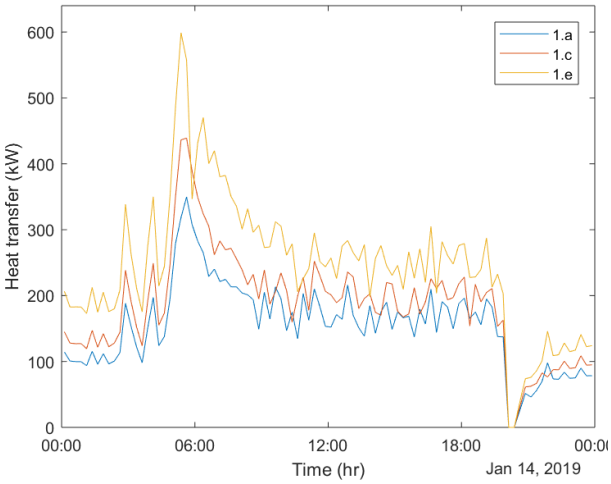

Figure 6.4: Heat transferred on source side of HX for No bleed (1.a), 10% (1.c) and 25% (1.e) bleed ratio

From the temperature observed and the dead-band control it appears that in all cases bleed is activated constantly throughout the day (bleed would stop if the outlet temperature of the SCW reaches 8.5 ˚C, which never happens on that day).

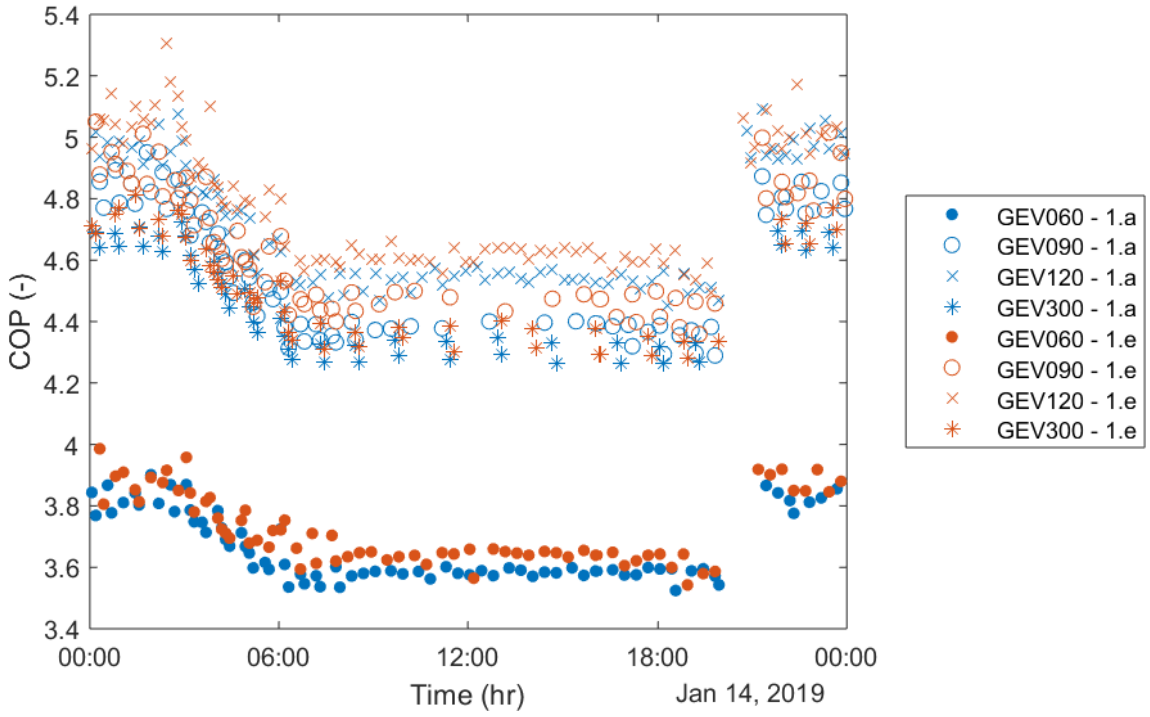

Figure 6.5: COP of heat pumps for the four models implemented in a no bleed and 25% bleed ratio scenario

The effect of a higher bleed ratio leads to higher temperature coming back from the well and then going in the heat pumps inlet. Figure 6.5 shows the COP of four selected heat pump models for that day in the two extreme configurations: No bleed and 25% bleed ratio. The increase of the temperature shows a little effect on the heat pumps COP, less than 0.1 difference between the two cases.

Even though the 25% bleed ratio shows good performance, especially for the peak auxiliary demand, it also asks for more pumping energy (twice as large as without bleed) and more groundwater is bled from the well. Section 6.3 will discuss groundwater volume bled and costs for all strategies presented.

Table 6.2: Summary of pumping energy and groundwater bled for no bleed, 10% and 25% bleed ratio during the heating peak day

Daily Values	**No Bleed**	**10% Bleed**	**25% Bleed**
Pumping Energy (kWh)	20.8	31.2	44.8
Groundwater Bled (m^3)	0	20	50

6.2.2 Linear Control for Bleed Flow Rate

In order to reduce the volume of groundwater bled, it seemed interesting to reduce the bleed ratio when the load is lower, e.g. by modulating the bleed ratio proportionally to the load. This section describes and compares three cases:

- 1.c: the good practice for bleed ratio (10% with dead band control) described above
- 2.a: linear control of bleed ratio with no minimum bleed ratio with a 25% maximum.
- 2.b: linear control of bleed ratio with a minimum bleed ratio with a 25% maximum.

The bleed flow rate occurring during the peak heat day is illustrated in Figure 6.6. The bleed rate with the good practice (1.c) is virtually constant, as the well is already cold from operations during the previous days. This leads to a high bleed flow rate throughout the day and night, even when the heating load is relatively small. Strategies 2.a and 2.b reduce the bleed flow rate at night but increase it during the day. The SCW outlet temperature is higher for strategy 1.c, leading to a reduced auxiliary heating load, even though the auxiliary heater is ON during the whole day for the 3 scenarios (see Figure 6.8). The reduced bleed ratio in 2.a and 2.b during the night has a negative impact on the SCW outlet temperature and heat exchange (Figure 6.7) during the morning peak, even though the bleed flow rate during that peak is increased. This seems to demonstrate the need to anticipate the morning peak when controlling the bleed ratio to “prepare” the well for a higher heat exchange, which resulted in the predictive scenarios investigated in section 6.2.3.

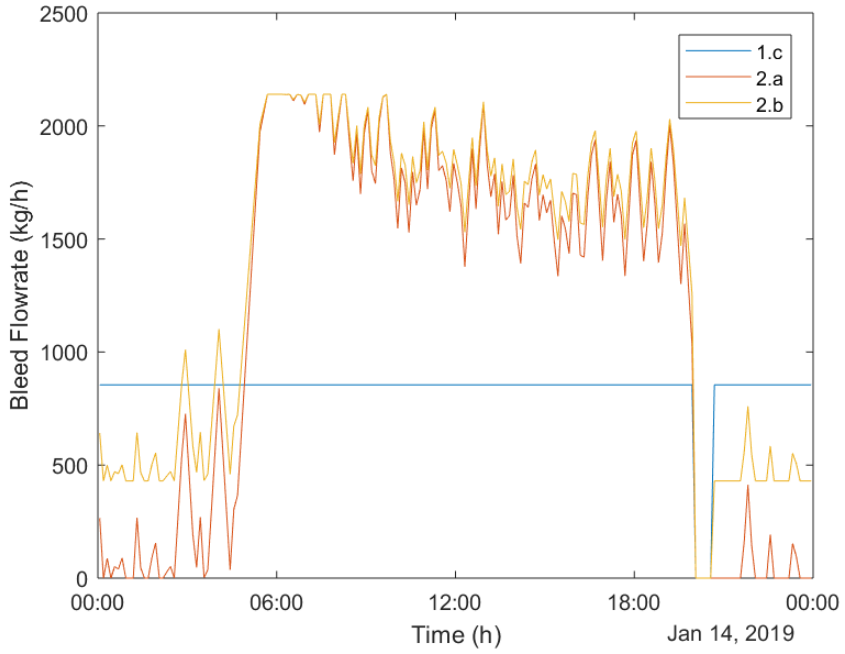

Figure 6.6 : Illustration of the bleed flow rate implemented in configurations 1.c, 2.a and 2.b during peak heating day.

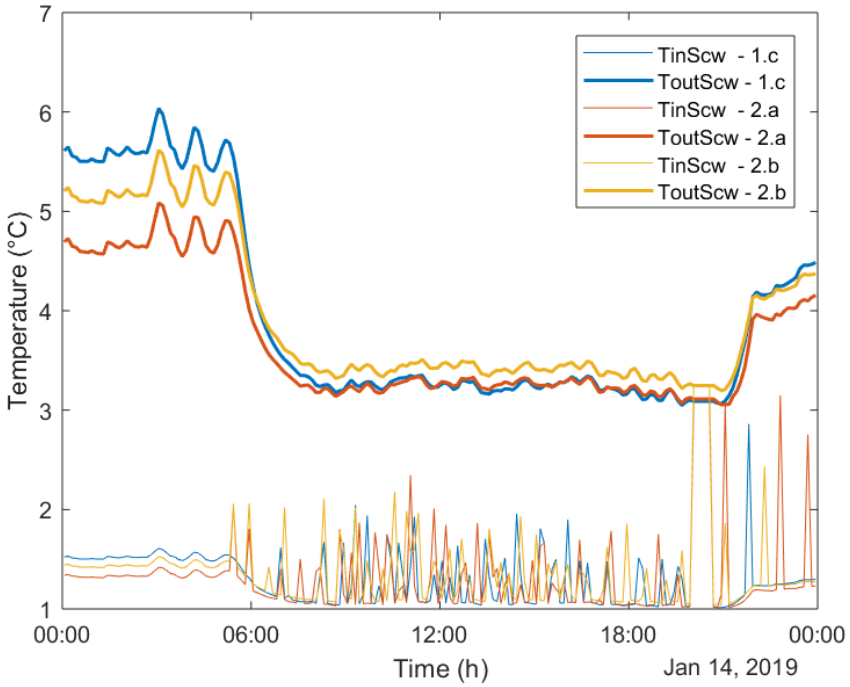

Figure 6.7: Inlet and outlet temperature of SCW for 1.c, 2.a and 2.b configuration

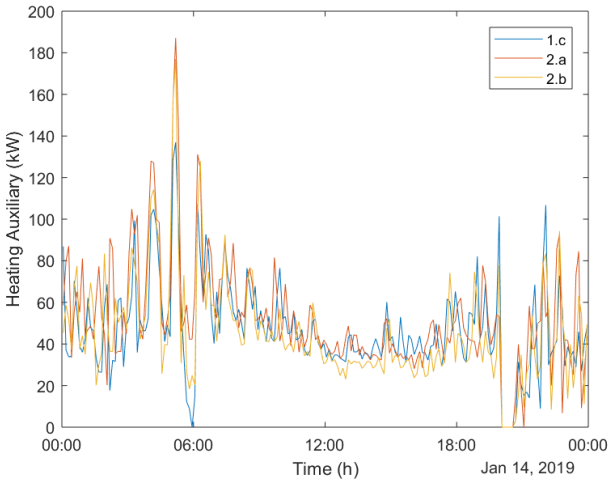

Figure 6.8 : Heating auxiliary power for configurations 1.c, 2.a and 2.b

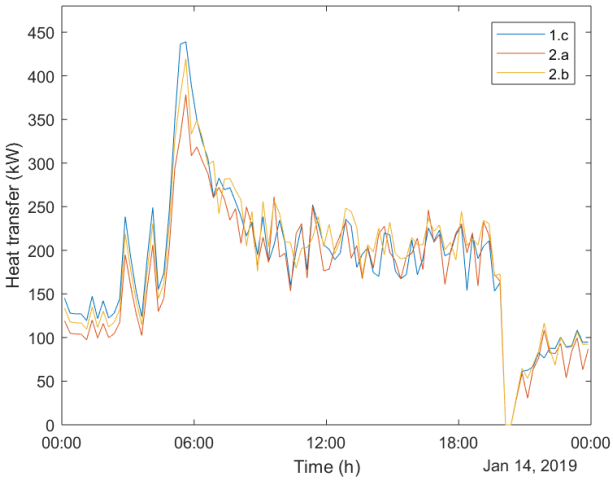

Figure 6.9 : Heat transferred on source side of HX energy for configurations 1.c, 2.a and 2.b

6.2.2.1 Sensitivity for Linear Bleed Rate Control

Scenarios 2.a and 2.b use the thresholds represented in Figure 6.1. In this section, 6 "excursion cases" implementing different thresholds of parameters A, B, and C illustrated in Figure 6.10 are investigated. The variants are also summed up in Table 6.3.

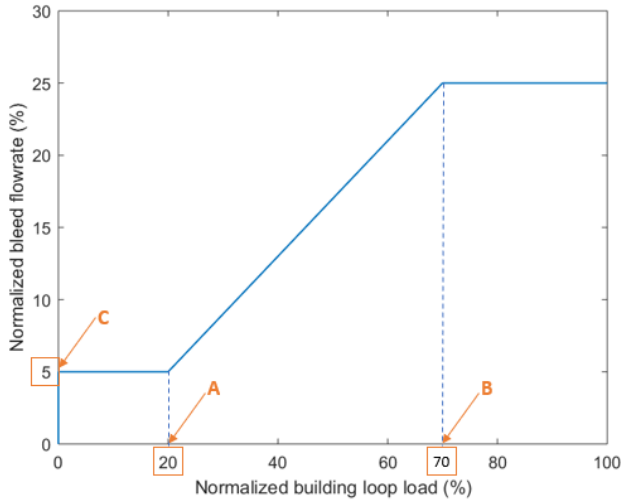

Figure 6.10: Illustration of the parameters tested in the sensitivity study for linear control of bleed flow rate

Table 6.3 : Summary of the cases tested in this sensitivity study

Parameter	A	B	C
Simulation Ref (2.b)	20	70	5%
Simulation 1	10	70	5 %
Simulation 2	30	70	5 %
Simulation 3	20	60	5 %
Simulation 4	20	80	5 %
Simulation 5	20	70	2.5 %
Simulation 6	20	70	7.5 %

Table 6.4 presents the annual results for all simulations. The variation of the parameter A (Simulations 1 and 2) shows an important variation of the ground water bled. Simulation 1 increases the volume of groundwater by 18% that leads to a reduction of the costs by 4%. The second simulation is interesting because the volume bled is reduced by almost 14% while maintaining the costs at the same level (0.2% variation). Concerning parameter B (Simulations 3 and 4), its variation increases the costs by less than 1% in both cases but simulation 3 increases the volume bled by 7% while simulation 4 decreases by 5%. Finally, the variation of the minimum bleed ratio (Simulations 5 and 6) shows the most important variation of the ground water volume bled (by almost 30%), with a comparatively smaller impact on operating costs.

Table 6.4: Summary of HVAC costs, energy and peak power demand of the building and groundwater volume for a yearly simulation

Simulation	Groundwater Volume (m^3)	Costs ($)	Energy (kWh)	Peak power demand (kW)
Ref (2.b)	2012	29 420 $	179897	292
1	2368 (17.7%)	28 140 $ (-4.3%)	177575 (-1.3%)	286 (-2.0%)
2	1738 (-13.6%)	29 350 $ (-0.2%)	181466 (0.9%)	301 (3.1%)
3	2148 (6.8%)	29 680 $ (0.9%)	179057 (-0.5%)	306 (4.7%)
4	1912 (-5.0%)	29 590 $ (0.6%)	180393 (0.3%)	299 (2.3%)
5	1416 (-29.6%)	30 220 $ (2.7%)	182988 (1.7%)	310 (6.2%)
6	2598 (29.1%)	27 700 $ (-5.8%)	176549 (-1.9%)	287 (1.7%)

6.2.3 Predictive Control

6.2.3.1 Predicted Load

As mentioned above, strategies 3 (3a to 3e) and 4 (4a to 4d) rely on a prediction of the heating load for a given horizon. The heating load which is of interest here is the building loop load, as opposed to the actual heating load of the building. The heat pump COPs are influenced by the building loop

supply temperature, so an accurate prediction of the building loop load would require an iterative process in which the predicted load would depend on the SCW behavior. Similarly to what was done in Section 6.1.1, a simplified approach was adopted where average annual COPs are used for all distributed heat pumps. The actual heating load of each zone (and that of fresh air) can be converted into a load on the building loop with that assumption. We assume perfect forecasts of the weather data and occupant behavior, so that heating loads are simply taken from a previous simulation which uses the good practice SCW control strategy (circulating flow rate of 3GPM/ton and bleed flow rate of 10% of 3 GPM/ton controlled by dead-band also known as *Good Practice 1*). The calculated building loop load is processed by calculating the maximum value over different prediction horizons, which are then written to a file to be read during simulations of "predictive control" strategies.

The predictive strategies use the maximum building loop load over the forecasting horizon, which is illustrated in Figure 6.11 for a 3-h horizon: at a given time step, the load used to control the bleed rate is the maximum value that will occur within the next 3 hours. This method was selected over using the average (or integrated) load over the horizon after a trial-and-error process.

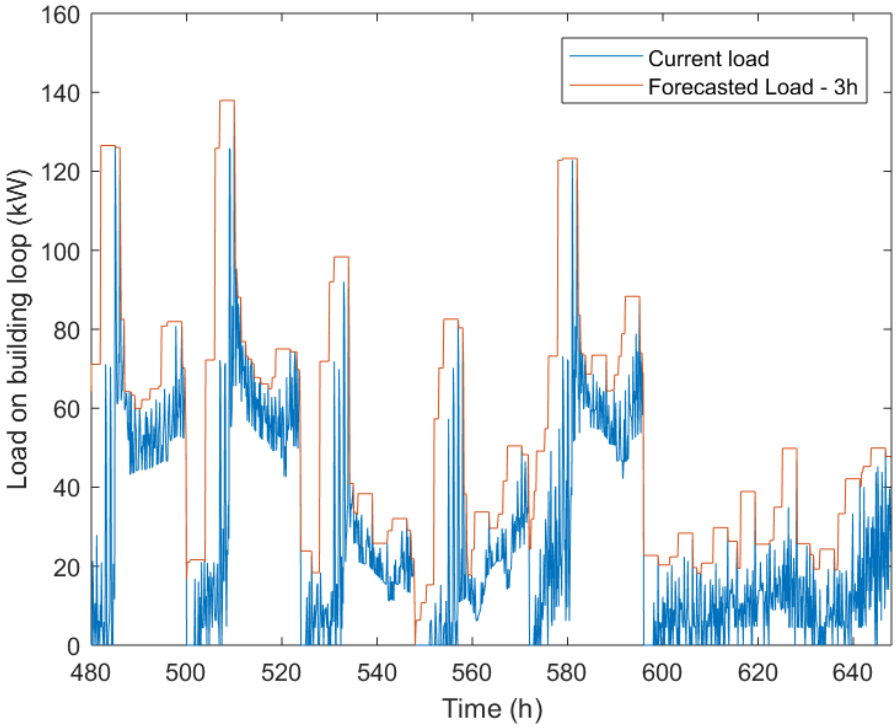

Figure 6.11: Current and forecasted load for the third week of the year using a 3-h horizon

6.2.3.2 Results

This section discuss the impact of predictive control strategy for bleed flow rate on peak heat day for simulation 2.b, 3.a and 4.a. Several periods of prediction were implemented and are presented with annual results in the next section, the curves shown here concern a 3h prediction period.

Controlling the bleed ratio on the future load on the building loop leads to a higher outlet temperature by almost 1 ˚C with the non-predictive linear control during night time and 0.3 ˚C during day time. When implementing a control strategy with no minimum bleed ratio, the increase of the outlet temperature is reduced but is still more interesting than a situation with no predictive control. The impact on temperature shows a diminution of the auxiliary system needs (Figure 6.13).

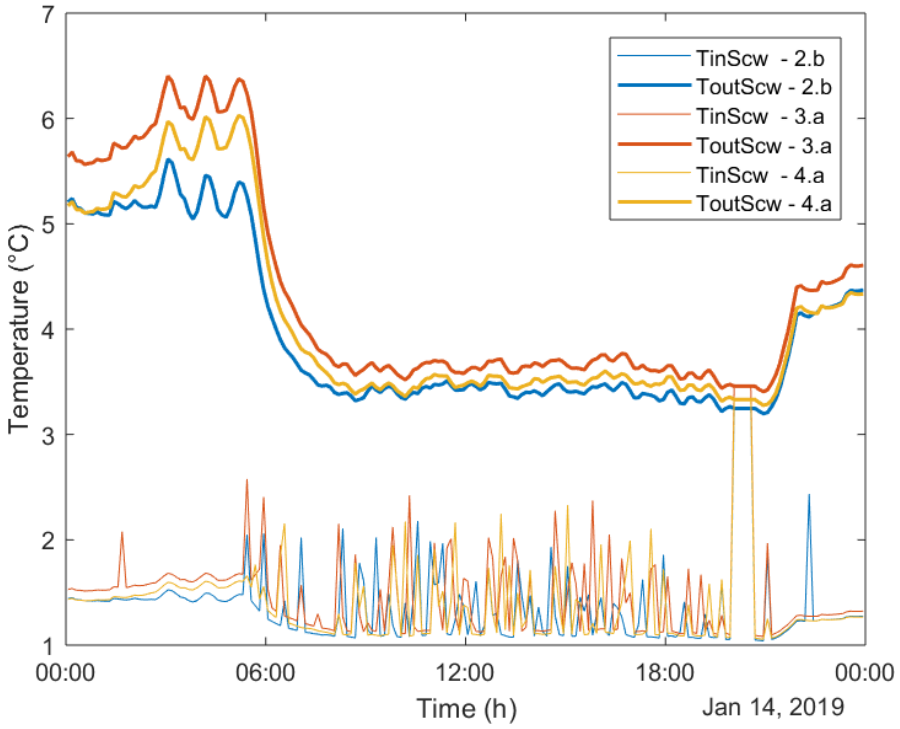

Figure 6.12 : Inlet and outlet temperature of the SCW for 2.b, 3.a and 4.a configuration

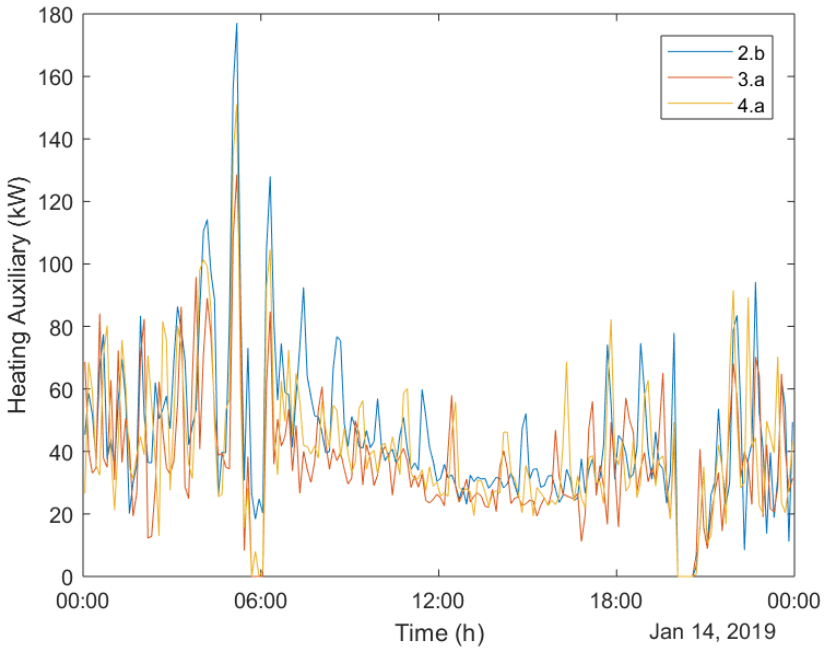

Figure 6.13 : Heating auxiliary energy for 2.b, 3.a and 4.a configurations

6.3 Annual Results

Figure 6.14 is divided in two parts and sums up the results for all simulations described in Table 6.1: (a) describes the annual costs and (b) shows the volume of groundwater annually bled in each case. In these graphs, the good practice or reference scenarios are colored in yellow and the optimum case found by pumping optimization in Chapter 5 is colored in red.

Scenarios 1.a to 1.e use a constant bleed rate activated by a dead-band. Their results show that increasing the bleed ratio beyond 15% seems unnecessary, as there are no cost savings but a significant increase in the volume of groundwater bled. It is interesting to note that 15% of 2 GPM/ton represents a flow rate of 0.3 GPM/ton, which is the same absolute value as the common practice identified in the literature review (10% of 3 GPM/ton).

Scenarios 2.a and 2.b are better than the *good practice 1 and 2* (GP1 and GP2) but cannot deliver a performance improvement compared to scenarios 1 – as mentioned above, controlling the bleed rate based on the current load does not seem to be an interesting option. A comparison between 2.b and 1.c, for example, shows that to bleed the same amount of water more continuously is better than reducing the bleed rate at night and increasing it at peak time.

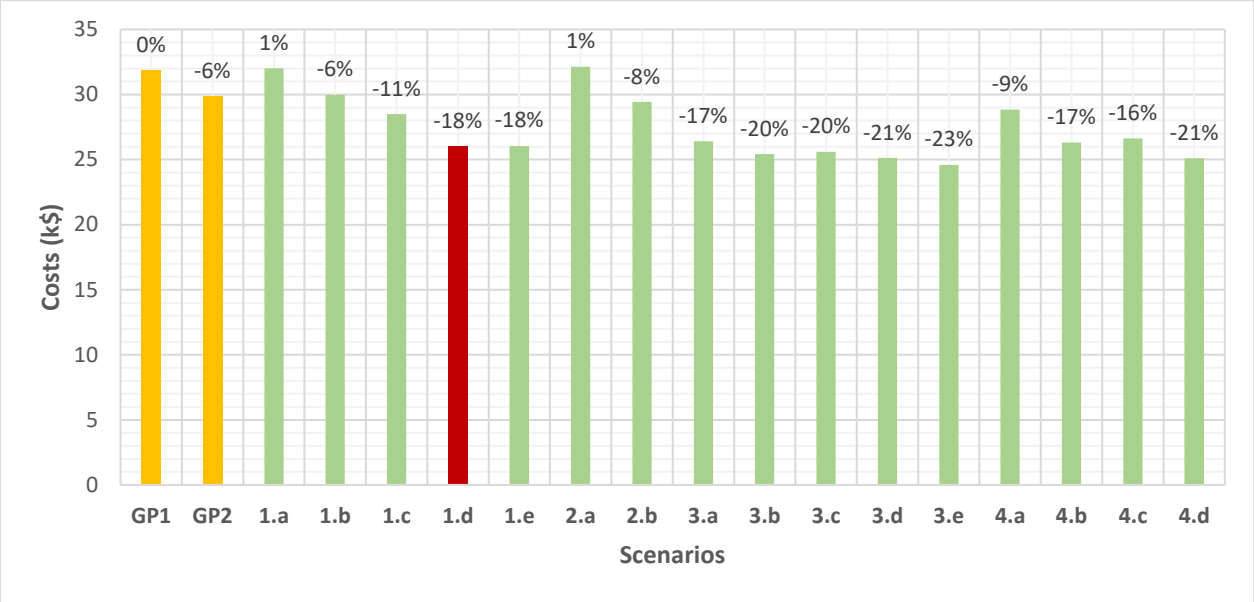

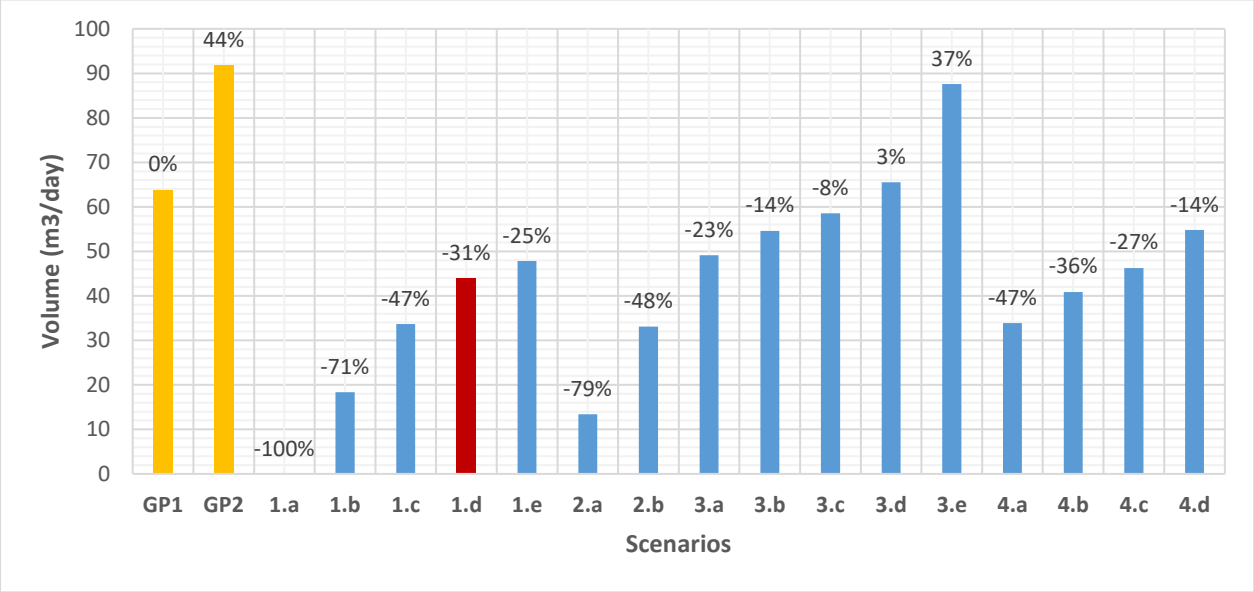

Figure 6.14 : Annual results for HVAC costs (a) and groundwater bled (b) for all configurations

The first set of predictive control with minimum bleed ratio shows cost savings of 17% to 23%. As the control depends on the maximum load occurring over the forecasting horizon, the volume bled is increasing with the duration of that prediction horizon. In particular, the 12-h and 24-h horizons lead to more water being bled compared to the good practice. A comparison between scenarios 3

and 4 shows that removing the minimum bleed ratio is beneficial, leading to similar costs with a much-reduced volume of water bled.

6.4 Conclusion

To conclude this chapter, the bleed control strategy has a major impact on the auxiliary power demand especially when operated before the morning peak so the well temperature is higher when the morning peak appears. The bleed control strategies seem to have little impact on the heat pumps COP since the variations of their inlet temperature are relatively small.

Figure 6.15 sums up all the strategies presented and discussed in this chapter as a function of the costs from HVAC systems and the volume of groundwater bled for annual simulations. All tested strategies offer a better overall performance than the *good practice* cases, showing reduction in costs and/or volume of water bled. A striking result is the comparison between scenario 1.a (which does not include bleed) and GP1: even without bleed, the 1.a operational costs are within 1% of the GP1 results.

All scenarios seem to show a similar trend of increasing groundwater volume bled for decreasing costs. Scenario 1.d (2 GPM/ton flow rate with linear modulations, and dead-band activated bleed rate of 15%) offers a good compromise between cost and water volume. Predictive control scenarios 4.b and 4.d offer a marginally better performance (with respectively slightly less water bled and slightly reduced operating costs), but their interest is questionable, keeping in mind that they would be more complex to implement and were assessed assuming perfect forecasts. Figure 6.16 shows the annual COP versus the volume of groundwater bled. Again, there seems to be a linear trend between the annual COP and the volume of water bled, with a significant potential for improvement compared to good practice.

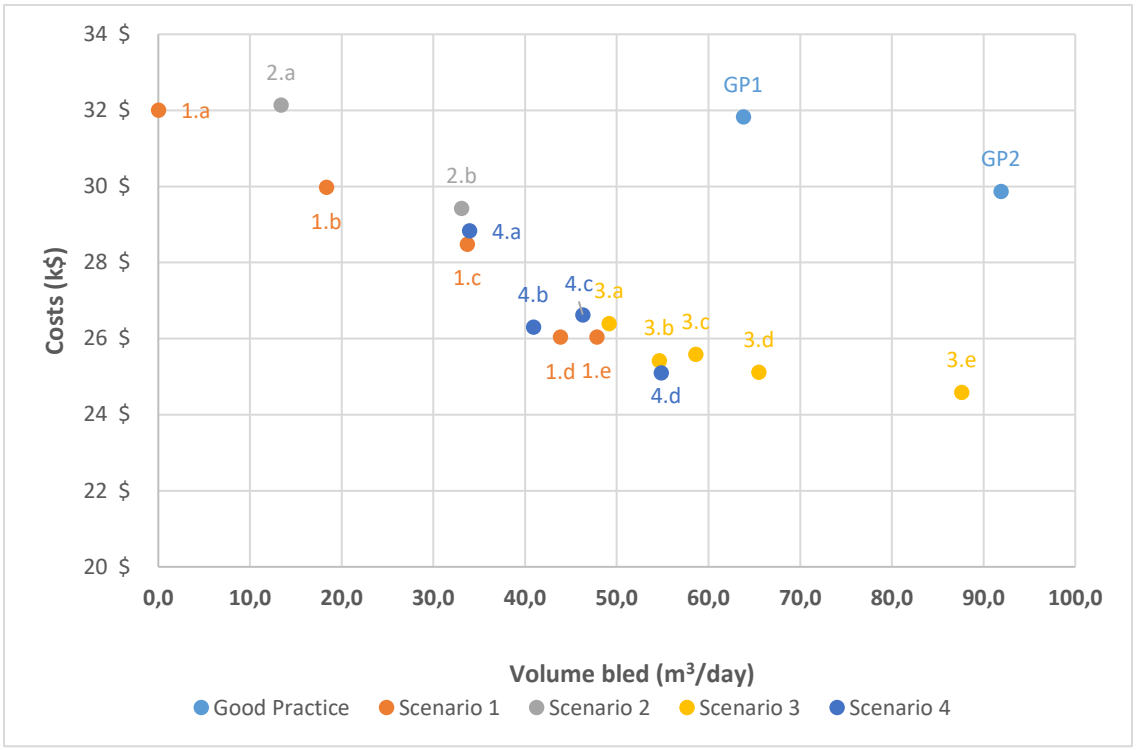

Figure 6.15 : Annual operating cost vs. annual volume of groundwater bled

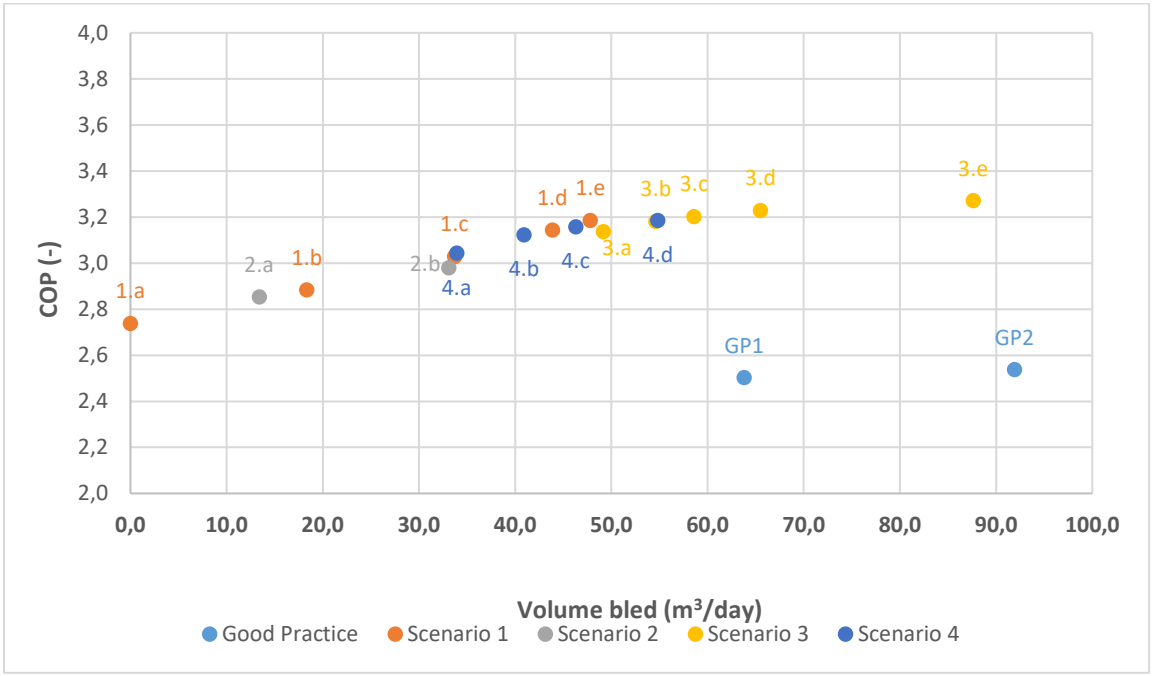

Figure 6.16 : Annual COP vs. annual volume of groundwater bled

CHAPTER 7 BUILDING CONTROL STRATEGIES AND OVERALL RESULTS DISCUSSION

The operation of SCW systems is mainly affected by pumping and bleed flow rate, as illustrated in the previous chapters. But these systems are also sensitive to control strategies selected for the building itself (in particular ramping up and down strategies to cope with the morning peak) and the auxiliary heating and cooling systems. This chapter presents an assessment of these two aspects, leading to a general discussion of all control strategies investigated in this master thesis.

7.1 Building Heating and Cooling Setpoints

The default setpoint profile for office buildings in the National Energy Code for Buildings (NECB) (CNRC, 2011) is shown in Figure 3.9. The heating setpoint during the day is set to 22 °C, with a night setback to 18 °C (also used during weekends and holidays). In the morning, the heating setpoint is raised to 20 °C for one hour before increasing to 22 °C, acknowledging the fact that most buildings cannot recover from a 4 °C setback in less than 2 hours – but this ramp still leads to large heating peaks in the mornings, particularly on Mondays. The cooling setpoint has no value at night or on weekends and holidays (the NECB indicates that cooling is "OFF"), so that the building temperature could reach high values and cause a significant peak in the morning after a warm and sunny weekend or holiday period.

One simple alternative to the NECB schedule to reduce the morning peaks would be to keep the day setpoints at all times, canceling the heating setback and cooling setup. This "Constant" scenario is represented in Figure 7.2. This scenario induces the lowest heating and cooling peaks but results in a higher annual energy use.

Several alternative setpoint profiles offering a compromise between the aggressive NECB setback and the increased energy use caused by constant setpoints were investigated. A trial-and-error process resulted in selecting the setpoint profile shown in Figure 7.3. This "smoother" scenario ramps the setpoints up (for heating) or down (for cooling) over 4 hours and will be referred to as the "Ramping" scenario.

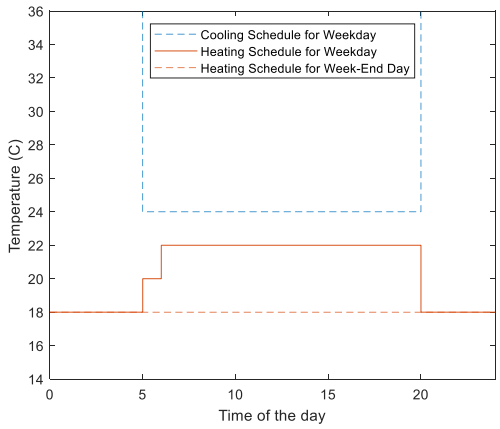

Figure 7.1: NECB setpoint profile

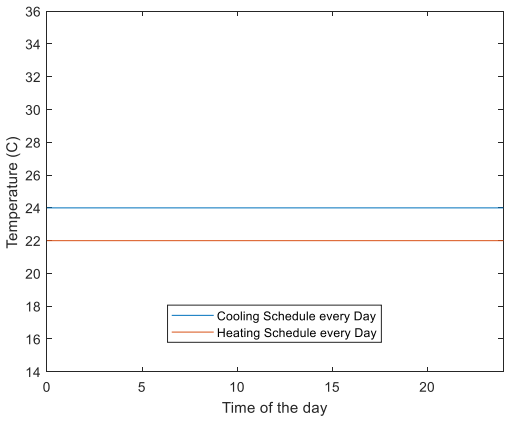

Figure 7.2: Constant setpoint profile

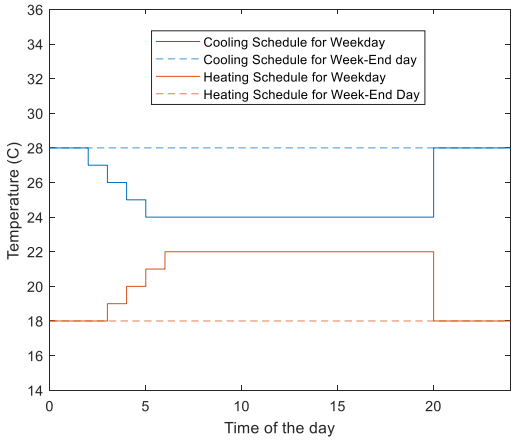

Figure 7.3: Ramping setpoint profile

These three setpoint profiles were simulated and the results for energy consumption and peak power demand of the building and HVAC costs are summed up in Table 7.1. These results were obtained with *Good Practice 1* control scenario for pumping power and bleed ratio.

Table 7.1: Peak power demand, annual energy use and costs for different setpoint profiles

	Energy		**Power**		**Costs**	
	kWh	%	kW	%	$	%
NECB	576 800	-	347	-	33 930	-
Constant	609 520	5,7%	265	-23%	26 610	-22%
Ramping/GP1	581 890	0,9%	328	-5%	31 830	-6%

The Constant setpoint profile achieves a significant reduction of the peak power but at the cost of a higher energy use. With the particular structure of Hydro-Québec M rate, which gives an important weight to peak power, the operating costs are significantly reduced, by over 20 %. A positive side effect of such a peak power reduction is that the required capacity for the auxiliary heating system would be reduced, likely reducing the associated capital cost.

The Ramping scenario offers a compromise between operating cost reduction and increased energy use, reaching an overall 6% cost reduction with an annual energy use 5% below the NECB scenario. This setpoint profile has been selected to assess pumping and bleed ratio control strategies in previous chapters. The rationale for selecting it over the constant profile despite a higher operating cost is as follows:

- GSHP systems in general, and SCW systems in particular, are often installed with an objective of reducing building energy use. It seemed unlikely that building operators would select operating setpoints that go against this overarching goal.
- Morning heating and cooling peaks can be mitigated by more sophisticated control strategies to manage thermal storage in the building structure and within the heating and cooling system (e.g. buffer tanks). Although such options were not considered in this master thesis, it is likely that their use would result in an overall setpoint profile maintaining some form of setback/setup to achieve energy savings during unoccupied hours.

7.2 Auxiliary Setpoint Temperature

As seen in chapter 3, heating and cooling auxiliary devices are installed at the inlet of the load side of the heat exchanger. This configuration ensures that the operative temperature of the SCW remains within an acceptable range, preventing freezing and excessive heating. In previous chapters, the setpoint temperature for the auxiliary heating has been set to 0.5 ˚C to maintain an inlet temperature to the SCW above the freezing point. This setting is achievable in simulation, but it might be deemed unsafe for real system operations. Simulations were performed to assess the impact of raising the auxiliary heating setpoint to 3 °C and 5 °C, offering a more comfortable safety margin against freezing. These results were obtained with the *Good Practice 1* control scenario for pumping power and bleed ratio.

The undisturbed ground temperature (around 10 °C for Montréal) is much closer to the lower operational limit (0 °C) than to the upper operational limit (fixed at 35 °C in our study, but this value could be higher depending on the heat pumps and local ground and water conditions). This means that the auxiliary cooling setpoint is less critical in a cold climate, and it was not investigated in this master thesis.

Figure 7.4 shows the minimum SCW inlet and outlet temperature for a yearly simulation and the maximum power demand from auxiliary systems. The SCW inlet temperature remains above 0 °C for all cases, being very close to the auxiliary heating setpoint. The difference between inlet and outlet temperatures is smaller when the auxiliary heating is set to a higher setpoint, indicated that the well is able to exchange more energy when operating at low temperature, since the pumping flow rate is identical in all simulations.

Figure 7.4 also shows the peak power demand from auxiliary systems in the three cases. As expected, if a higher temperature must be maintained in the building loop, the peak power demand of the auxiliary system will also be higher. It increases by 27% and 60% respectively for the 3 ˚C and 5 ˚C setpoints, compared to the 0.5 ˚C setpoint. Although not shown in the figure, the annual energy use shows a similar trend to the peak demand. The auxiliary heating setpoint is critical for the SCW performance, which can only be fully utilized if the water getting back to the ground is very close to the freezing point.

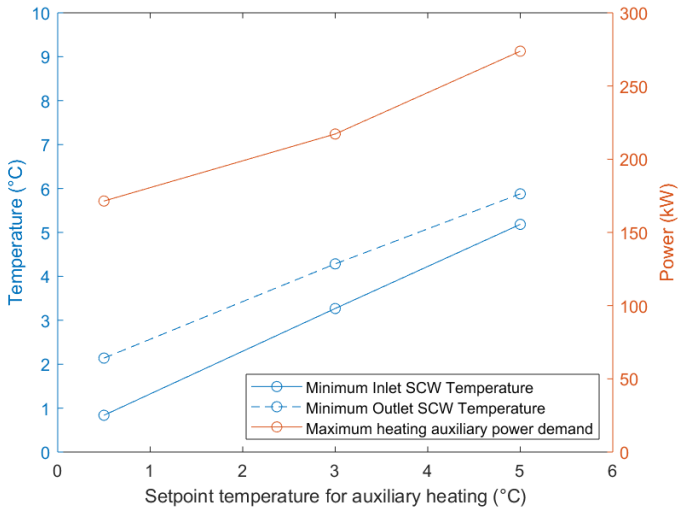

Figure 7.4: Impact of auxiliary heating setpoint temperature on peak power demand and SCW temperatures

The bleed control strategy in the *Good Practice 1* scenario activates the 10% bleed when the SCW outlet temperature falls below 5.5 ˚C and deactivates it above 8.5 ˚C. In the case of a 5 ˚C setpoint temperature for the auxiliary heating system, the outlet temperature is always above the 5.5 ˚C limit and bleed is never activated. This illustrates the need to carefully select the different control strategies and their parameters to optimize the overall operation of SCW systems.

Table 7.2 presents the annual operating cost, annual energy use, and the overall building peak power demand for the 3 auxiliary setpoint values. The strong increase in peak demand and operating costs for more conservative setpoints illustrates the challenges of operating SCW systems in cold climates – to achieve the full potential of these systems, a great attention must be paid to control parameters, including the auxiliary heating setpoints, which should not be considered as a secondary variable in SCW system design.

Table 7.2 : Peak power demand, annual energy use and costs for different auxiliary setpoint

	Energy		**Power**		**Cost**	
	kWh	%	kW	%	$	%
Aux0.5/GP1	581 890	0,0%	328	0,0%	31 830	0,0%
Aux3	613 690	5,5%	373	13,7%	39 570	24,3%
Aux5	653 490	12,3%	412	25,8%	48 500	52,4%

Results show that a 0.5 °C auxiliary heating setpoint maintains the SCW inlet temperature above 1 °C, thereby preventing freezing efficiently. However, it should be noted that using such a low heating setpoint is not common in building systems which are intended to protect the equipment from freezing. A typical setpoint for frost protection is 5 °C, and a quick survey of commercially available freeze protection switches has shown that they can typically be set to a minimum value equal to or larger than 1 °C. It is likely that using a 0.5 °C setpoint would require ad hoc controls and freeze protection devices with very tight tolerances.

7.3 Overall Discussion of Control Strategies

The previous sections show that control strategies for the building itself (zone temperature setpoints) and the auxiliary heating and cooling systems have a significant impact on the SCW thermal performance. A complete picture of the impact of different control strategies can be obtained by combining the different options investigated throughout this master thesis and the reference scenarios. Figure 7.5 and 7.6 show a summary of the simulations presented in this research work respectively as the annual costs and COP versus the average daily groundwater volume bled.

The different bleed ratio scenarios seem to offer the best performance for various levels of trade-off between the volume of groundwater bled and the operating costs or COP. They were obtained with the "ramping" building temperature setpoint, a 0.5 °C setpoint for the auxiliary heating, and a linear modulation of the total pumping flow rate up to 2 GPM/ton (0.036 L s^{-1} kW^{-1}), and these control strategies are the best options according to our simulations. Changing the auxiliary heating setpoint or the (total) pumping flow rate control strategy can have a large impact on the performance, leading to large operating costs increase (or large COP reduction) for a given volume of groundwater bled.

When using the best options for total pumping flow rate, building setpoints, and auxiliary heating setpoints, the achievable operating costs and COP seem to vary almost linearly over a large range of volume of groundwater bled: increasing bleed will increase thermal performance, but at a cost in terms of total volume of groundwater diverted from the SCW. When bleed occurs has an impact on performance, but that impact is smaller in comparison, for the scenarios tested in this work.

As discussed in Chapter 6, the predictive control strategies that were tested in this master thesis deliver modest improvements that do not seem to justify the increased complexity, especially given that they were simulated in ideal conditions (assuming perfect forecasting). The best compromise is found for a non-predictive control strategy called scenario 1.d in chapter 6. Its comparison with *Good Practice 1* shows that the annual COP can be increased from 2.5 to 3.2 with cost savings of 17%, while it bleeds 30% less groundwater.

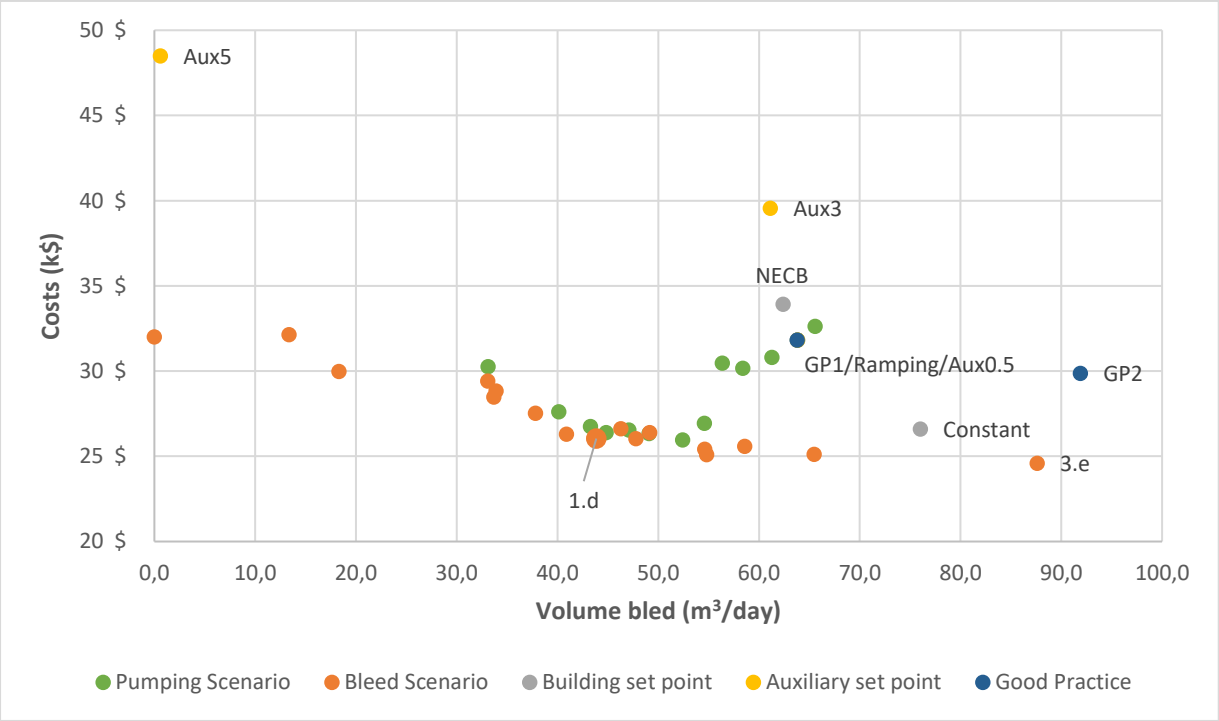

Figure 7.5: Annual operating cost vs. annual volume of groundwater bled

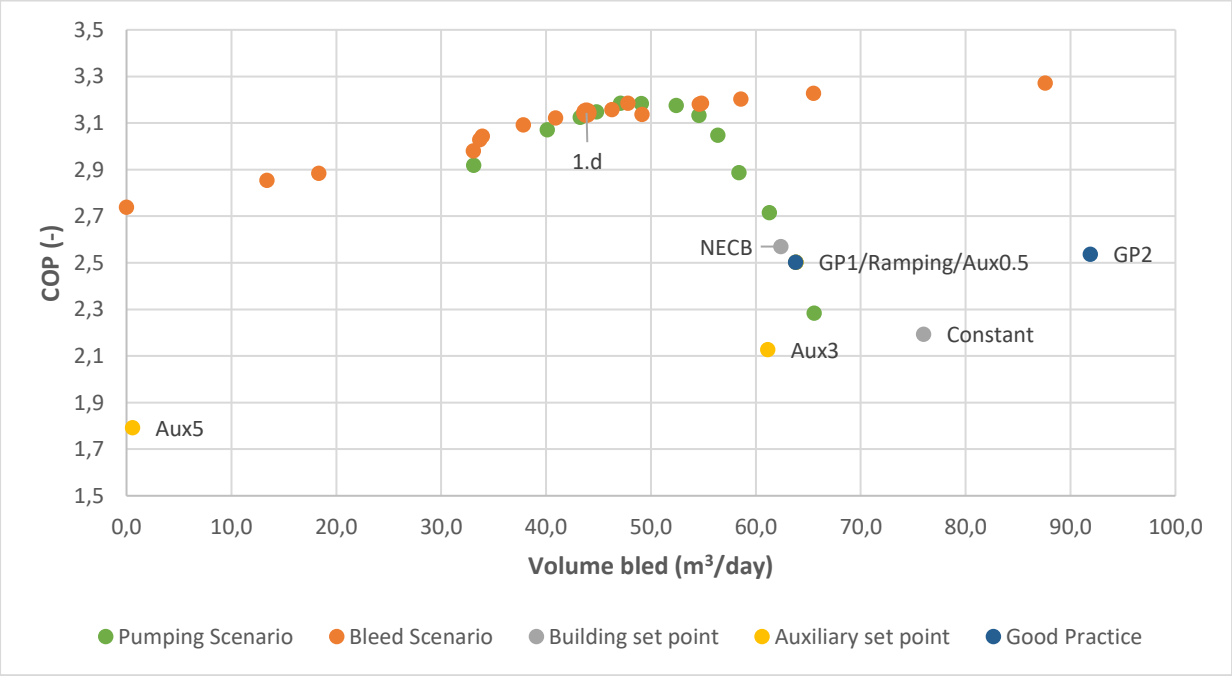

Figure 7.6 : Annual COP vs. annual volume of groundwater bled

CHAPTER 8 CONCLUSION

The aim of this research work was to design and assess control strategies adapted to Standing Column Wells (SCWs) operating in a cold climate and to provide guidelines to reduce overall energy consumption, peak electrical power demand, and total groundwater volume discharged ("bled") to the injection well.

The first contribution is the elaboration of a detailed model of a typical office building in a cold climate including a model of a building loop serving distributed (zone) heat pumps. The model is developed in TRNSYS and includes 15 thermal zones heated or cooled by On/Off heat pumps served by a building loop. The building loop is connected to the SCW through a plate heat exchanger. The TRNSYS model is coupled to an existing detailed model of the SCW implemented in Matlab. The SCW model was modified to include a detailed assessment of the head loss in the ground loop that considers different flow rates, temperatures, and bleed scenarios. The head loss model allows to assess the pumping energy accurately in different system configurations and operating conditions, which represents the second contribution of this work.

The detailed TRNSYS/Matlab model of the building and the SCW allows to assess different control strategies for the different subsystems, including the building itself (zone setpoint profiles and auxiliary devices setpoint). This detailed model is a main addition compared to a first iteration of this master thesis work which was presented in a conference paper (Beurcq et al., 2018, included in Appendix F). A reference scenario is defined (same HVAC system without SCW) and good practice control strategies inspired by the literature are also implemented to provide a reference scenario with an SCW.

Existing good practice and new proposed control strategies for the total flow rate are assessed based on their annual operating costs, energy and peak demand, and groundwater bled. Operating costs are assessed using Hydro-Québec Rate M, which includes a relatively low cost for energy and a significant penalty for peak power.

The third contribution of this work, presented in chapter 5, shows the impact of reducing the flow rate compared to good practice recommendations (3 GPM/ton, or 0.054 L s^{-1} kW^{-1}) increases the residence time in the well, leading to a higher SCW outlet temperature in heating and reducing the need for auxiliary heating. In particular, we show the interest of using a variable-speed pump and

propose controlling the flow rate linearly as a function of the load on the building loop, and the results show that this linear control strategy with a maximum flow rate of 2 GPM/ton (0.036 L s^{-1} kW^{-1}) delivers up to 8 % savings in operating costs compared to the *Good Practice 1*, with an equivalent or reduced volume of groundwater bled.

The fourth contribution is an assessment of different bleed rate control strategies, including a modulation proportional to the current building loop (as for the total flow rate) which is not beneficial and a modulation proportional to the forecasted maximum load over a given horizon. These predictive strategies are compared to constant bleed ratios activated by a dead-band control on the SCW outlet temperature, recommended in the literature. The tested predictive strategies deliver marginal improvements, making their use difficult to justify given the large increase in complexity. A systematic study of different constant bleed ratios shows that, when combined with the proposed linear modulation of the total flow rate, it is possible to select different operating points according to the constraints placed on the volume of groundwater bled. Over a large range of operating parameters, the annual operating cost decreases almost linearly with the volume of water bled, showing that the optimum operation necessarily results from a trade-off between these two aspects. The proposed strategies allow to select the minimum operating cost (or the maximum annual COP, if desired) for a given volume, and deliver significant improvements over the good practice scenarios.

The last contribution is an overall assessment of the system performance when modifying control parameters related to the building, namely the zone setpoint profile and the auxiliary devices setpoints. In heating mode, the undisturbed ground temperature (around 10 °C) is relatively close to the minimum allowable value (above freezing), so the setpoint of the auxiliary heater has a major impact on the overall system performance. We recommend a value of 0.5 °C, recognizing that this would likely require tightening the control tolerance of controls and safety devices compared to standard building practice. The zone setpoint profile also has a large impact on the overall system performance: as for all heat pump systems, attempting to recover quickly from large night setback/setup will cause large peaks and require more auxiliary energy, leading to a significant reduction of the annual COP. The recommended profile implements “smooth” ramps to recover from night setpoints, which is a compromise between a constant setpoint (reducing peaks even further but increasing annual energy use) and typical schedules e.g. proposed in the Canadian

National Energy Code for Buildings. The significance of these building-related control parameters has not, to our knowledge, been mentioned in the literature. The overall optimized system delivers up to 8 % operating costs savings (also showing a 26 % COP increase) compared to good practice scenarios or allows to operate with a better performance and with a reduced volume of groundwater bled.

8.1 Recommendations

The detailed building model uses On/Off heat pumps for the zones and a relatively simple modulating model for fresh air conditioning. With variable capacity heat pumps becoming more common, the model could be modified to include these new heat pumps, including a detailed model for fresh air conditioning.

The relatively simple predictive strategies investigated in this work could also be expanded and use the building heating and cooling loads (rather than the load on the building loop, which depends in fact on the SCW operation). Our study seems to indicate that a 12-h horizon is a good compromise, so simple scenarios based on heuristics (e.g. bleed at night if the next morning is forecast to have a high heating load) could be investigated. Predictive scenarios could also use the ambient temperature, for which good forecasts could realistically be obtained. A scenario based on the current ambient temperature would also be interesting to explore, similar to the “heating curve” typically applied in heating systems.

The strategies were evaluated regarding the energy consumption, power demand and volume of groundwater bled, however a complete lifecycle costs evaluation would be more accurate as it would also consider the size of the equipment needed for auxiliary systems etc.

Our work showed the need to optimize concurrently all the operating parameters (pumping, bleed rate, zone setpoints, and auxiliary setpoint), but the approach used in this master thesis relied on a multi-step approach involving a fair amount of trial-and-error. A more systematic optimization would be interesting, although the computational effort in terms of simulation time with the current model would represent an obstacle.

Finally, the potential of SCWs and their optimum control parameters should be investigated for different building types and different climate zones across Canada.

REFERENCES

Abu-Nada, E., Akash, B., Al-Hinti, I., Al-Sarkhi, A., Nijmeh, S., Ibrahim, A., & Shishan, A. (2008). Modeling of a geothermal standing column well. *International Journal of Energy Research, 32*(4), 306-317.

ASHRAE. (2010). *Energy Standard for buildings except low-rise residential buildings (Standard 90.1-2010)*. Paper presented at the Atlanta, GA, USA: American Society of Heating, Refrigerating and Air-conditioning Engineers.

ASHRAE. (2013). *Chap. 24: Airflow around buildings. In ASHRAE Handbook of Fundamentals*. Atlanta, GA, USA: American Society of Heating, Refrigerating and Air-conditioning Engineers.

ASHRAE. (2013). *Energy Standard for Buildings excep Low-Rise residential Buildings (Standard 90.1-2013).* Atlanta, GA, USA: American Society of Heating, Refrigerating and Air-conditioning Engineers.

Bear, J. (1979). *Hydraulics of groundwater*. New York: McGraw-Hill.

Beaudry, G., Pasquier, P., & Marcotte, D. (2018). *Hydrogeothermal Characterization and Modelling of a Standing Column Well Experimental Installation*. Paper presented at the International Ground Source Heat Pump Association (IGSHPA) Conference, Stockholm, Sweden.

Cho, J.-H., Nam, Y., & Kim, H.-C. (2016). Performance and Feasibility Study of a Standing Column Well (SCW) System Using a Deep Geothermal Well. *Energies, 9*(2), 108.

Churchill, S.W. 1977, 'Friction Factor Spans All Fluid Flow Regimes' Chem. Eng. (Rugby, U.K.) 84(24), pp.91-91

Commission Européenne. (2016). *Vers un secteur du chauffage et du refroidissement intelligent, efficace et durable.* Retrieved from a european commission memo.

Conseil national de recherches du Canada. (2011). *Code national de l'énergie pour les bâtiments*. Ottawa, ON: Conseil national de recherches du Canada.

Croteau, J. É. (2011). *Évaluation des paramètres influençant les températures d'opération des puits à colonne permanente.* (Mémoire de maîtrise, École Polytechnique de Montréal, Montréal, QC).

Deng, Z. (2004). Modeling of standing column wells in ground source heat pump systems. (Thèse de doctorat, Oklahoma State University, Stillwater, Oklahoma).

Deng, Z., Rees, S., & Spitler, J. (2005). A model for annual simulation of standing column well ground heat exchangers. *Hvac&R Research, 11*(4), 637-655.

Deng O'Neill, Z., Spitler, J. D., & Rees, S. J. (2006). Performance Analysis of Standing Column Well Ground Heat Exchanger Systems. *ASHRAE transactions, 112*(2).

Environment Canada. 2010. *Canadian Weather Energy and Engineering Data Sets (CWEEDS Files) and Canadian Weather for Energy Calculations (CWEC Files) Updated User's Manual*. Ottawa, ON, CAN: Environment Canada.

Eppner, F. (2016). *Évolution thermo-hydro-géochimique d'un puits à colonne permanente conduisant à la précipitation et à la dissolution de la calcite.* (Thèse de doctorat, École Polytechnique de Montréal, Montréal, QC).

Eppner, F., Pasquier, P., Baudron, P., (2017). *A coupled thermo-hydro-geochemical model for standing column well subject to CO 2 degassing and installed in fractured calcareous aquifers.* Geomechanics for Energy and the Environment 11, 14–27.

Eppner, F., Pasquier, P., Baudron, P., (2017). *Investigation of Thermo-hydro-geochemical Processes in a Standing Column Well Intersected by a Fracture*, in: Proceedings of the IGSHPA Technical/Research Conference and Expo 2017. Denver, USA, p. 9.

Gowri, K., Winiarski, D., &Jarnagin, R. (2009). *Infiltration Modeling Guidelines for Commercial Building Energy Analysis* (Report PNNL-18898). Richland, WA, USA: Pacific Northwest National Laboratory.

Hydraulic Institute (1990). *Hydraulic Institute Engineering Data Book* (2nd edition). Parsipanny, NJ, US: Hydraulic Institute.

Hydro-Québec. (2018). Electricity Rates. Chapter 4: Rated for medium power. Montréal, QC: Hydro-Québec.

Kavanaugh, S. (1998). Development of design tools for ground-source heat pump piping. *ASHRAE Transactions, 104* 932.

Klein, S. A., W.A. Beckman, J.W. Mitchell, J.A. Duffie, N.A. Duffie, T.L. Freeman, J.C. Mitchell, et al. (2018). "TRNSYS 18 – A TRaNsient SYstem Simulation Program, User Manual. Version 18." Madison, WI: University of Wisconsin-Madison.

Lund, J. W., & Boyd, T. L. (2016). Direct utilization of geothermal energy 2015 worldwide review. *Geothermics, 60* 66-93.

The MathWorks. (2017). MATLAB User's Guide (2017a) [logiciel]. The MathWorks, Inc., Natick, Massachusetts, United States. Retrieved from https://www.mathworks.com

McGowan, M. K. (2018). Propelling St. Patrick's Cathedral Forward. *Ashrae Journal, 60*(8), 54-62.

Ng, B. M., Underwood, C. P., & Walker, S. L. (2011). Standing column wells—Modeling the potential for Applications in Geothermal Heating and Cooling. *HVAC&R Research, 17*(6), 1089-1100.

Nguyen, A., Pasquier, P., & Marcotte, D. (2012). Multiphysics modelling of standing column well and implementation of heat pumps off-loading sequence. Paper presented at the Comsol Conference, Boston, USA.

Nguyen, A., Pasquier, P., & Marcotte, D. (2013). Development of an ODE model featuring a three level bleed control and an off-loading sequence for standing column wells. *Proceedings of BS2013, Chambéry, France* 26-28.

Nguyen, A., Pasquier, P., & Marcotte, D. (2015a). Thermal resistance and capacity model for standing column wells operating under a bleed control. *Renewable Energy, 76* 743-756.

Nguyen, A., Pasquier, P., & Marcotte, D. (2015b). Influence of groundwater flow in fractured aquifers on standing column wells performance. *Geothermics, 58* 39-48.

Nguyen, A., & Pasquier, P. (2015c). An adaptive segmentation Haar wavelet method for solving thermal resistance and capacity models of ground heat exchangers. *Applied Thermal Engineering, 89* 70-79.

Oliver, J., & Braud, H. (1981). Thermal exchange to earth with concentric well pipes. *Transactions of the ASAE, 24*(4), 906-0910.

Orio, C. D. (1994). Geothermal heat pumps and standing column wells. *Transactions-Geothermal resources council* 375-375.

Orio, C. D., Johnson, C. N., & Poor, K. D. (2006). Geothermal Standing Column Wells: Ten Years in a New England School. *ASHRAE transactions, 112*(2).

Orio, C. D., Patnaude, Z. J. (2014). Eight years of operation of 615 tons geothermal nursing home in Northern tier. *ASHRAE Transactions, 120* 1CC.

Pasquier, P., Nguyen, A., Eppner, F., Marcotte, D., & Baudron, P. (2016). Standing column wells. In *Advances in Ground-Source Heat Pump Systems* (pp. 269-294): Elsevier.

Rees, S. J., Spitler, J., Deng, Z., Orio, C., & Johnson, C. (2004). A study of geothermal heat pump and standing column well performance. *ASHRAE Transactions, 110*(1), 3-13.

RNCan. (2016a). Base de données nationale sur la consommation d'énergie – Consommation d'énergie secondaire du secteur résidentiel par source d'énergie et utilisation finale. Ressources Naturelles Canada, Ottawa. Retrieved from http://oee.rncan.gc.ca/organisme/statistiques/bnce/apd/showTable.cfm?type=HB&sector=res&juris=00&rn=1&page=0 dernière visite le 2018-03-14.

RNCan. (2016b). Base de données nationale sur la consommation d'énergie – Consommation d'énergie secondaire du secteur résidentiel et commercial par source d'énergie et utilisation finale et type d'activité. Ressources Naturelles Canada, Ottawa. Retrieved from

http://oee.rncan.gc.ca/organisme/statistiques/bnce/apd/showTable.cfm?type=HB&sector=com&juris=00&rn=1&page=0 dernière visite le 2018-03-14.

RNCan. (2018). Faits sur l'électricité. Ressources Naturelles Canada, Ottawa. Retrieved from https://www.rncan.gc.ca/energie/faits/electricite/20079 dernière visite 2018-03-14.

Spitler, J. D., Rees, S. J., Deng, Z., Chiasson, A., Orio, C. D., & Johnson, C. (2002). R&D studies applied to standing column well design. ASHRAE research project RP-1119. Atlanta, GA: American Society of Heating, Refrigerating and Air-Conditioning Engineers.

TESS. (2012). TESSLibs 17 - Component Libraries for the TRNSYS Simulation Environment. Madison, WI, USA: Thermal Energy Systems Specialists.

Thulukkanam, K. (2013). *Heat exchanger design handbook*: CRC press.

Trane. (2018). Water Source Heat Pump Axiom Horizontal/Vertical - GEH/GEV. Dublin, Irlande: Trane.

USDOE-BTO. (2017). 'Commercial Prototype Building Models.'. Washington, DC, USA: U.S. Department of Energy, Buidling Technologies Office. https://www.energycodes.gov/development/commercial/prototype_models.

Yuill, G. K., & Mikler, V. (1995). Analysis of the effect of induced groundwater flow on heat transfer from a vertical open-hole concentric-tube thermal well. Paper presented at the American Society of Heating, Refrigerating and Air-Conditioning Engineers winter meeting and exhibition, Chicago, Illinois, USA.

APPENDIX A PERFORMANCE MAP FOR TYPE 919

Type 919 is a water source heat pump model from the Tess component library in TRNSYS. This model is based on user-supplied data files containing catalog data for the normalized capacity (both total and sensible in cooling mode), and normalized power, based on the entering water temperature to the heat pump, the entering water flow rate and the air flow rate. Other curve fits are used to modify the capacities and power based on off-design indoor air temperatures. The component requires four supplied data files : cooling and heating performance data files and cooling and heating correction factor data. The model description mentions that the values in the files for the catalog data files for both heating and cooling mode should include the indoor fan.

The rated conditions for each heat pumps are summed up in appendix C and corresponds to a scenario with an entering water flow rate at 2.5 GPM/ton at 25 ˚C in cooling mode and 0 ˚C in heating mode while the rated air flow rate corresponds to a 400 cfm/ton (except for the GEV060 model, it is 380 cfm/ton).

The goal of this appendix is to provide in informations on the performance map used in Type 919 for our simulations and especially the processed used to transform the constructor catalog information (Trane here) into a correct file for TRNSYS.

In both performance data file, the power provided is the sum of the compressor power and the blower power chosen (appendix B). The cooling capacities are reduced with the fan power while the heating ones are increased by the amount of the fan power assuming its energy consumption is helping the heat pump in heating mode while it is a disadvantage in cooling mode.

The Trane catalog also gives correction factors for variation in entering air temperature that provides the data for the correction factor files. An example of the constructor table available is shown below. For an easier comprehension, the coefficients of columns 2 and 3 will be called *a* and *b*, the one in columns 4 to 8 will be called *c* and finally coefficient for heating in columns 10 and 11 are called *d* and *e*. Note that all the fields with '-' were filled by zeros in the code and the field with '*' means that the total capacity equals the sensible capacities. Based on the rated capacities without the blower included it would mean that for those coefficient *c:*

$$a \times Rated\ Total\ Cooling\ Capacity = c \times Rated\ Sensible\ Cooling\ Capacity$$

$$c = \frac{a \times Rated\ Total\ Cooling\ Capacity}{Rated\ Sensible\ Cooling\ Capacity}$$

Table 151. Correction factors for variation in entering air temperature 7.5 tons GEV090

Cooling Entering Air WB F	Cooling Capacity	Cooling Comp Power Watts	Sensible vs. Entering Dry Bulb Multipliers					Heating Entering Air DB F	Heating Capacity	Heating Comp Power Watts
			65.6	70.6	75.6	80.6	85.6			
44.5	0.943	0.981	0.994	1.058	1.125	*	*	43	1.068	0.713
49.4	0.944	0.981	0.995	1.059	1.125	*	*	48	1.057	0.768
56.3	0.945	0.981	0.806	1.020	1.127	*	*	53	1.042	0.824
60.3	0.946	0.982	0.615	0.837	1.067	*	*	58	1.028	0.880
63.2	0.963	0.988	0.459	0.690	0.920	1.140	*	63	1.014	0.938
66.2	1.000	1.000	–	0.535	0.767	1.000	1.210	68	1.000	1.000
72.1	1.088	1.023	–	–	0.455	0.688	0.920	73	0.988	1.066
77.1	1.169	1.037	–	–	–	0.415	0.652	78	0.974	1.133

Notes: * = Sensible equals total capacity

We have to transform those coefficients for the TRNSYS type because the rated capacities of the component include the fan power which is not the case in the constructor data. The new coefficients or variables will be noted with * (example a*, b*,etc.) when the blower impact is included.

For cooling power (X) the new coefficient b* is computed as below. Note that it is the same process for heating power and capacity.

$$b \times X = X_{corrected}$$

and $$X^* = X + Blower$$

then $$b^* \times X^* = X_{corrected} + Blower$$

In the end, the new coefficient is : $b^* = \frac{b \times X + Blower}{X + Blower}$

In the case of the cooling total and sensible capacities (Y) the coefficient a and c are modified as following :

$$a \times X = X_{corrected}$$

and $$X^* = X - Blower$$

then $$a^* \times X^* = X_{corrected} - Blower$$

In the end, the new coefficient is : $a^* = \frac{a \times X - Blower}{X - Blower}$

Finally, in all performance data, we added some values to zero in order to counter the effect of TRNSYS interpolation and make sure the heat pump capacity and power are zero when the operative temperature of the heat pump is not met (under 3.88 ˚C in heating mode and over 48.9˚C in cooling mode).

APPENDIX B FAN CHOICE FOR HEAT PUMPS

Type 919 requires to include the fan power in the parameters and performance map of the heat pump. This appendix illustrates the method for the fan choice for each heat pump.

The first column corresponds to the heat pump model from the Trane catalog (Water Source Heat Pump Axiom Horizontal/Vertical from 2018). The second column corresponds to the nominal air flow rate that is provided to the thermal zone when the heat pump is ON. The third column computes the corresponding power from the ASHRAE recommendation 90.1 with equation 3.5. For each model of heat pump the Trane catalog gives several option of fan models. In this work we chose an average model among the one proposed. The fan power from the catalog is shown in the fourth column in horse power. Column five computes the fan power selected in column 4 assuming a 65% efficiency. The last column computes the difference between the ASHRAE recommendation and the fan selected.

Heat Pump	**Nominal Air Flow rate**	**Power From ASHRAE 90.1**	**Trane Catalog Power for fan**	**Fan power (ε_{fan} = 65%)**	**Difference**
Units	cfm	kW	HP	kW	%
GEV036	1140	0.91	0.5	0.57	38%
GEV042	1330	1.07	0.5	0.57	47%
GEV048	1520	1.22	1	1.13	7%
GEV060	1900	1.52	1	1.13	26%
GEV072	2400	1.93	1	1.13	41%
GEV090	3000	2.41	2	2.26	6%
GEV120	4000	3.21	3	3.40	6%
GEV150	5000	4.01	3	3.40	15%
GEV180	6000	4.81	5	5.66	18%
GEV240	8000	6.42	7.5	8.49	32%
GEV300	10000	8.02	7.5	8.49	6%

APPENDIX C TYPE 919 PARAMETERS

N°	Parameter name	Units	GEV060	GEV090	GEV120	GEV300
6	Number of Water Flow Steps	\	7	5		
7	Number of Water Temperatures - Cooling	\	9	11		
8	Number of Water Temperatures – Heating	\	8	9		
9	Number of Wet Bulb Temperature Steps	\	7	8		
10	Number of Dry Bulb Temperature Steps – Cooling	\	5	5		
11	Number of Dry Bulb Temperature Steps – Heating	\	7	8		
12	Number of Airflow Steps – Cooling	\	8	5		
13	Number of Airflow Steps – Heating	\	8	5		
17	Blower Power	kJ/h	4 076	8 153	12 229	30 572
21	Total Air Flow rate	L/s	897	1 416	1 888	4 719
22	Rated Total Cooling Capacity	kJ/h	62 287	95 876	126 405	324 876
23	Rated Sensible Cooling Capacity	kJ/h	45 933	73 454	93 804	241 527
24	Rated Cooling Power	kJ/h	19 736	25 433	34 225	91 412
25	Rated Heating Capacity	kJ/h	56 091	74 938	100 854	274 185
26	Rated Heating Power	kJ/h	19 664	25 073	34 189	93 248
27	Rated Air Flow rate	L/s	897	1 416	1 888	4 719
28	Rated Liquid Flow rate	L/s	1.06	1.7	2.27	5.68

APPENDIX D ITERATIVE VERSUS TIMESTEP CALLING OF TYPE 155

The following figure shows the results of two simulations implementing a timestep versus iterative calling of the type 155 in the simulation. This choice allows a reduction of the simulation time by 10 (30 hours to 3 hours). Both simulations were implemented with the *good practice 1* scenario parameters. The overall energy consumption difference is 2.4%.

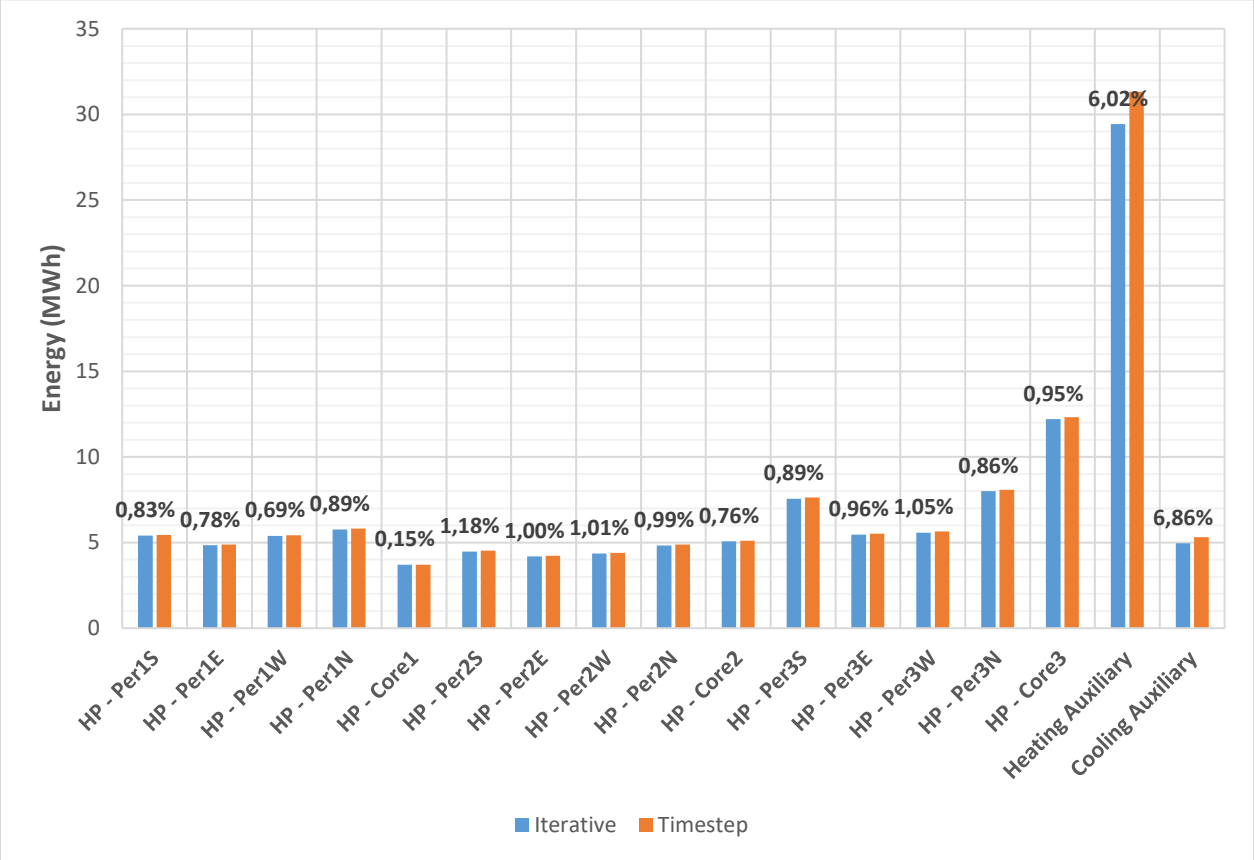

APPENDIX E BUILDING LOOP LOAD ESTIMATION

For the linear control strategies implemented, we processed an estimation of the building loop load based on *Good practice 1* scenario. The annual simulation allowed to process an annual COP for each heat pump in cooling and in heating.

$$COP_{yearly,heat} = \frac{Q_{zone,heat}}{W_{c,heat}} \quad \text{and} \quad COP_{yearly,COOL} = \frac{Q_{zone,cool}}{W_{c,cool}}$$

With Q_{zone} the heating or cooling energy transferred to the zones and W_c is the energy consumed by the heat pump compressor in the considered mode (cooling or heating).

The estimated building zone is the sum of the heat injected by each heat pumps in cooling mode minus the sum of the heat extracted by the heat pumps in heating mode. As the heat pumps compressor consumption and heat needs from building loops is influence by the SCW operative control sequence we use the annual average COP for each heat pump to compute for each timesteps the energy extracted or injected by each heat pumps (Core zones might be in cooling zone when perimeter zones are in heating mode then the building loop is reduces).

$$Q_{loop} = Q_{bldg} - W_c \qquad Q_{loop} = Q_{bldg} + W_c$$

$$\text{with } COP_{heat} = \frac{Q_{bldg}}{W_c} \qquad \text{with } COP_{cool} = \frac{Q_{bldg}}{W_c}$$

$$Q_{loop} = Q_{bldg}\left(1 - \frac{1}{COP_{heat}}\right) \qquad Q_{loop} = Q_{bldg}\left(1 + \frac{1}{COP_{cool}}\right)$$

HEATING COOLING

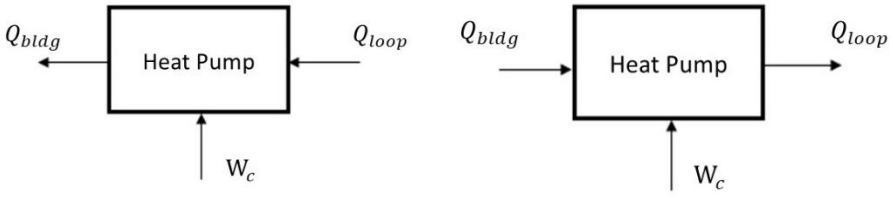

The following equation computes the overall estimation the building loop used in control strategies :

$$Q_{bldgloop} = -\sum_{1}^{n=16} Q_{loop,heat,i} + \sum_{1}^{n=16} Q_{loop,cool,i}$$

with n the number of zones including the heat pump for fresh air conditioning.

APPENDIX F ARTICLE 1: OPTIMIZED CONTROL FOR STANDING COLUMN WELLS IN COLD CLIMATE

C. BEURCQ[1], M. KUMMERT[1], P. PASQUIER[2]

(1) Polytechnique Montréal, dept. of Mechanical Engineering, Montréal (Québec), Canada

(2) Polytechnique Montréal, dept. of Civil, Geological and Mining Engineering, Montréal (Québec), Canada

ABSTRACT

This paper aims at developing and assessing control strategies for Standing Column Well (SCW) ground-source heat pump systems. Pumping flowrate and bleeding ratio (fraction of the flow rate which is not directly reinjected in the SCW) are controlled to minimize the operating cost and risks, while reducing the peak demand and yearly energy use. The building is modelled in TRNSYS and coupled to a Matlab model of the SCW. The SCW model is based on a thermal resistance and capacity model and includes the impact of bleeding and hydrogeological conditions on thermal performance. Some "reactive" control strategies recommended in the literature are assessed and compared to new strategies that use information on the building loads. Results show that different control strategies can have a large impact on operation costs. The load-dependent strategies investigated in this paper can deliver savings from 4% to 8% compared to a well-tuned best-practice control strategy. Optimized control strategies for bleeding ratio can also reduce the total diverted flow rate, reducing environmental risks and maintenance costs. System sizing also has a large impact on performance, and both sizing and operation guidelines are required to ensure the success of SCW systems in cold climates.

Keywords: Standing Column Well, ground-source heat pump, Bleed control strategies, Geoexchange

1. INTRODUCTION

In Canada, cooling and heating energy represents two thirds of the energy used in the commercial and institutional sector while it is almost 80 % in the residential sector. Ground-source heat pumps

(GSHPs) can provide heating and cooling efficiently using renewable energy from the ground, benefiting from the constant temperature of the soil beyond a certain depth.

Standing Column Wells (SCWs) are ground heat exchangers that use groundwater to transfer heat from and to the ground and can lead to significant capital cost savings compared to conventional closed-loop geothermal systems if installed in suitable hydrogeological environments. According to recent studies, for a similar installed thermal power, SCWs can show savings on construction costs between 49% to 78% when compared to closed-loop systems (Deng O'Neill et al., 2006). A 9-year monitoring study in the United States showed that six SCWs of 455 m were are able to generate energy savings of more than 685,000 kWh per year in a relatively cold climate (Orio et al., 2006). These large savings with a relatively small number of wells were possible due to the significant thermal power supported by each well (more than 110 kW per SCW).

The real potential of SCWs lies in their capacity of being installed in dense urban areas or in historic districts where a lack of land area impedes the installation of a wide closed-loop system (Pasquier et al., 2016). Another advantage of SCWs is their ability to operate efficiently in porous or rocky geological formation having a low permeability, where an open-loop system would not be a viable option. Despite a significant potential, SCWs are not widely used outside the north-east of the United States. This is mainly due to a lack of technical expertise outside the geographical areas where SCWs initially emerged.

Figure 1 shows a typical SCW system where a building loop (heat sink or source for decentralized heat pumps) and a loop are connected by a plate heat exchanger. The performance of the decentralized heat pumps connected to the building loop is directly impacted by the fluid temperature at their inlet, i.e. by the temperature at the load side of the heat exchanger. The ground loop consists of a submersible pump immersed in the SCW and a return pipe which is typically inserted within the well. Before reinjecting the groundwater into the SCW, part of the flow rate can be diverted into a separate injection well. This process is called “bleed” and normally improves the system performance by attracting water from the undisturbed neighbouring ground through aquifer fractures. The maximum bleed fraction is dictated by ground conditions and is usually in the order of 10 % to 30 % (Pasquier et al., 2016). This means that 90 % to 70 % of the well flow rate is reinjected directly in the SCW, while the rest is diverted to a nearby sewer, river or injection well.

Note that some jurisdictions require to reinject the bleed water to its original aquifer, which is usually achieved by an injection well.

The bleed flow rate cannot usually be maintained at high levels for long periods of time, due to the risk of bringing the water level down too much in the SCW or overflowing the injection well in low permeability aquifers. Bleeding continuously the SCW also increases the risk of clogging the fracture network around the injection well. The total pumping flow rate also influences the residence time of water in the well, which impacts the SCW performance. The pumping power can represent a significant share of the operational costs, and is influenced by two parameters: total flow rate in the ground loop and pumping head. The latter is caused by the activation of the bleed which lowers the groundwater level in the SCW and increases the pumping head.

The total flow rate and the ‘’bleed ratio’’ (fraction of the flow rate diverted) are two control variables important for SCWs installed in cold climate because of the low available margin between the ground undisturbed temperature (typically around or below 10 °C) and the minimum acceptable temperature (above freezing). Auxiliary heating devices with a lower efficiency (e.g. electric resistance heating, natural gas furnaces and conventional chillers for cooling) are typically used when the SCW cannot insure acceptable temperature conditions in the building loop. The setpoints for these auxiliary devices and the control strategy for total flow rate and bleeding will have a significant impact on annual energy use, peak demand, and costs.

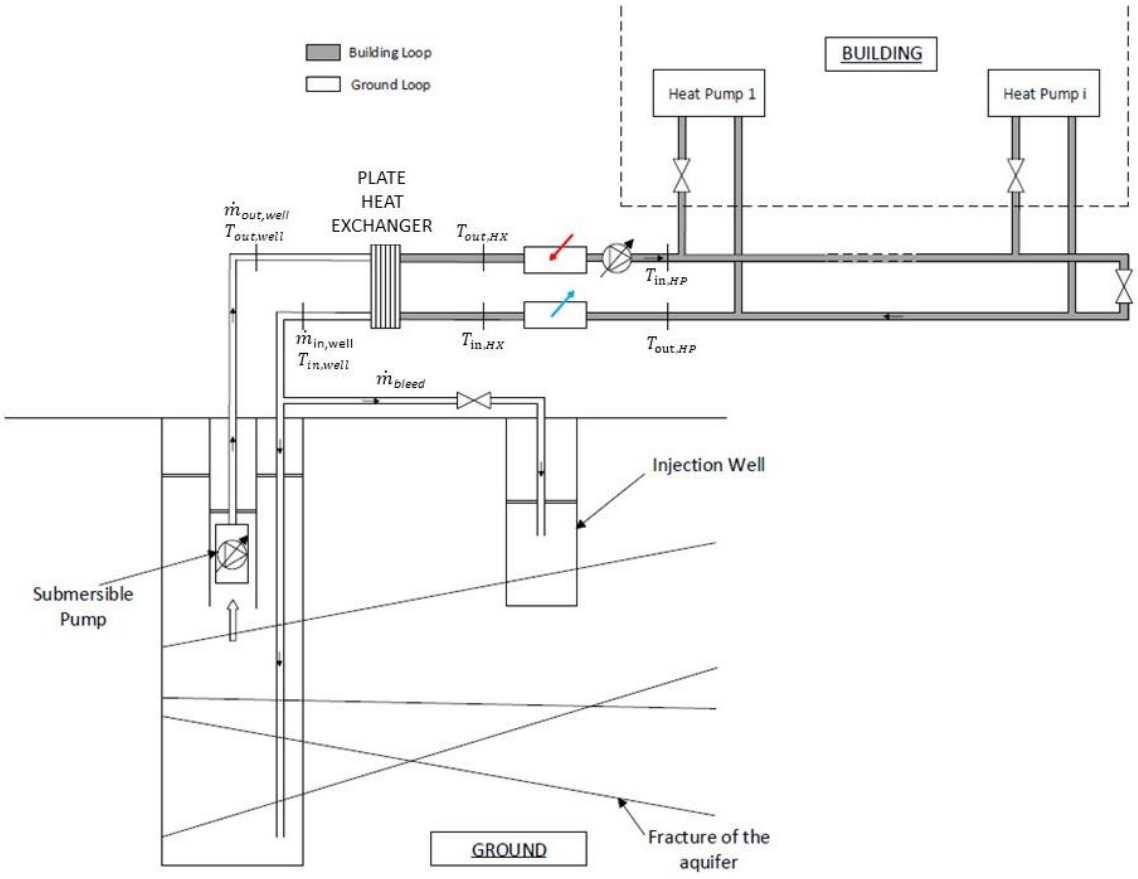

Figure 1: Schematic of the SCW system

1.1.Control strategies: literature review

Only a few papers investigating bleed control strategies for SCWs were found in the literature. Rees et al. (2004) proposed the following logic:

- Temperature difference: if the difference between the temperature entering and leaving the well is above a given threshold, bleeding is used. The authors use the value of 5.6 °C and a constant 10% bleed ratio.
- Dead-band on well leaving temperature: under a certain temperature coming out of the well, bleeding is used. Bleeding stops when the return temperature from the well has returned above the initial value plus a dead-band. The authors use a level of 5.83 °C to start using bleed and a level of 8.6 °C to stop bleeding, in heating mode (other values are used in cooling mode). Again, a constant 10% bleed ratio is used.

Minea (2013) suggests initiating a 10% bleed in heating mode when the temperature of the groundwater drops below 4.6 °C.

Nguyen et al. (2013) implemented an off-loading sequence of the GSHPs with a three-level bleed control (10%, 20% and 30% of the total flow rate) triggered when the temperature leaving the SCW falls below a prescribed temperature. The control sequence was also designed to start an auxiliary heating system when the groundwater was approaching 4 °C in heating. The main goal of this work was to prevent any risk of groundwater freezing and operational problems with the GSHP while increasing the running time of the heat pumps.

The reviewed control strategies were shown to perform adequately in simulation by their respective authors, but none of the studies presented an explicit optimization of the strategies themselves or their parameters (i.e. thresholds and dead-bands).

2. OBJECTIVES AND METHODOLOGY

The aim of this paper is to investigate control strategies for SCW systems, addressing both the modulation of the (total) pumping flow rate and the modulation of the bleed ratio. Control strategies will be compared to the ones found in the literature in terms of energy use, peak demand, and electricity cost. Conclusions will then be drawn on recommendations for cold-climate SCW control strategies.

The system presented in Figure 1 is modeled in TRNSYS, except for the SCW model, which is implemented in Matlab. The two software programs communicate through a TRNSYS component that allows the user to exchange inputs and outputs (Type 155).

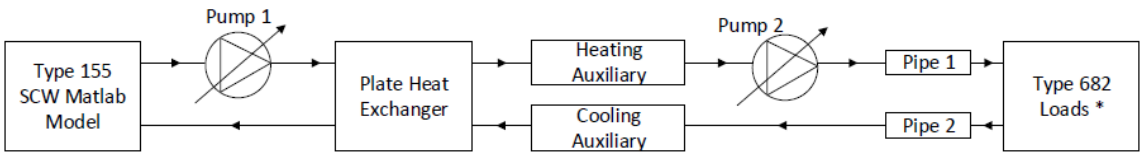

Figure 2: Pattern of the system implemented in TRNSYS

* The load imposed by Type 682 on the building loop corresponds to the heat transfer on the source-side of decentralized heat pumps in the building, as explained in section 2.2.1.

Building Loads

A medium three-storey office inspired by the U.S. Department of Energy Prototype Buildings (USDOE-BTO, 2017) is modeled in TRNSYS using the 3D Sketchup plugin and the TRNBuild interface.

Performance parameters and simulation assumptions (e.g. internal gains) follow the ASHRAE Standard 90.1 – 2010 specifications (ASHRAE, 2010). The simulation uses a typical weather file for Montreal, QC (Environment Canada, 2010). The simulated building is artificially scaled up or down to result in peak building loads of 25, 50 and 75 kW as detailed below. Daily average and peak heating and cooling loads are shown in Figure. Plotted values represent the heat that must be added to or removed from the building to maintain the desired temperature setpoint. Figure 3 includes the load corresponding to service water heating. No efficiency or coefficient of performance are included.

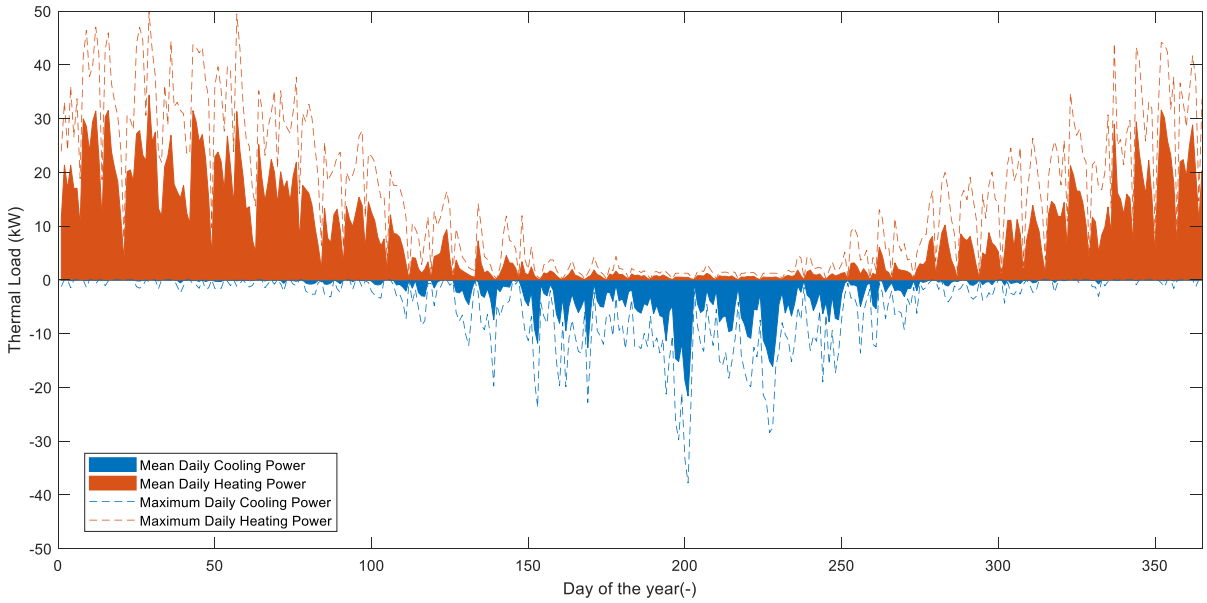

Figure 3: Building thermal load (heating and cooling)

Building loop

2.2.1. Load

The calculated building thermal load (heating or cooling) is converted into a thermal load on the building loop by a simple heat pump model. Figure presents the method implemented in TRNSYS. To keep the simulation simple, hourly building loads for space heating, service hot water, and space cooling are pre-calculated and read-in by a data reader (Type 9c). Figure 4 and 5 shows the calculation of the thermal load on the building loop using a simple heat pump model.

Some of the heat pumps provide heat to the loop while some others extract heat from it. It is assumed that the actual extra heating or cooling load needed by the loop is provided either by the SCW or the auxiliary system. In the end, the calculated building loop load is sent to a component (Type 682) that imposes the load on its incoming flow stream.

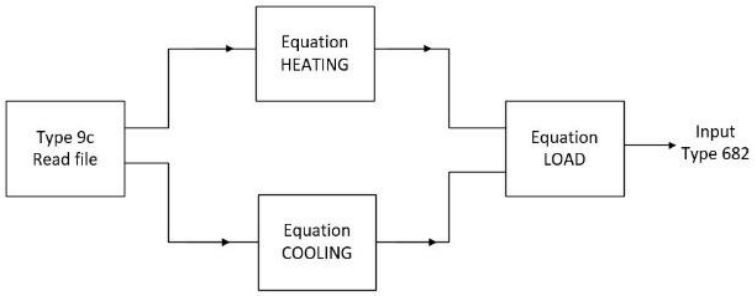

Figure 4: Converting building loads to thermal loads on the building loop.

The TRNSYS equations blocks used in Figure 3 implement the following relationships for the heating and cooling cases (see the nomenclature at the end for a variable description):

$$Q_{loop} = Q_{bldg} - W_c \qquad Q_{loop} = Q_{bldg} + W_c$$

with $COP_{heat} = \frac{Q_{bldg}}{W_c}$ with $COP_{cool} = \frac{Q_{bldg}}{W_c}$

$$Q_{loop} = Q_{bldg}\left(1 - \frac{1}{COP_{heat}}\right) \qquad Q_{loop} = Q_{bldg}\left(1 + \frac{1}{COP_{cool}}\right)$$

HEATING COOLING

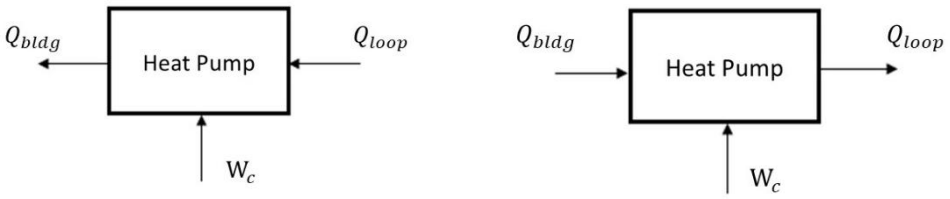

Figure 5: Heat pump in heating mode (left) and cooling mode (right)

In the previous equations, the coefficients of performance (COP) are evaluated with the following equations. Typical values are taken from (Bernier et al., 2007) for heating and cooling and adapted for service water heating (which requires a higher temperature for the delivered heat):

$$COP_{heat} = 3.49 + 0.061 \times T_{in,HP}$$

$$COP_{cool} = 7.92 - 0.117 \times T_{in,HP}$$

$$COP_{swh} = 1 + 0.061 \times T_{in,HP}$$

Figure 6 shows the load on the building loop after calculation. The curves above the horizontal axe represents heating loads while the one under are for cooling loads. Also, the colored areas show the daily mean loads whereas the dotted curves show the maximum load reached during the considered day.

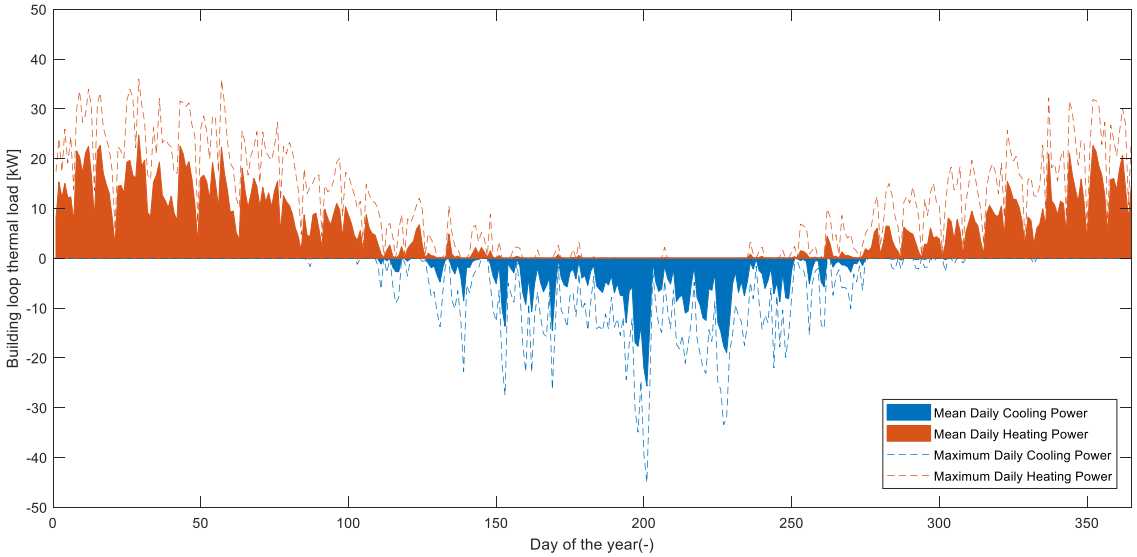

Figure 6 : Daily loads on the building loop. A negative value corresponds to cooling mode

As shown in the equations above, the electrical power used by the heat pump is subtracted from the heating building load but added to the building cooling load to calculate the load on the building

loop, which changes slightly the balance between heating and cooling. It also results in a peak cooling load on the building loop which is higher than the peak heating load, while the situation was reversed for the “pure” building loads. Heat pump COPs depend on their inlet temperatures, and the values plotted in Figure 6 were obtained reference scenario 2 described below. Values of the building loop loads will vary slightly for each case.

Pump control in the building loop

In the building loop, the fluid can experience a slightly negative temperature, so a mix of water and glycol is needed to prevent freezing of the fluid in the heat pumps during their operation in heating mode. A fluid composed of 25% of propylene glycol and 75% of water was then selected. The fluid properties were adjusted according to this concentration of propylene glycol.

The pump on the building loop is set to provide a maximum temperature difference of 3 °C at the maximum load on the loop. Figure 7 shows the control of the pump as a function of the load. In this figure, the maximum load for the simulation is 50 kW.

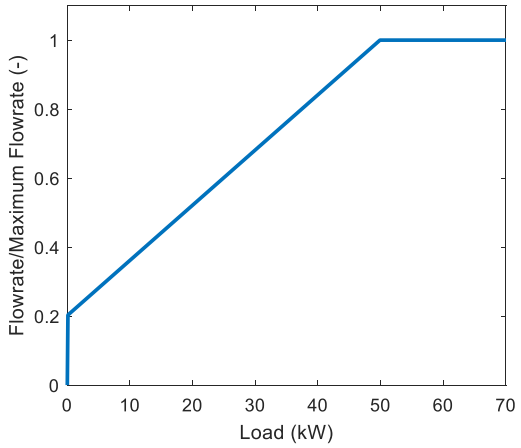

Figure 7: Control Strategy for the pump on the building loop for a 50 kW maximum load.

2.2.3. Auxiliary heating and cooling

In the building loop there are two auxiliary systems for cooling and heating. They operate when the well cannot maintain the building loop within acceptable levels by itself. The auxiliary heating system helps maintaining a minimum temperature of 3 °C in the building loop if the temperature coming back from the well is less than 5 °C with a 1 °C dead-band. This dead-band means that the auxiliary system will start when the temperature coming out from the well is under 4.5 °C and stops

when it is above 5.5 °C. For heating, the auxiliary is an electrical resistance with a coefficient of performance set at 1.

For the cooling mode, the same dead-band is applied for a setpoint temperature of 35 °C if the groundwater comes back at more than 30.5 °C. The cooling auxiliary is conventional chiller that has a performance coefficient of 3.

The power and capacity are supposed to be sufficient to maintain the setpoint temperature at all time. The consumption of the auxiliary system is studied and part of the cost calculation.

2.2.4. Pipes

The heating and cooling system used for the building includes a piping network that connects the water-to-air heat pumps to the plate heat exchanger as illustrated in Figure 2. The simulation model includes the TRNSYS type 31 for pipes before and after the location of the Load type that simulates the action of the water-to-air heat pumps on the loop. The size of the pipes was adapted to represent a reasonable approximation of the system's thermal mass. The selected value also ensures that the volume of fluid in the pipes is larger than the volume that can be displaced within one time step (1 h) at the maximum flow rate (this helps avoid numerical oscillations). This led to 50-m long pipes with a 0.45-m diameter.

2.3. Ground loop

2.3.1. Matlab Model for the SCW

The SCW model used to perform the simulations is the Thermal Resistance and Capacity Model (TRCM) developed in A. Nguyen et al. (2015b) and A. Nguyen et al. (2015a). The model is written in Matlab and integrates the geometry, thermal conductivity and diffusivity of the surrounding ground, vertical pipes and groundwater through a network of interconnected thermal resistances and capacities. Solution of the model also takes into account the vertical displacement of the groundwater in the SCW and the groundwater flow in the aquifer induced by the bleed. Bleeding results in a reduction of the water level in the extraction well (drawdown D) and in an increase of the water level in the injection well (impression I). The various formulae used to evaluate the resistances and capacities of the network are presented in the original paper describing the model. Note that the model has been validated against several numerical reference solutions.

Table 1: Parameters of the SCW.

Parameter	Value
Borehole Length	300 (m)
Hydraulic conductivity	5.7e-7 (m/s)
Borehole diameter	0.15 (m)
Pump pipe diameter	77.5 (mm)
Porosity	2 (%)

The Matlab model is linked to the simulation via the TRNSYS Type 155. The main parameters of the SCW used are shown in Table 2 and were obtained from the experimental system described by Beaudry et al. (2018). During the simulations, the model receives inputs from TRNSYS and gives back the outputs summarized in Table 3.

Table 2: Inputs and outputs of type 155.

No	Input		Output	
	Name	Unit	Name	Unit
1	Inlet Temperature to the well - $T_{in,well}$	°C	Outlet Temperature of the well - $T_{out,well}$	°C
2	Inlet Flowrate to the well - $\dot{m}_{in,well}$	kg/hr	Outlet Flowrate of the well - $\dot{m}_{out,well}$	kg/hr
3	Bleed flow rate - $\dot{m}_{bleed}$	kg/hr	Bleed flow rate - $\dot{m}_{bleed}$	kg/hr
4	-	-	Drawdown – D	m
5	-	-	Pressure Drop	kPa
6	-	-	Impression in the injection well	m

2.3.2. Submersible Pump (SP)

The submersible pump is responsible for the flow rate on the source side of the plate heat exchanger. The pump is designed with a variable frequency drive that is meant to provide the best efficiency at every time step. The efficiency of the motor and the pump are then set to constant values for our simulation.

Table 3: Parameters for the submersible pump.

Parameter	Value (unit)
Pump efficiency	0.6 (-)
Motor efficiency	0.76 (-)

The simulation of the submersible pump is a key component in the simulation because the electrical consumption of the submersible pump has a significant impact on the overall consumption of the system. The pump consumption is function of the flow rate and pressure drop in the ground loop.

The latter includes the pressure drops caused by the drawdown of the dynamical water level in the SCW and pressure drops in the piping network. The pump is modeled by Type 742, which takes an externally calculated pressure drop as an input as well as the flow rate.

The pressure drop is calculated and returned by the Matlab model. It is a function of the temperature and the flow rate, and represents the sum of the pressure drops in: the pipes, the heat exchanger, the elbows and valves of the system. It also considers the drawdown induced by bleeding of the SCW. Table 5 sums up the parameters used for each component included in the total pressure drop.

Table 4:Parameters for the calculation of pressure drop in the ground loop.

Parameter	Units	Length (m)	Diameter (mm)
Rising pipes	1	28	77.5
Reinjection pipe	1	225	48.68
Elbows	6	-	77.5 (3)/ 48.68(3)
Valves	2	-	77.5 (1)/ 48.68(1)

The pressure drop for the plate heat exchanger is a combination of a computation based on Thulukkanam (2013) and manufacturer data of the heat exchanger used in Varennes. The roughness of the pipes used is 0.0000212 and corresponds to the roughness of HDPE pipes.

2.3.3.Bleed and injection well

Different bleeding control strategies are implemented in the simulations. For instance, to prevent the injection well from overflowing, the bleed ratio is set to zero if the water level in the injection well is less than 5 m from the surface. This threshold was chosen based on observations made by Orio et al. (2005) that observed a static water level for commercial buildings that are usually between 5 to 12 m from the surface, with a median value of 6 m. Setting the threshold at 5 m gives a safety margin of 1 m.

Computation of energy costs

To analyze the simulations, the electricity bill is calculated according to the M rate of the local electricity provider (Hydro-Québec). The billing is divided in two parts for energy and power. The output of the simulation is treated to provide monthly results for energy and power considering heating and cooling provided by the heat pumps and by the auxiliary systems, and the energy used by the submersible pump. The Rate M structure is as follows (units are Canadian Dollars, abbreviated as $ here):

- 14.46 $ per kW for the monthly peak power demand;
- 4.99 ¢/kWh (0.05 $/kWh) for the first 210,000 kWh of the month; and
- 3.70 ¢/kWh (0.037 $/kWh) for the remaining consumption of the month.

The billing demand is the maximum power used by the system during the current month, but is at least 65% of the power used between the 1st of December and 31st of march. For example, if the yearly peak demand occurring in January is 100 kW, and the peak monthly demand for August is 50 kW, the monthly bill for August will use a value of 65 kW (65 % of the winter maximum) and not 50 kW.

3.SIMULATED CASES

We implemented a model that allows us to control the pumping and bleeding flowrates with various control strategies. To obtain consistent results, we compared eight control strategies (Scenarios 1 to 8) to two reference scenarios (Reference 1 and 2). The first reference scenario implements the same building loop without the ground heat exchanger, and relies on auxiliary heating and cooling only. This reference scenario aims at identifying the gain of using a ground heat exchanger. The second reference scenario combines the control strategies usually implemented according to a literature review (dead-band of 3 °C, pumping flow rate of 3GPM/ton (54 L/s-MW) and a 10% bleed ratio). Note that the pump is switched off when there is no load on the building loop. Also, as the temperature thresholds are location dependent, we simulated different cases to derive the best auxiliary heating and cooling setpoints for our case, which correspond to temperatures of 5 °C and 29 °C, respectively. This was done to ensure that the reference scenario presents a good level of performance with well-tuned simple control strategies.

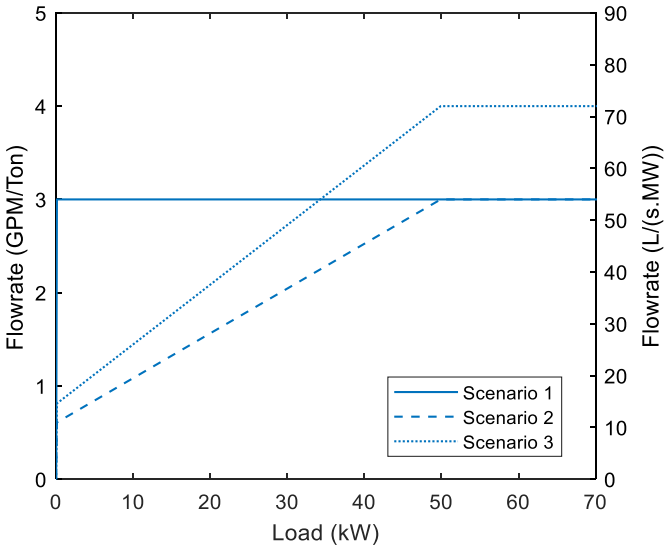

Figure 8: Pumping flow rate control strategies

Scenarios 1 to 3 investigate the control strategies for the total pumping flow rate of the ground loop. These control strategies are shown in Figure 8 and were selected after performing a few preliminary tests. We selected a constant pumping flow rate of 3 GPM/ton (Scenario1) and a linear control of the pumping flow rate as a function of the load applied on the building loop (Scenario 2 and 3). The linear controls have a minimum flow rate corresponding to 20% of the maximum flow rate to account for practical limitations of variable speed drives. Note that these scenarios consider no bleed and a maximum peak load of 50 kW.

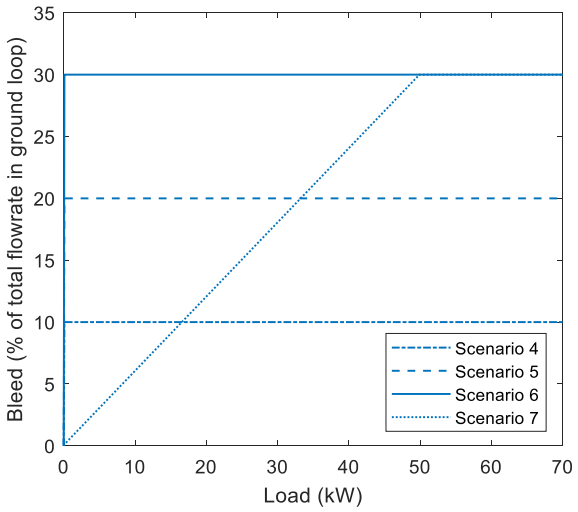

Figure 9: Bleed flow rate control strategies

Scenarios 4 to 7 aim at comparing various control strategies for the bleed and are illustrated in Figure 9. These control strategies are based on the scenario 3 for the pumping flow rate and will be adding a control over bleeding with a constant bleed ratio (Scenario 4 to 6) or a bleed ratio that varies linearly from 0 to 30% as a function of the load applied on the loop.

In Figure 9, the bleed ratio is controlled based on the ratio between the current load and the maximum absolute load, whether the current load is positive (heating) or negative (cooling). Comparing with Figure 7 shows that, since the maximum heating and cooling loads are different, the maximum flow rate will never be reached in one of the modes. With the situation illustrated in Figure 7, the maximum cooling load on the building loop is about 45 kW and the maximum heating load is about 35 kW. The control law in Figure 9 would calculate the bleed ratio based on the ratio between the current load and 45 kW, therefore only reaching 78 % (=35/45) in heating.

In a last variant (scenario 8), the law represented in Figure 9 is implemented separately for heating and cooling, with their respective maximum values. Using the same example as above, the bleed ratio in heating would be proportional to the ratio between the current heating load and 35 kW, while the bleed ratio in cooling would be proportional to the ratio between the current load and 45 kW.

4. RESULTS AND DISCUSSION

The simulated temperatures on each side of the plate heat exchanger for a peak demand day both in cooling and heating mode are illustrated in Figure 10. In cooling mode, the temperatures remain below 30 °C, which means that the cooling auxiliary (AC) is not used. As the building is designed for a heating-dominated climate, it is not surprising to observe cooling is covered entirely by the geothermal system. We can observe a 3 °C temperature difference between entering and leaving water temperature on the load side of the plate heat exchanger. This observation is consistent with the settings of the simulation as the peak demand of the year is presented in Figure 10. In heating mode, we can observe a temperature close to zero, the freezing point. On that day, the auxiliary heating (AH) system is always operating because the temperature leaving the SCW is always lower than the setpoint of 5 °C mentioned in Section 3. It should be mentioned that the temperature difference is less than 3 °C because the peak demand in heating is lower than in cooling.

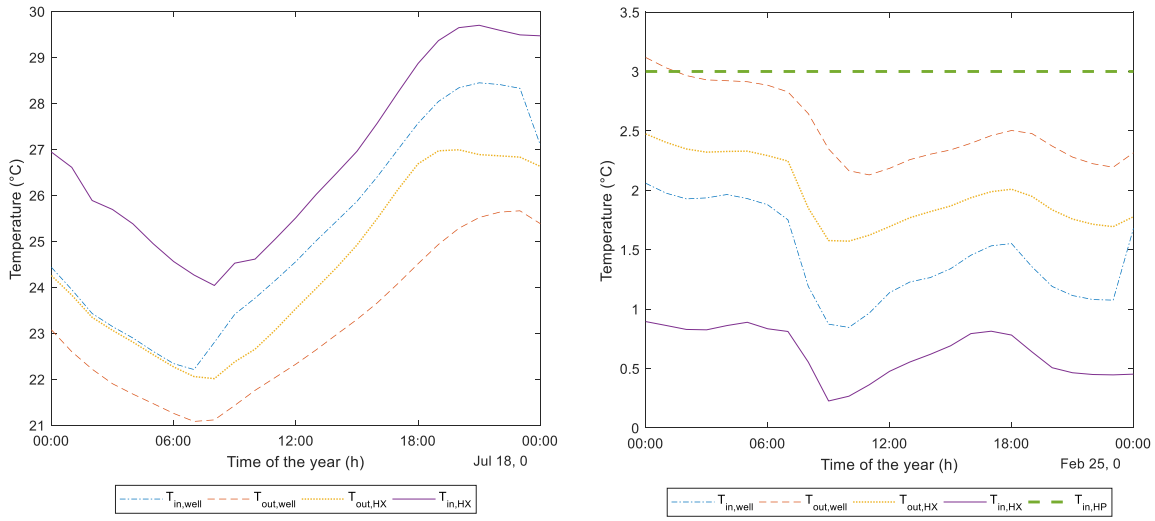

Figure 10: Temperature at the plate heat exchanger for (left) a peak day in cooling mode and (right) a peak day in heating

Looking at figure 9, it is important to note that in cooling mode, $T_{out,HX}$ is equal to $T_{in,HP}$, $T_{out,HP}$, $T_{in,HX}$ because none of the auxiliaries are working. In heating mode, the auxiliary heating is working so $T_{in,HP}$ is different from $T_{out,HX}$ while $T_{out,HP}$ and $T_{in,HX}$ are the same.

4.1 Control of the total pumping flow rate

In this section, the energy consumption and the maximum power demand corresponding to the first three scenarios are compared to the first reference case where no SCW is used to exchange heat with the building loop. Figure 11 summarizes the results and also shows the portion of the energy or power demand associated to the operation of the heat pumps (HP), auxiliary cooling (AC), auxiliary heating (AH) and submersible pump (SP).

Our results indicate that using a SCW halve the energy consumption and reduce by approximately 30% the power demand (compare Scenario 1 to 3 to Reference 1). This first result confirms the potential of ground heat exchangers to reduce the energy bill. We also observed that using a linear control for the pumping flow rate (Scenario 2 and 3) decreases the total energy consumption and the pumping energy significantly by comparison to the use of a constant flow rate (Scenario 1). Indeed, using a linear control reduces the pumping energy even though the off-peak flowrates lead to less heat exchange and therefore to a higher use of the auxiliary systems.Comparing the results of Scenario 2 and 3 shows a slight reduction of the energy consumption and power demand when

using a maximum flow rate of 4 GPM/ton (Scenario 3). Indeed, a higher flow rate increases the heat exchanged by the SCW, which in turn will help reducing the operation of the auxiliary systems. On the basis of this result, a maximum flow rate of 4 GPM/ton will be used for Scenarios 4 to 8.

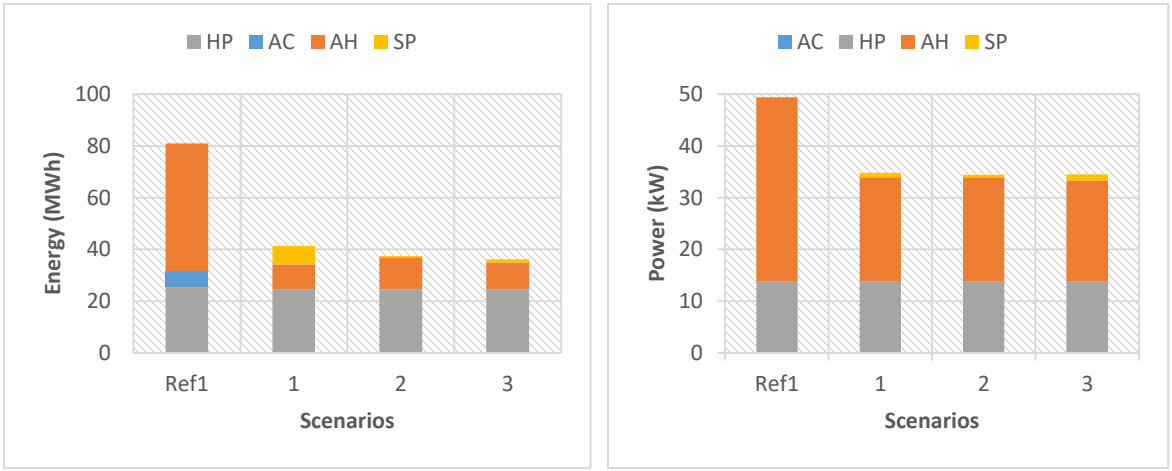

Figure 11: Energy consumption (left) and power demand (right) for Scenario 1,2 and 3.

Control of the bleed ratio

Figure 12 shows the impact of the control strategy of the bleed flow rate on the energy consumption and the maximum power demand. Our results indicate that using the more complex control strategy of Scenario 4 to 8 helps reducing the energy consumption of approximately 15 to 20% by comparison to the reference scenario 2. The impact on the power demand is however limited and a small variation of only 1.25 kW is observed between the studied cases.

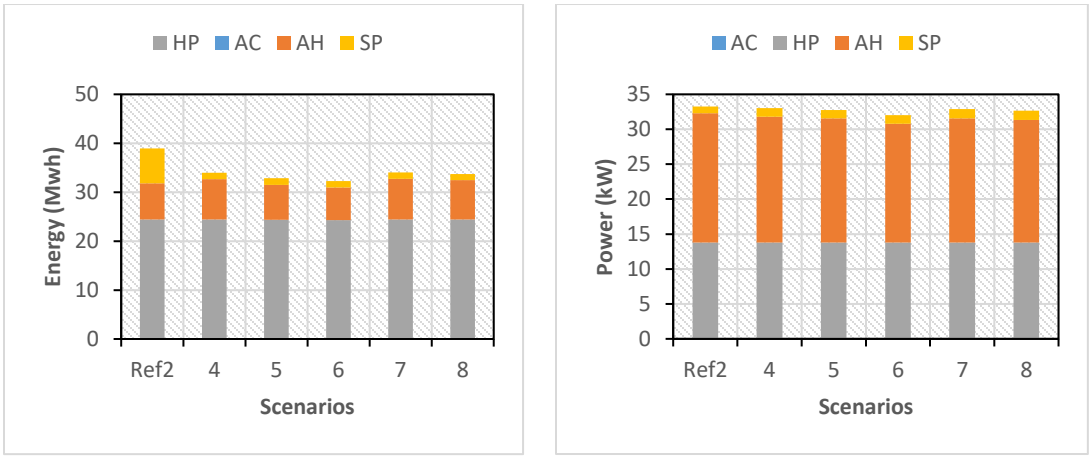

Figure 12: Energy (left) and maximum power (right) for simulations bleeding control

Figure 13 shows the amount of groundwater bled during a year with the control strategies used for the simulations. The volume of groundwater discharged to the injection well varies from 2480 to 7640 m^3 per year for Scenario 4 to 8, with a minimum for Scenario 7 and 8. This is an interesting result because discharging groundwater in the injection well oxygenates the water, which in turn promotes mineral and biological clogging of the injection well. Reducing the volume of groundwater bled is then desirable for the operation of SCW systems. Consequently, the energy consumption and power demand being similar for Scenario 4 to 8, the controls of Scenario 7 and 8 should be preferred since they show a significantly smaller discharged volume of groundwater.

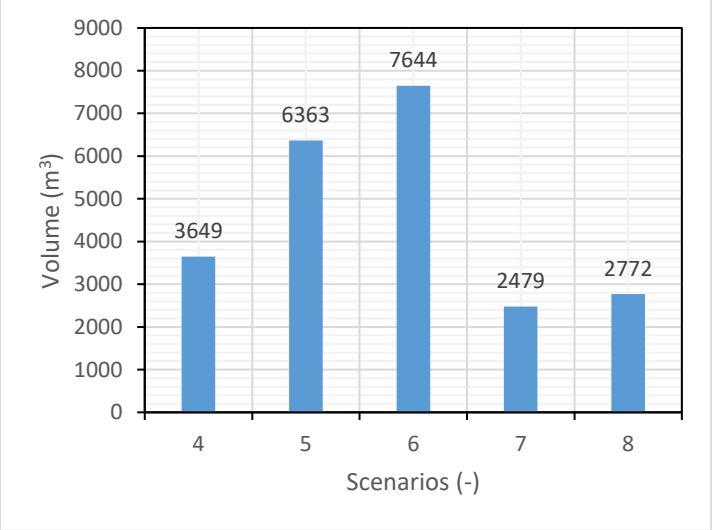

Figure 13: Volume of groundwater bled for different bleed controls

4.3 Financial savings

Table 6 shows the financial savings achieved in comparison to the reference scenarios. Our results indicate that the SCW system provides savings ranging between 39% and 46% with respect to a system having no ground heat exchanger. The savings achieved by improving control strategies are in the range of 4 to 8%, but it should be stressed that the Reference 2 scenario has been tuned by trial and error to the simulated case and represents an “optimized best practice” case.

Table 5: Savings on costs compared to the reference cases

	Reference scenarios		Scenarios Without Bleed control			Scenarios With Bleed control				
	1	2	1	2	3	4	5	6	7	8
Operational Costs ($)	10370	6050	6370	6160	6090	5790	5690	5580	5770	5730
Savings compared to Reference 1 (%)	-	-	38.6	40.6	41.2	44.2	45.1	46.2	44.3	44.8
Savings compared to Reference 2 (%)	-	-	-	-	-	4.3	5.9	7.8	4.6	5.3

4.4. Influence of system sizing (fraction of the building load covered by the SCW)

Figure 14 shows the operating costs for buildings having different peak loads but connected to a single SCW. Unsurprisingly, we can see that as the peak load diminishes, the operating cost also diminishes. The reduction is however much more interesting for the geothermal system since the load covered by the SCW increases with a smaller building.

The non-geothermal references show a total cost divided in 40% for energy and 60% for power costs. For the 50 and 75 kW cases, power is responsible for 70% of the total cost. Regarding the billing rates, it is better to give priority on lowering the peak power and then the energy.

These figures also show how important it is to size SCW systems (as all types of geothermal systems) properly to match their capacity to the building needs. Proper sizing allows to limit the use of auxiliary heating and cooling and to maximize the savings of ground-source systems.

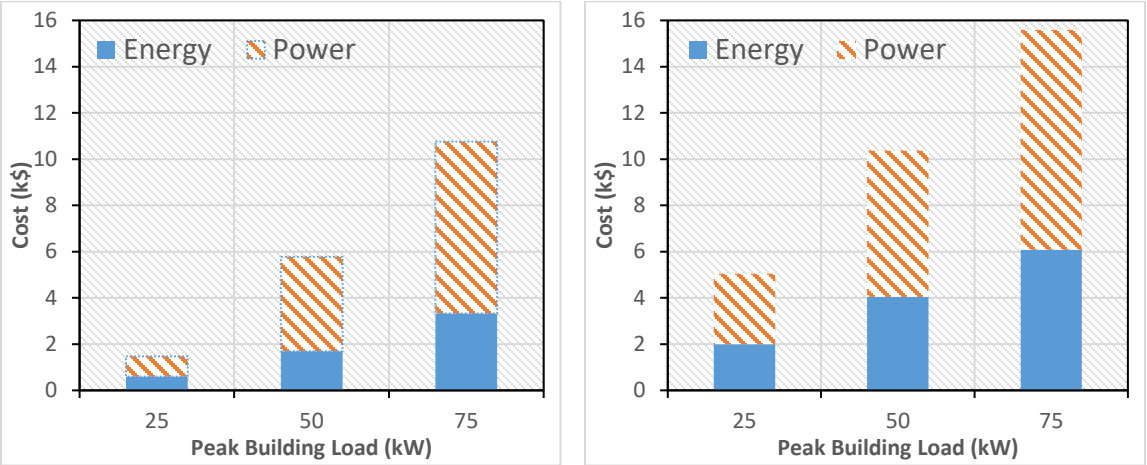

Figure 14: Comparison of the power and energy costs for the different peak power demand (25, 50 and 75 kW) with (left) a SCW system and (right) no geothermal system

5. CONCLUSION

The operation of SCW systems involves two major control variables: the total pumping flow rate (water extracted from the SCW) and bleeding ratio (fraction of the flow rate which is not directly reinjected in the same well).

The results presented in this paper show that using a linear control on the pumping flow rate has a major influence on the pumping energy required. The control strategy must achieve a balance between pumping energy use and using more auxiliary energy for heating or cooling. The control of bleeding ratio shows cost savings from 4 to 8% compared to bleed control strategies found in the (scarce) literature on SCW systems. The most important point about bleed control is the reduction of the volume of groundwater bled which will have a significant impact on operational cost of the SCW system especially concerning the injection well maintenance.

It seems necessary to develop design guidelines for SCW system to help sizing underground components compared to building loads. Guidelines are also lacking to select control strategies for the total pumping flow rate and the bleeding ratio, and the authors help that this paper will be a first step towards developing such guidelines for cold climate operation.

Further work should address more complex control strategies such as predictive control, and assess system performance for different combinations of building types, control strategies, and climates.

6.REFERENCES

ASHRAE. (2010). *Energy Standard for buildings except low-rise residential buildings (Standard 90.1-2010)*. Paper presented at the Atlanta, GA, USA: American Society of Heating, Refrigerating and Air-conditioning Engineers.

Beaudry, G., Pasquier, P., & Marcotte, D. (2018). *Hydrogeothermal Characterization and Modelling of a Standing Column Well Experimental Installation*. Paper presented at the International Ground Source Heat Pump Association (IGSHPA), Conference 2018.

Bernier, M., Kummert, M., & Bertagnolio, S. (2007). *Development and application of test cases for comparing vertical ground heat exchanger models.* Paper presented at the International Building Performance Simulation Association (IBPSA) Conference 2007.

Deng O'Neill, Z., Spitler, J. D., & Rees, S. J. (2006). Performance Analysis of Standing Column Well Ground Heat Exchanger Systems. *ASHRAE Transactions, 112*(2).

EnvironmentCanada. (2010). *Canadian Weather Energy and Engineering Data Sets (CWEEDS files) and Canadian Weather for Energy Calculations (CWEC files) updated user's manual.* Paper presented at the Ottawa, ON, CAN: Environment Canada. Retrieved from http://climate.weather.gc.ca/prods_servs/engineering_e.html.

Minea, V. (2013). Experimental investigation of the reliability of residential standing column heat pump systems without bleed in cold climates. *Applied Thermal Engineering, 52*(1), 230-243.

Nguyen, Pasquier, P., & Marcotte, D. (2013). Development of an ODE model featuring a three level bleed control and an off-loading sequence for standing column wells. *Proceedings of BS2013, Chambéry, France*, 26-28.

Nguyen, A., Pasquier, P., & Marcotte, D. (2015a). Influence of groundwater flow in fractured aquifers on standing column wells performance. *Geothermics, 58*, 39-48.

Nguyen, A., Pasquier, P., & Marcotte, D. (2015b). Thermal resistance and capacity model for standing column wells operating under a bleed control. *Renewable Energy, 76*, 743-756.

Orio, C. D., Chiasson, A., Johnson, C. N., Deng, Z., Rees, S. J., & Spitler, J. D. (2005). A Survey of Standing Column Well Installations in North America. *ASHRAE Transactions, 111*(2).

Orio, C. D., Johnson, C. N., & Poor, K. D. (2006). Geothermal Standing Column Wells: Ten Years in a New England School. *ASHRAE Transactions, 112*(2).

Pasquier, P., Nguyen, A., Eppner, F., Marcotte, D., & Baudron, P. (2016). Standing column wells *Advances in Ground-Source Heat Pump Systems* (pp. 269-294): Elsevier.

Rees, S. J., Spitler, J., Deng, Z., Orio, C., & Johnson, C. (2004). A study of geothermal heat pump and standing column well performance. *ASHRAE Transactions, 110*(1), 3-13.

Thulukkanam, K. (2013). *Heat exchanger design handbook*: CRC press.

USDOE-BTO. (2017). Commercial Prototype Building Models. Retrieved February 28, 2017, from https://www.energycodes.gov/development/commercial/prototype_models.

7.NOMENCLATURE

AC – Auxiliary Cooling

AH – Auxiliary Heating

COP – Coefficient of performance (subscript will indicate if it is for cooling, heating or service water heating)

D – Drawdown (lowering of the water level in the extraction well due to bleeding)

GPM – Gallons Per Minute

GSHP – Ground Source Heat Pump

HDPE – High-Density Polyethylene

HP – Heat Pump

I – Impression (water level rise in injection well due to bleeding)

$\dot{m}_{bleed}$ – Bleed Flowrate

$\dot{m}_{in,well}$ – Flowrate entering the well (flow rate leaving the well minus the bled flow rate)

$\dot{m}_{out,well}$ – Flowrate leaving the well

Q_{bldg} – Building thermal load

Q_{loop} – Thermal load on the building loop

SCW – Standing Column Well

SP – Submersible Pump

SWH – Service Water Heating

$T_{in,well}$ – Temperature of groundwater entering the well

$T_{out,well}$ – Temperature of groundwater leaving the well

$T_{in,HX}$ – Temperature entering the heat exchanger on load side

$T_{out,HX}$ – Temperature leaving the heat exchanger on load side

$T_{in,HP}$ – Temperature entering the heat pumps on building loop

$T_{out,HP}$ – Temperature leaving the heat pumps on building loop

TRNSYS – Transient System Simulation tool

W_c – Energy consumption of the heat pump (energy required by the compressor)